FLOW AND ACOUSTIC ANALYSIS OF TWO-WHEELER MUFFLER

A THESIS SUBMITTED IN PARTIAL FULFILLMENT OF THE
REQUIREMENT FOR THE AWARD OF THE DEGREE OF

MASTER OF TECHNOLOGY
(COMPUTATIONAL DESIGN)
TO

DELHI TECHNOLOGICAL UNIVERSITY

SUBMITTED BY

JITENDER SAINI
ROLL NO. - 2K14/CDN/07

UNDER THE GUIDANCE OF

ROOP LAL
ASSISTANT PROFESSOR

DELHI TECHNOLOGICAL UNIVERSITY

**DEPARTMENT OF MECHANICAL, PRODUCTION & INDUSTRIAL
AND AUTOMOBILE ENGINEERING
DELHI TECHNOLOGICAL UNIVERSITY
BAWANA ROAD, DELHI-110042
JUNE 2016**

DELHI TECHNOLOGICAL UNIVERSITY

(Formerly Delhi College of Engineering)

Shahbad Daulatpur, Bawana Road,

Delhi-110042

STUDENT'S DECLARATION

I, **Jitender Saini,** hereby certify that the work which is being presented in this thesis entitled **"Flow and acoustic analysis of two wheeler muffler"** is submitted in the partial fulfillment of the requirement for degree of **Master of Technology (Computational Design)** in Department of Mechanical Engineering at **Delhi Technological University** is an authentic record of my own work carried out under the supervision of **Assistant Professor Roop Lal.** The matter presented in this thesis has not been submitted in any other University/Institute for the award of Master of Technology Degree. Also, it has not been directly copied from any source without giving its proper reference.

Signature of Student

This is to certify that the above statement made by the candidate is correct to the best of my knowledge.

Signature of Supervisor

The Master of Technology Viva-Voce examination of Mr. Jitender Saini has been held on ………………. and accepted.

Signature of Supervisor   **Signature of HOD**

Signature of External Examiner

I

CERTIFICATE

This is to certify that this thesis report entitled, **"Flow and acoustic analysis of two wheeler muffler"** being submitted by **Jitender Saini (Roll No. 2K14/CDN/07)** at Delhi Technological University, Delhi for the award of the Degree of Master of Technology as per academic curriculum. It is a record of bonafide research work carried out by the student under my supervision and guidance, towards partial fulfillment of the requirement for the award of Master of Technology degree in Computational Design. The work is original as it has not been submitted earlier in part or full for any purpose before.

Roop Lal

Assistant Professor

Mechanical Engineering Department

Delhi Technological University

Delhi-110042

ACKNOWLEDGEMENT

Throughout the work a positivity always surrounds me which keeps me motivated and inspired me to do better. Thanks to god, for his blessings and for the strength and energy, he has given me to complete this work.

I would also like to thank **Prof. R. S. Mishra, Head,** Department of Mechanical Engineering, for the resources made available to carry out this research work and **Dr. A. K. Agrawal, M.Tech. Coordinator and Associate Professor,** Department of Mechanical Engineering, whose perception and interpretation of the things and guidance from time to time helped me for the continuous improvement.

I want to express my sincere gratitude to my research supervisor, **Roop Lal, Assistant Professor,** Department of Mechanical Engineering, for allowing me to carry out the research work jointly with Omax Autos Ltd, Gurgaon. His humble and kind nature made me very comfortable to share and discuss problems. I am very grateful for his support throughout the work.

I would like to extend my gratitude to **Mr. Amit Gulavani, Head, Innovomax, an Omax R&D Centre,** for providing me the opportunity to work on this project and all my seniors in Omax Autos Ltd, Gurgaon, especially **Mr. Abid Hussain** for his guidance and encouragement during the project work.

Last but not the least, I want to thank my family, for believing in me.

JITENDER SAINI
M.TECH (COMPUTATIONAL DESIGN)
2K14/CDN/07

ABSTRACT

Muffler manufacturers are being confronted with the problem of designing mufflers with low restriction as well as low radiated exhaust noise. Increased competition and stricter regulation norms have intensified the need for development of an efficient muffler. The traditional "build & test" procedure which is time consuming and expensive, can nowadays be assisted by simulation models which are able to predict the performance of several different muffling systems in a short time, thus saving time and resources.

Generally, mufflers should be designed to satisfy the two requirements. One is high noise attenuation performance, which is a fundamental requirement of a muffler. An exhaust muffler should muffle the frequency range of interest, especially the low frequency range, because it is well known that most of the noise is limited to the engine rotational frequency and its first few orders & the second is minimum back pressure, the extra static pressure exerted by the muffler on the engine through restriction in the flow of exhaust gases. This needs to be kept to a minimum, because a large back pressure will result in reduction of volumetric efficiency and the specific fuel consumption rate. These two important design requirements for a muffler are often contradictory.

The purpose of this work is to investigate the flow and acoustic performance of a 100 cc two wheeler muffler. The computational fluid dynamic (CFD) analysis is done to predict the flow performance by finding the flow parameters, pressure and velocity. When it comes to acoustical performance, there are several parameters that describes the characteristics of a muffler, the transmission Loss (TL) is the most popular amongst them because of the reason that it is a property of the muffler only and it doesn't depend upon the sound source. It can also be useful, to check the validity of a mathematical model. For acoustic analysis, the transmission loss of the present muffler was predicted using commercial software package. At first the design was investigated for single expansion chamber, by doing harmonic acoustic analysis and the validation is made with the analytical results. Then the validated procedure is adopted for the concept muffler and results are compared with the experimental results. Comparing measured and FEA results allowed assessment of the accuracy and reliability of the simulation

TABLE OF CONTENTS

LIST OF FIGURES

CHAPTER 3   MEASUREMENT & CALCULATION

CHAPTER 4   MODELLING & SIMULATION

CHAPTER 5   RESULTS & DISCUSSION

LIST OF TABLES

CHAPTER 1
INTRODUCTION

In 21st century, automobile industries are booming at an unimaginable pace. In order to survive in this continuously changing environment, they need to keep improving the performance of their product without increasing its cost. Until recently, during the advancement of the computer age there was a great deal of limitation for predicting muffler performance. In the past, the mufflers often needed to be scaled down to a simplified model which left out some key factors that contributed to the overall sound pressure level. Although the underlying theory was in place due to M. L. Munjal's classical book on duct and muffler acoustics [2], the tools and resources to fully characterize the entire system were not available until computer solvers for Finite Element Methods (FEM) and Computational Fluid Dynamics (CFD) became readily available. The methods in place to predict muffler performance never took the entire picture into account. The thesis aims to analyze the behavior of the muffler completely as well as to find the limitation of the solver used for the analysis.

1.1 Background

Internal combustion (IC) engine noise has been drawing significant attention from automotive manufacturers. Emission requirements have also become much more stringent on engine noise and emission levels over the last decade and a half. That is the reason for increasing popularity of noise control amongst wide variety of OEM (original engine manufactures) designers. This is one of the prime importance for OEM to be competitive or to keep a given supremacy in the market. To effectively reduce the noise level, the first step is the identification of noise sources.

An IC engine noise signal is composed of many components from different sources. These sources include combustion, mechanical, and the combination of both. A major factor in engine and vehicle emitted noise is the exhaust system. With regard to the sound pressure levels, the untreated exhaust noise is often ten times greater than all the structural noise of the system combined [1].

The following figure shows the contributions of noise by various automotive systems.
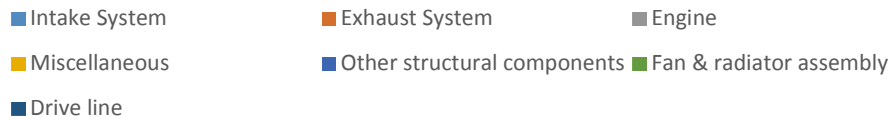
Fig. 1.1: Noise Contributions by Various Automotive Systems

So the problems of reducing engine noise consist, mainly in attenuating exhaust noise.

In determining the lowest frequencies of interest, it is essential to understand the application of the exhaust system. The primary parameter of interest is the firing frequency of the engine which is the rate of in-cylinder fuel ignition which takes all active cylinders into account [3].

A high intensity pressure wave generated by combustion in the engine cylinder propagates along the exhaust pipe and radiates from the exhaust pipe termination. The pulse repeats at the firing frequency of the engine which is defined by

$$CFR = \frac{Engine\ speed\ in\ RPM}{60} \qquad for\ 2-stroke\ engine \qquad (1\text{-}1)$$

$$= \frac{Engine\ speed\ in\ RPM}{120} \qquad for\ 4-stroke\ engine \qquad (1\text{-}2)$$

$$EFR = n \times (CFR) \qquad n\ is\ no.\ of\ cylinders \qquad (1\text{-}3)$$

Where CFR; Cylinder firing frequency

and   EFR; Engine firing frequency

NOTE: For calculating the target frequencies engine max power rpm is required

The firing frequencies are also called exhaust tones (frequencies) of the engine. Majority of the pulse energy lies in the frequency range of 0-1800 Hz. Exhaust mufflers are designed to reduce sound levels at these frequencies/tones.

Other frequencies expected in the spectrum are harmonic orders of both the firing frequency and crankshaft speed, usually with diminishing amplitudes as a function of frequency. Typical firing frequencies for various types of engines are shown in Fig. 1.2.
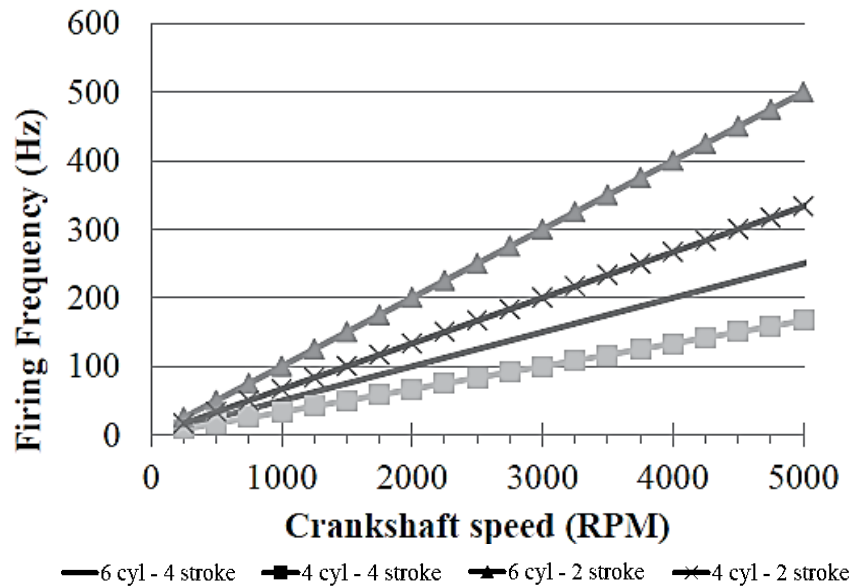
Figure 1.2: Typical first order firing frequencies for various engine configurations.

1.1.1 Remedial measures of noise control

There are three basic elements in any noise control system

- The source of the sound
- The path through which the sound travels
- The receiver of the sound (Faulkner, 1976).
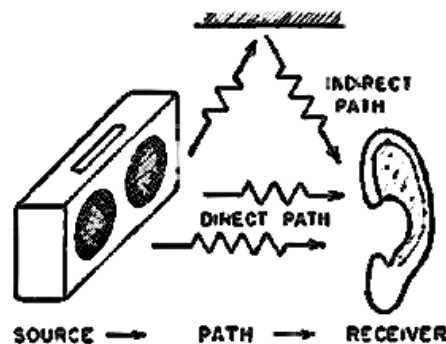
Fig. 1.3: Three components of a general noise system: source of noise, path of noise & the receiver. The path may be direct or indirect to the receiver

3

Accordingly, corrective measures can be taken to stop the noise, here are discussed some methods:

1.1.1.1 Stopping it at the source

- Improving the engineering in many noisy objects has cut noise nearly by 30 decibels (i.e. snow mobiles)
- Reducing sound at the sources by an average of 10 decibel cuts soundness in half.

1.1.1.2 Substitution of mechanical power generation & transmission equipment

- Electric motors for internal combustion engines or gas turbines
- Belts or hydraulic power transmissions for gear boxes

1.1.1.3 Noise attenuating devices

- By the use of mufflers or silencers
- Active noise cancellation devices

1.1.1.4 Shielding your ears

- Without doubt, plugging up your ears is the cheapest and easiest method of noise control

1.2 Motivation

Noise reduction is one of the highest prior target for IC engine development because of the stricter engine noise limits. To increase the sales amount and profit in marketing, the low-noise design of a product has become essential. To depress the low-frequency noise in two wheelers, muffler is habitually in use.

Mufflers with very complicated internal acoustic components such as inlet/outlet tubes, thin baffles, perforated tubes, and sound absorbing materials have been introduced in automobiles. The complex internal components of mufflers would be adopted so as to improve the silencing efficiency, but introduce much difficulty in the analysis and design of the silencer because new designs should be analyzed with respect to both acoustics and back pressure.

Motivation of this work came from the fact that muffler design is restricted to trained personnel and is commercially expensive, in particular for preliminary design evaluation. Most muffler manufacturers are small and medium companies with a limited number of resources. They thereby require cost effective, simple and fast modeling tools, especially in the preliminary design evaluation stages.

1.3 Muffler selection criteria & its classification

Engine exhaust noise is controlled through the use of silencers and mufflers. Generally speaking, there is no technical distinction between a silencer and muffler and the terms are frequently used interchangeably. A silencer has been the traditional name for noise attenuation devices, while a muffler is smaller, mass-produced device designed to reduce engine exhaust noise.

Exhaust silencer is needed to reduce the engine exhaust noise. In most applications the final selection of an exhaust silencer is based on a compromise between the predicted acoustical, aerodynamic, mechanical and structural performance in conjunction with the cost of the resulting system.

In internal combustion engines, mufflers are connected along the exhaust pipe as a part of the exhaust system

1.3.1 Acoustical performance

The minimum reduction of the noise by the muffler is usually specified as a function of frequency. The most frequently used acoustic performance parameters include the insertion loss, IL, which is the difference in sound pressure level for the surroundings due to the insertion of the silencer into the system; the noise reduction, NR, which is the difference in sound pressure level between the point immediately upstream and the point immediately downstream of the muffler; and the transmission loss, TL, which is the change in sound power level across the muffler, if there were no energy reflected back to the muffler in the tail pipe. The insertion loss and the noise reduction usually depend on the characteristics of the tail pipe, in addition to the muffler parameters. The transmission loss usually depends only on the characteristics of the muffler.

Of the three performance parameters just discussed, insertion loss is clearly the only one that represents the performance of the muffler truly. Therefore, there must be adequate insertion loss so that the exhaust (or intake) noise is reduced to the level of the noise from other components of the engine (or compressor or fan, as the case may be), or as required by the environmental noise pollution limits.

1.3.2 Aerodynamic performance

Muffler could lead to a decline of engine power and economy caused by the exhaust resistance while reducing noise. Increasing competition between manufacturers

necessitates the need of lower back pressure mufflers. This could be possible if the volume is increased but due to the space constraints it is not feasible. Therefore, the optimum design requires which has the minimal (or optimal) mean pressure drop so that the source machine does not have to work against undue or excessive backpressure.

1.3.3 Mechanical performance

Although the internal gauge pressure within most mufflers is relatively small, the mechanical design of the muffler must be considered. In applications involving high-temperature gases or corrosive gases, the materials selected for the muffler must be compatible with the fluid handled. If there are suspended particles (soot, for example) in the gases, the mechanical design must be such that these particles are not easily trapped within the muffler. This requirement may interact with the geometric requirements.

1.3.4 Structural performance

In many cases, such as in automotive applications, there are limitations on the physical size and the shape of the muffler because of the performance and other important parts of automotive. Thus, while designing the muffler its volume must be taken into account. This requirement often interacts with the acoustic requirements therefore both criteria should be considered simultaneously for an optimum design of muffler.

1.3.5 Muffler types

Despite the terms and large number of configurations, the silencer can be broken into two fundamental types: active & passive. Each type of silencer has specific performance attributes that can be used independently or in combination to produce the required IL for a specific application.
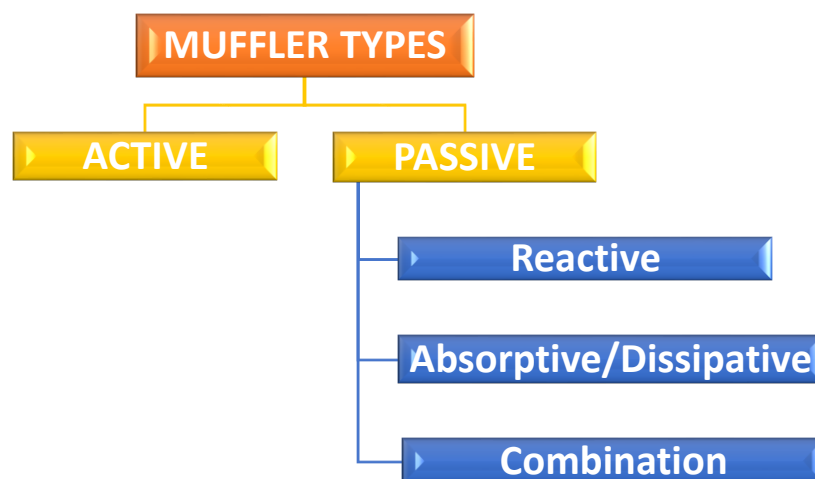
Fig. 1.4: Classification of mufflers

6

1.3.5.1 Reactive muffler

Reactive silencers comprise different elements i.e. a series of a resonating and expansion chambers that are designed to reduce sound pressure level at certain frequencies. It works on the principle that whenever an area discontinuity is encountered, the sound waves experiences an impedance mismatch which in turn causes reflection of a part of the sound wave back toward the source or back and forth among the chambers. The reactive silencers are more effective at lower frequencies than at high frequencies, and are most widely used to attenuate the exhaust noise of internal combustion engines.
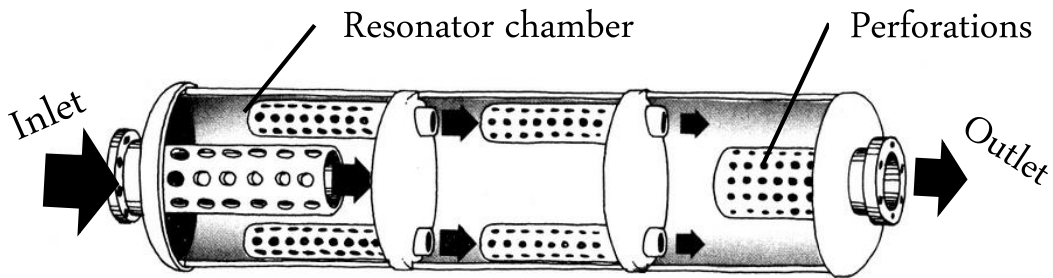
Fig. 1.5: Reactive muffler cut view

1.3.5.2 Absorptive/dissipative silencer

Absorptive silencers contain fibrous or porous sound-absorbing materials and attenuate noise by converting the sound energy propagating in the passages into heat caused by friction in the voids between the oscillating gas particles and the fibrous or porous sound-absorbing material.
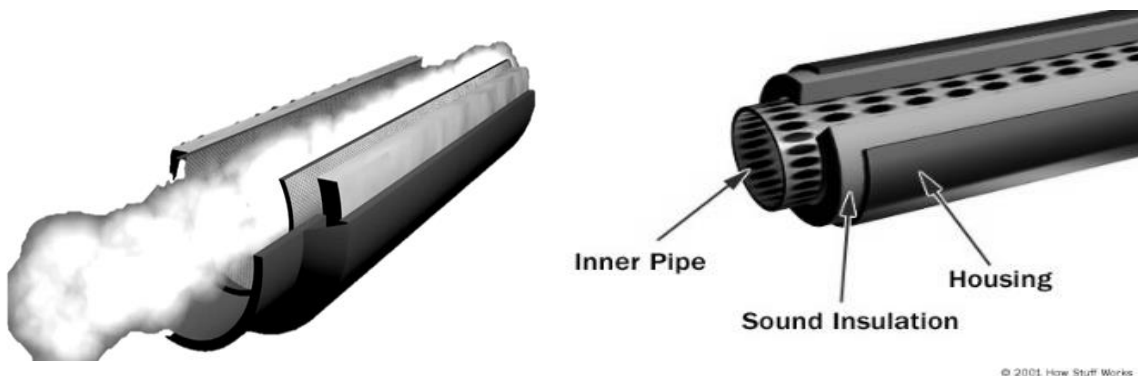
Fig. 1.6: Absorptive muffler

Absorptive silencers usually have relatively wideband noise reduction characteristics at middle and higher frequencies. Absorptive silencers are often used to attenuate the engine intake noise or supplement the performance of reactive silencers for the engine exhaust noise control. The sound absorbing materials are generally held in position by the use of a

perforated metal liner. Knowledge of the structural content of an exhaust system is important when considering the inclusion of a catalytic element or Selective Catalytic Reduction (SCR) system in conjunction with the silencer. Particulate migration of the insulation into the exhaust stream over a period of time can cause the catalytic element to become fouled and substantially impact or impede its performance.

1.3.5.3 Combination silencer

Some silencers combine both reactive and absorptive elements to extend the noise attenuation performance over a broader noise spectrum. Therefore, they can work at low, mid or high level frequency range. Low level frequencies are taken care by reactive elements and high level frequencies by absorptive elements. Combination silencers are also widely used to reduce engine exhaust noise. Figure 1.8 shows typical noise attenuation curves of reactive, absorptive, and combination silencers.

Fig. 1.7: Combination muffler
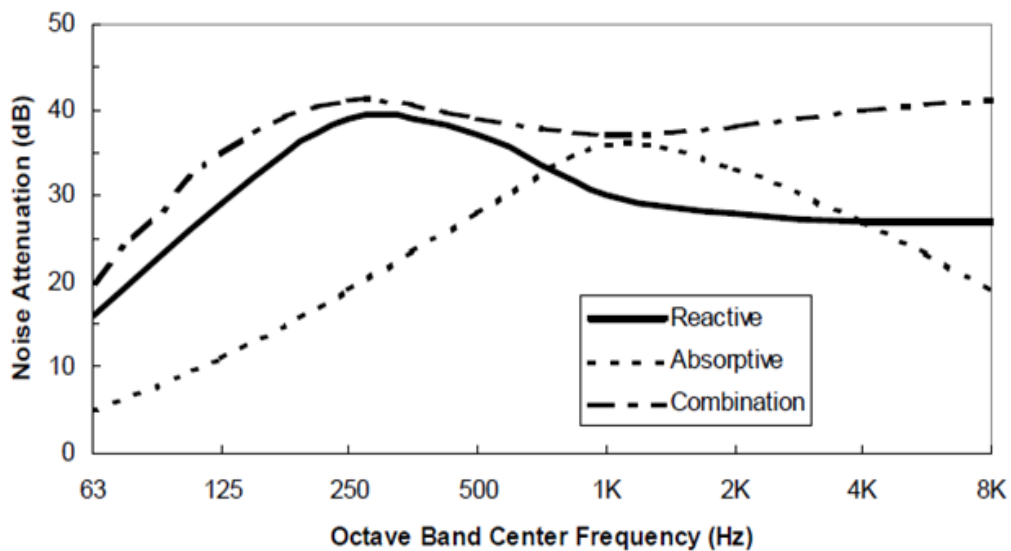
Fig. 1.8: Typical noise attenuation curves

1.3.5.4 Active silencer

Active silencing, or sound cancellation systems, employ detectors used in sensing the noise in an exhaust pipe and a loudspeaker that is used to reintroduce an inverted signal that is developed to reduce low frequency noise. This will affect the noise attenuation greatly as the sound attenuation is 100%.

It is possible to produce a sound wave that is exactly the opposite of another wave. This is the basis for those noise-canceling headphones you may have seen. Take a look at the figure below. The wave on top and the second wave are both pure tones. If the two waves are in phase, they add up to a wave with the same frequency but twice the amplitude. This is called constructive interference. But, if they are exactly out of phase, they add up to zero. This is called destructive interference. At the time when the first wave is at its maximum pressure, the second wave is at its minimum. If both of these waves hit your ear drum at the same time, you would not hear anything because the two waves always add up to zero.

At first this idea seems to be very fascinating but there are a variety of complications and problems because the sound from the exhaust is unpredictable and highly fluctuating in nature. Also at present it is very expensive as compared to the other less costlier products. The performance of active silencing deteriorates at high frequencies. Therefore, its widespread use is possible with the advancement in the technology.
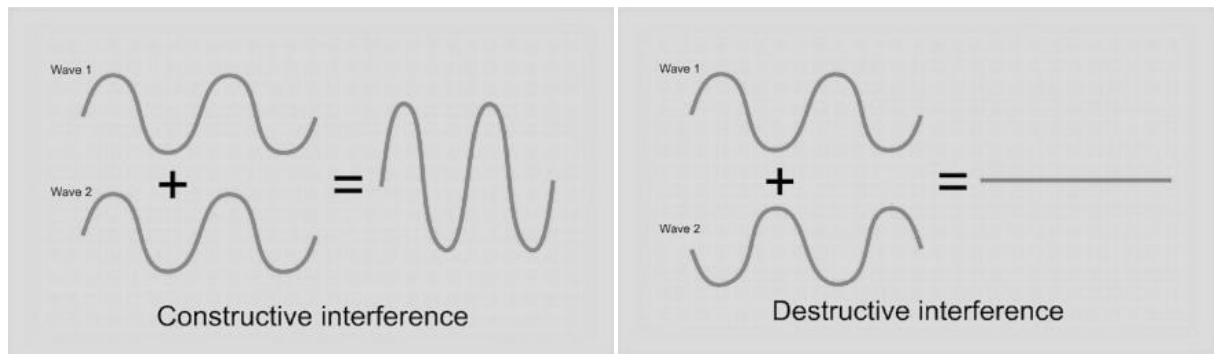
Fig. 1.9: Wave interference phenomenon

1.4 Literature review

Over the last four decades' mufflers have been the focus of many research programs that improved the understanding of the basic phenomenon and resulted in more accurate design methods.

Passive Mufflers based on impedance mismatch, called reflective or reactive Mufflers have been most common in the automobile industry. Recently, better methods have been developed to produce long durable fibrous materials with controllable physical and chemical properties, making it possible for the absorptive mufflers to be used with automobiles. Reflective types of muffler, on the other hand, do not pose any such problems. But, they, in general, produce more back pressure than their counterparts. Pressure drop in the muffler determines the impact of the muffler on the mechanical performance of the source, thereby putting a restriction on their use in many situations. Both of these have their respective frequency range of good and poor acoustic performances. So, to take advantage of both the types of muffler and to overcome their limitations, they are combined to give the required performance over a broader frequency range of interest.

Shital Shah et al. [1] paper provided a practical approach to design, develop and test muffler particularly reactive muffler for exhaust system, which will give advantages over the conventional method with shorten product development cycle time and validation. It also emphasis on how modern CAE tools could be leveraged for optimizing the overall system design balancing conflicting requirements like Noise & Back pressure.

STEP-1: Target setting and Benchmarking

Get basic engine inputs	→	Benchmark engine with same power	→	Set target for design
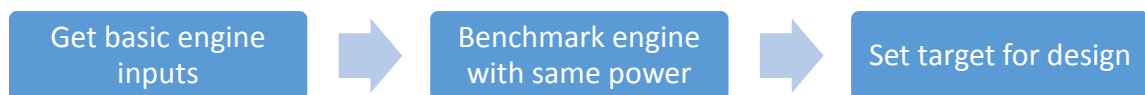
STEP-2: Calculation of target frequencies

Calculation CFR based on basic engine data	→	Calculation of EFR based on CFR

STEP-3: Muffler volume calculations

Refer the engine basic data	→	Calculate muffler volume

STEP-4: Internal configuration and concept design

Refer benchmarking data & target frequencies	→	Internal configuration calculation based on step 2	→	Concept design finalization

STEP-5: Modelling and Simulation

Refer concept design	→	CFD analysis for backpressure measurement	→	Harmonic acoustic analysis for TL	→	Comparison of results
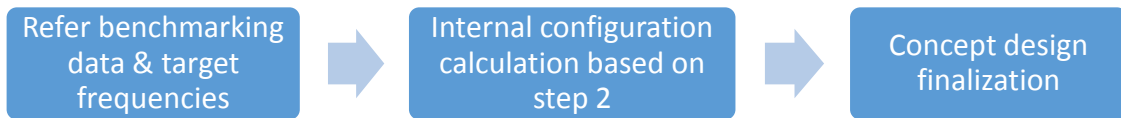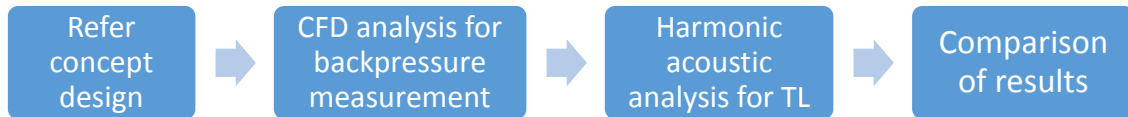
STEP-6: Prototype manufacturing

Refer design from step 5	→	Manufacturing of prototype

STEP-7: Experimental testing and design finalization

Measurement for TL	→	comparison of simulation & experimental results	→	concept finalization
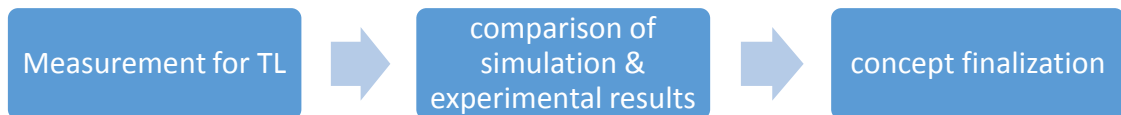
Daniel [17] work also presented principles of muffler design and explains the main advantages of various styles of mufflers. The work describes various functional requirements whether acoustical or non-acoustical, that should be considered for designing a muffler. Measurements are also taken for insertion loss on formula SAE vehicle to assess the style of muffler and its attenuation characteristics.

The calculations considering various parameters like maximum attenuation, temperature of exhaust gas and criteria laid down by ASHRAE Technical Committee for the design of muffler elements was provided by M. Rahman et al [16].

Hak-Son Han et al [15] works helps in benchmarking of muffler as he had done analysis for the target frequencies in the base muffler. The temperature distribution in the exhaust pipes is considered for analysis and the method to enhance the acoustic performance of the muffler is established.

A. I. E1-Sharkawy and N. M. E1-Chazly [18] provided different theories which were compared and evaluated, including the transmission line theory which adopts the plane-wave propagation only, the single pulse theory which takes into consideration the gas flow conditions, and the exact modal analysis which considers all possible radial and spinning modes in addition to the plane-wave.

Mehdizadeh & Paraschivoiu [19] implemented a three-dimensional finite element method and applied it to solve several noise control problems. More specifically, three-dimensional time-harmonic wave propagation in air and porous media is modeled whereby porous materials may be used as acoustic absorbers or as filters in mufflers and silencers. Therefore, finite element modeling can be used for predicting the transmission loss (TL) in the problem of interest at a given frequency range.

Abdullah A. Dhaiban et al. [20] evaluated the performance of elliptical chamber mufflers of different configurations by 3D finite element modeling in ANSYS and the results are compared with the experimental and transfer matrix method. A comparison of TL for a circular expansion chamber and analytical plane wave theory is also made. Comparison made of cut-off frequency obtained from analytical formula and FE model. Wei Fan and Li-Xin Guo [21] improved the work in the area of 3D FE modelling in conjunction with the computational fluid dynamic analysis (CFD) by accounting the effect of the mean flow in evaluating the acoustic performance of mufflers. They imported the mean flow data to the acoustic field by mesh mapping, acoustic response analysis is performed to acquire acoustic pressure at the inlet and outlet. To validate the accuracy of the 3Dnumerical method, published experimental and numerical results for the studied silencers are compared with the present predictions. Zeynep Parlar et al. [22] investigated the flow and acoustic performance of a reactive perforated muffler by using FEA tool COMSOL and the results are compared with the experimental values. An error of 20% is found between the experimental and numerical values.

Peter & Nicole [23] uses four different commercial acoustic softwares namely ANSYS, COMSOL, Virtual Lab and VA-One to show their capabilities of modelling complex muffler geometries. They performed the FE simulation for three reactive muffler designs and then compared it with experimental results by the two microphone method. Differences in the computational predictions were generally observed only at higher frequencies and this is attributed to differences in the computational meshes, different finite element formulations and different approaches used to obtain the transmission loss. Comparison of the computational results with those obtained experimentally showed that the models over-

predicted the magnitude of the transmission loss at resonant frequencies. This is attributed to the fact that no damping is included in the computational models, which all assume inviscid fluid and rigid walls.

Panicker & munjal [24] gives the transfer matrices of various muffler elements for the evaluation of noise characteristics of muffler. The losses in stagnation enthalpy or pressure occurring at these elements are taken into consideration explicitly. The experimental verification is carried out for the new transfer matrix.

El-Sharkawy and Nayfeh [25] work reveals that the performance of an expansion chamber is greatly affected by the expansion ratio, the sound frequency and to a lesser extent the chamber length. This conclusion was verified experimentally. It is shown that plane-wave theory is valid only at low sound frequencies and small expansion ratios. It is also concluded that expansion-chamber mufflers are efficient in attenuating low-frequency sound, which make them ideal for 'automotive silencing applications.

Erdem Özdemir et al. [26] studied the effect of various geometric parameters on the flow & acoustic performance of a cross-flowed perforated and 3-expansion-chambered reactive muffler. It is known that an increase in the total muffler axial length results in a better noise attenuation performance. Also a 30% reduction on length of rear chamber did not make any difference on acoustic characteristics. To generate crossflow, inlet and outlet pipe's perforated part stand in the middle chamber. A decrease at the length of middle chamber prevents the cross flow. Thus, it can be concluded that a greater pressure loss occurs at this model.

Thawani and Doige [27] investigated the performance of reactive muffler considering the effect of mean flow and damping. Mathematical models for sound propagation through a uniform duct in case of no flow, mean flow are given followed by models including damping effects. The solution of the governing equations is presented in the form of 2×2 transfer matrix.

K. Byrne et al. [28] also investigated the performance of a small expansion chamber muffler considering the effect of mean flow and wall compliance through the presented experimental method. The attenuation in the straight through plastic pipe was subtracted from the total attenuation measured with the muffler in place to give the attenuation due to the muffler alone. It was found that, relatively low mean flow velocities have very little effect on the sound transmission loss. The effect of different length to diameter ratio on the transmission loss using two load method is also studied [29]. Volume of the Expansion

chamber is kept constant for all the modeling and designing work. It was observed that with increase in the expansion ratio the average transmission loss increases.

Some authors have also worked to found out the effect of various positioning of inlet and outlet duct on the sound transmission loss [30]. The transmission loss improved by increasing the offset distance of outlet radially from central position. Maximum transmission loss occurred when inlet and outlet are 900 offset with each other.

It was observed that number of holes and size of holes in the perforated tube affects the transmission loss of muffler. Larger diameter of holes lowers the backpressure and the transmission loss. Also with increase in the length of the perforated tube transmission loss increases [31].

Panigrahi and Munjal [32] discussed some techniques with reference to a few novel muffler configurations, sudden area expansion and contraction, and the crossflow expansion and contraction, of reactive automotive mufflers in order to reduce the backpressure. The analysis is carried out with the Computational Fluid Dynamics (CFD) based commercial software FLUENT9, 10. The 3-D acoustic performance analysis (axial transmission loss evaluation) of the mufflers is performed using SYSNOISE11, a finite element (FE) method based commercial software. Empirical expressions have been derived for the pressure drop in each of these four cases in terms of the most significantly affecting parameter. These expressions have been derived in such a way that they can be used to evaluate the pressure drop of more complex muffler systems where these elements are used in conjunction.

Lian-yun LIU et al. [33] proposed a multidimensional CFD approach for transfer matrix calculation of six acoustic loads, four straight pipes and two expansion chambers. They were simulated as 2D axisymmetric CFD models. The absorptive material, heat transfer, and mean flow effects are also taken into account. Also the exhaust noise with one of the loads and the exhaust muffler installed was predicted based on Thevenin's theorem.

An approach for modelling glass wool is also presented [34]. The glass wool is modelled as a porous domain and performed CFD analysis on a muffler in both cases with and without glass wool to show the percentage deviation with the experimental data. To reduce prototype cost and design process Porous coefficients of glass wool, was calculated from 1D simulation (e.g. WAVE) instead of experimental data.

Two different models of a muffler that are designed for the engine output of a light commercial vehicle's diesel engine are analyzed [35]. The models were constructed in CATIA and analyzed in ANSYS FLUENT 14.5. After the construction of exhaust muffler model in CATIA it is analyzed in ANSYS FLUENT 14.5. Two types of inlet boundary

conditions, velocity inlet and pressure inlet are considered for carrying out the analysis in FLUENT.

To properly predict the performance of a silencer system, many factors need to be involved in the calculation. Geometrical concerns, absorptive material characteristics, flow effects (turbulence), break out noise, self-generated noise, and source impedance all need to be included in the design calculations of insertion loss (IL). IL values are preferred for most applications as a final design criterion, however, the TL values are still very useful when comparing the performance of one silencer geometry to the next. The methods are applicable only to transmission loss (TL) calculations.

It is very important to note that the method derivations, and their use with the FEM and BEM are based on plane wave propagation sound sources (i.e. the entire face of the inlet section moving in unison) and an anechoic termination. Situations other than these will need to be addressed on a specific basis.

Bilawchuk and Fyfe [36] uses the SYSNOISE ability to perform both FEM and BEM computations in order to compare the virtues of the traditional, the 4-pole and the 3-point method, with both the FEM and BEM approach. In terms of computational time required for solution, the 3-point method was found out to be generally faster than either the traditional or 4-pole methods. Also, the FEM was much faster than the BEM due to the fact that the BEM utilizes a full coefficient matrix when solving, while the FEM coefficient matrix is only sparsely populated.

Tao and Seybert [9] carried out a review of various techniques available for measuring the sound transmission loss of muffler. The methods that are discussed in their work are decomposition method, two source method, and two load method. The results indicated the limitations of the decomposition method in the absence of a good anechoic termination. The decomposition method does not lead to the four-pole parameters of the muffler; these are necessary for predicting the IL of the system.

S. N.Y. Gerges et al. [38] used the transfer matrix method based on the plane wave theory and convective state variables and applied it to the eight different muffler configurations. The experimental measurements for these configurations are compared with the numerical results obtained from the transfer matrix method.

K.S. Andersen [39] showed how the transfer matrix may be extracted using the complex wave amplitudes at two specific points on the inlet side and outlet side, while running only a single simulation at multiple frequencies. 3D simulations in COMSOL of different

muffler configurations are verified by measurements in a flow acoustic test rig using the two source method.

Israel Jorge Cárdenas Nuñez et al. [40] investigated the sound transmission loss of compressor suction muffler using various methodologies and compared it with the results obtained by the experimental method. He also performed finite element analysis on ANSYS, for the acoustical performance of the muffler.

1.5 Research gap

Reviewing various literatures helps in finding out that not much work has been done or published on the acoustic analysis of mufflers using Altair products. As most of the manufactures uses HyperMesh (a Hyperworks product, by Altair) for preprocessing of their product. Therefore, it could prove to be very useful in both ways i.e. faster modelling and simulation, if it is possible to find a tool for flow and acoustic analysis, by Altair itself. Luckily, there is option available in the solvers AcuSolve and OptiStruct (another Hyperworks product, by Altair). OptiStruct which is a structural solver has capability for the acoustical analysis and it is less costly as compared to the various other commercially available software packages for acoustics and AcuSolve is one of the best CFD tool available in market.

Therefore, it would be first of its kind & also a good alternative if the setup for the problem, FLOW AND ACOUSTIC ANALYSIS OF TWO WHEELER MUFFLERS can be made using only the Altair products.

1.6 Objectives of the research

The main objective of the present study is to build a three dimensional finite element approach (3D-FEM) for a sample muffler, to study its flow and acoustic attenuation

performance. The details of the objectives are as follows:

- Create three dimensional model of the concept muffler of a two wheeler using NX (an integrated product design, engineering and manufacturing solution by Siemens)
- Perform a fluid flow analysis using Computational Fluid Dynamics (CFD) solver, AcuSolve for velocity, pressure and temperature inside the muffler.
- Harmonic acoustic analysis using OptiStruct solver, to get the sound pressure values inside the muffler and to carry out calculation for the acoustic performance parameter, transmission loss (TL).

- Validation of the acoustic analysis results (OptiStruct) for the different muffler configurations.
- Comparison of the flow & acoustic results of the concept muffler with the ANSYS and experimental data respectively.

CHAPTER 2
THEORY OF MUFFLERS

Due to increased environmental concerns requiring less noise emissions combined with reduced emission of harmful gases, it is becoming very crucial to carefully design the exhaust system mufflers for road transport applications. Maximum acoustic performance is usually desired under the limit of space constraints. Today, a significant part of the available space is also used by so called after treatment devices, i.e., devices used for emission control of harmful gases. This has increased the complexity of the design task and created a need for more advanced design approaches such as optimization which requires a better understanding of the flow and acoustic behavior of muffler.

2.1 Flow through muffler

Muffler could lead to a decline of engine power and economy caused by the exhaust resistance while reducing noise. Increasing competition between manufacturers necessitates having being reduced weight, having capability of higher sound absorption and lower back pressure mufflers. Lightness could be possible if the thickness is decreased or the volume is reduced. However, this causes high back pressure. Therefore, the optimum design requires.

In two stroke engines, which use the crankcase as a scavenging pump, the dynamic effect plays a fundamental role in filling the cylinder with fresh charge. Every time the exhaust flow meets a section increase, a negative pressure is generated and propagates in the opposite direction of flow with the speed of sound. On the other hand, if the flow finds a restricted section, a positive pressure wave always propagates in the opposite direction with the speed of sound.

Backpressure has a significant effect on performance of two stroke engine. The pressure in two-stroke engine can be considered atmospheric when the cylinder filling (scavenging) is superimposed to the exhaust phase, i.e., with the exhaust port opened to the external atmosphere. The effectiveness of the cylinder filling with fresh charge depends on small differences of pressure, and the two stroke engine can only tolerate small amounts of exhaust back pressure.

In four stroke engines the most obvious effect is the increase in size of the pumping loop as

the backpressure increases, due to the extra work done by the piston on the gas in pumping it out of the cylinder during the exhaust stroke
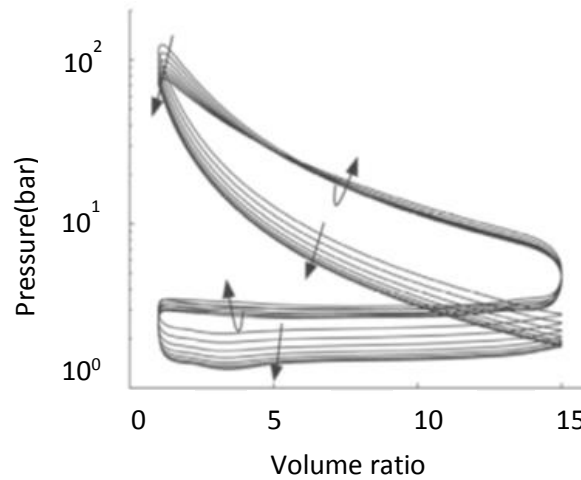
Fig 2.1: The P-V diagram of a cylinder for various backpressure. Arrows shows direction of change with increasing backpressure

This represents the extra work that must be done by the engine as the backpressure increases, in addition to meeting the constant load demand. Although the maximum cycle pressure decreases due to the reduced compressor pressure ratio, the engine pressure ratio remains effectively constant. The gradient of the power stroke curve also decreases with increased back pressure. This is due to the increase in the burn duration that occurs with reduced maximum cylinder pressure. Thus, excessive backpressure can adversely affect performance, resulting in reduced power and increased fuel consumption, exhaust temperatures and emissions. Also it is imperative that exhaust backpressure is kept within specified limits for those engines subject to emissions legislation.

The power P delivered by the engine and absorbed by the dynamometer is directly proportional to the volumetric efficiency. From the definitions of engine power, mean effective pressure, and fuel conversion efficiency, and fuel air ratio, and volumetric efficiency, the following relationships between engine performance parameters can be developed for power P [12]:

$$P = \frac{n_f \; m_a \; N \; Q_{Hv} \; (F/A)}{n_R} \tag{2-1}$$

From this relation it can be seen that as the volumetric efficiency increases the power available at the crankshaft increases.

An ideal muffler for a reciprocating internal combustion engine should function as a low pass filter. The steady or mean flow should be allowed to pass unimpeded through the muffler while the fluctuating flow which is associated with the acoustic pressure fluctuation is impeded. If the steady flow is not significantly impeded the so-called 'back pressure' will be very low and the engine will function more efficiently. It is desirable to be able to predict the pressure drop associated with the steady flow through the muffler. Perforated tubes are commonly used inside automotive mufflers. They can be found in the form of perforated tubes to confine the mean flow in order to reduce the back-pressure to the engine

On the other hand, if the flow is forced through the perforations, this provides a significant back pressure on the engine. Being able to theoretically model perforated mufflers enables car manufacturers to optimize their performance and increase their efficiency in attenuating engine noise, and at the same time to minimize the back pressure exerted on the engine

The burning gases enters with high temperature at inlet pipe, the heat is dissipating on the muffler structure and exit with an average temperature of 50°C. At inlet pipe the burning gases have a high pressure which decreases with the recirculation of the gases through the perforated pipes of the exhaust muffler.

Silencer's performance is mainly dependent on the values of backpressure. Pressure drop of exhaust system includes losses due to piping, silencer, and termination. High backpressure can cause a decrease in engine efficiency or increase in fuel consumption, overheating, and may result in a complete shutdown of the engine potentially causing significant damage.

2.1.1 Pressure Drop Considerations

Mean flow through the muffler passages encounters a drop in its stagnation pressure. The engine or fan source must push the gases or air against this back pressure. This results in pumping losses in the engine power output. When back pressure is high, it results in a drop in volumetric efficiency, which in turn would result in a further loss in engine shaft power and an increase in the specific fuel consumption (SFC) of the engine. In the case of a fan, the power load on the motor is proportional to the product of the flow rate Q and total pressure drop, Δp.

The latter is the sum of the pressure drops in the intake system and discharge/exhaust system. Thus, electrical power consumption of a fan motor is directly proportional to the total back pressure experienced by the fan. Therefore, prediction and minimization of the stagnation pressure drop across mufflers (or silencers) is an integral part of the discipline of analysis and design of mufflers.

Two primary mechanisms of the stagnation pressure drop are wall friction in the boundary layer, and eddy and vortex formation in the free shear layer at area discontinuities and perforated sections.

Pressure drop can be normalized in terms of dynamic head, H. Thus,

$$\Delta p = K \cdot H \qquad\qquad H \equiv \frac{1}{2}\rho_o U^2 \qquad\qquad (2\text{-}2)$$

Here, K is called the dynamic pressure loss factor or coefficient. Empirical expressions of K for different muffler elements with turbulent mean flow are given below

Pressure loss factor for turbulent flow through a pipe or duct of length l_p and (hydraulic) diameter d_p (Fig. 2.2):
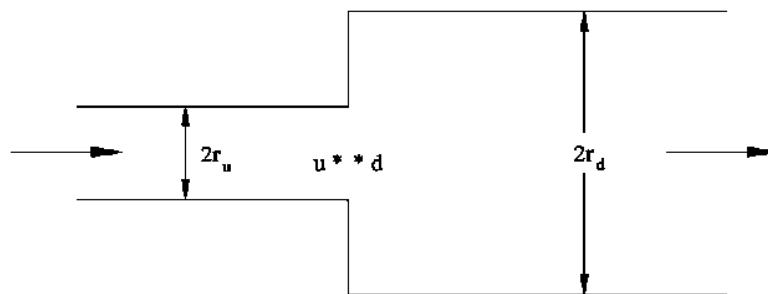
Fig 2.2: Sudden expansion

$$K \equiv \frac{\Delta p}{H} = F \cdot \frac{l_p}{d_p} \qquad\qquad (2\text{-}3)$$

where F is the Froude's friction factor given by

$$F = 0.0072 + 0.612 / R_e^{0.35} \quad , \quad R_e < 4 \times 10^5 \qquad\qquad (2\text{-}4)$$

$R_e = U d_p \rho_o / \mu$ is the Reynold's number, and μ and ρ_o are the coefficient of dynamic viscosity and mass density, respectively

21

Typically, $F \simeq 0.016$ for the mild steel pipes used in exhaust mufflers. However, roughness of fiberglass-lined pipes is much more than that of the normal unlined rigid pipes, and therefore, $F \simeq 0.032$ for the lined pipes as well as the perforated unlined pipes, as in a concentric tube resonator (Fig. 2.3).
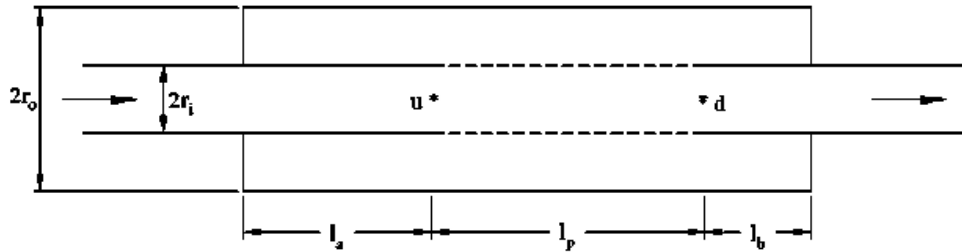
Fig 2.3: Concentric tube resonator

Pressure loss factor for a sudden contraction (Fig. 2.4):
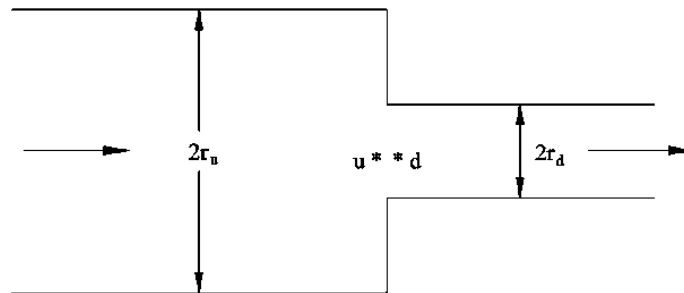
Fig 2.4: Sudden contraction

$$K \simeq (1 - n)/2, \qquad n = (r_d/r_u)^2 \qquad (2\text{-}5)$$

Pressure loss factor for a sudden expansion (Fig. 2.5):
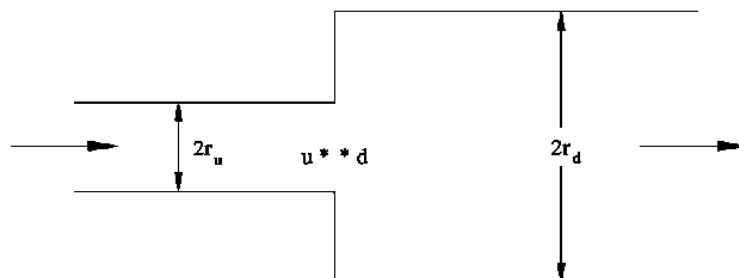
Fig 2.5: Sudden expansion

$$K \simeq (1 - n)^2, \qquad n = (r_u/r_d)^2 \qquad (2\text{-}6)$$

22

Note that for both the sudden area discontinuities, n is defined as ratio of cross-section of the narrower pipe to that of the wider pipe. Thus, n is less than unity in both Eqs. (2-5) and (2-6).

Pressure loss factor for extended outlet (Fig. 2.6), extended inlet (Fig. 2.7), and flow reversal with contraction or expansion (Fig. 2.8):
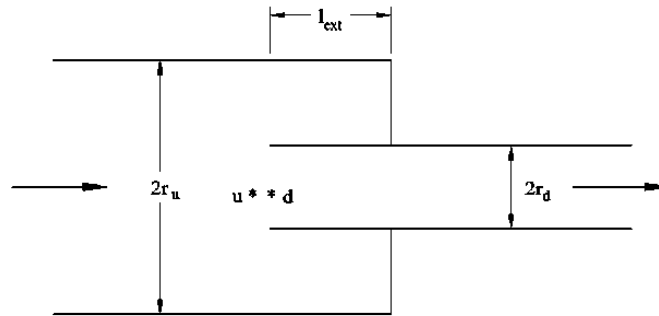
Fig 2.6: Extended outlet
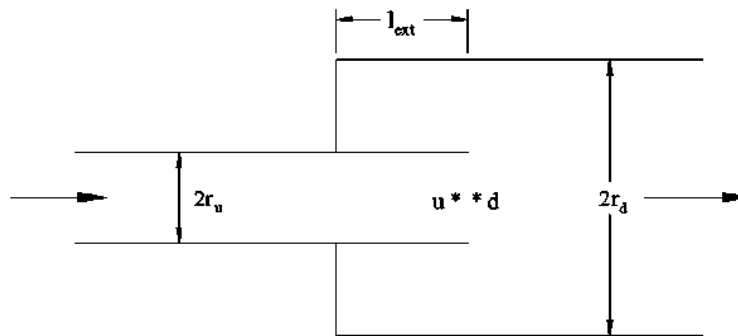
Fig 2.7: Extended inlet
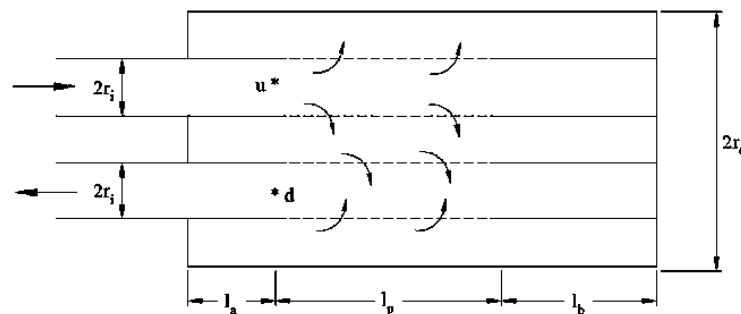
Fig 2.8: Reversed flow, three duct, closed - end element

$$K \simeq 1.0 \qquad (2\text{-}7)$$

Pressure loss factors for bell mouth, gradual contraction, gradual expansion, etc. are much lower than those for the corresponding sudden or step area changes. However, gradual area changes lead to poor TL and therefore are not always desirable.

Pressure loss coefficient of the plug muffler (Fig. 2.9):
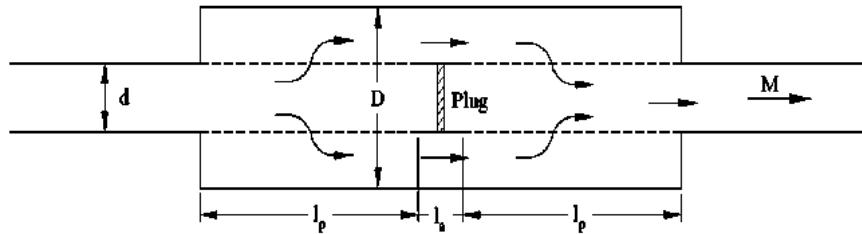
Fig 2.9: Plug muffler

$$K = 5.6e^{-0.23x} + 67.3^{-3.05x}, \quad 0.25 < x < 1.4 \tag{2-8}$$

Where x is the open-area ratio of the cross-flow expansion (Fig. 2.10) and cross-flow contraction (Fig. 2.11), assumed to be equal. The open-area ratio is defined by

$$\text{Open area ratio, } X = \frac{2\pi r_1 l_p \sigma}{\pi r_1^2} = \frac{2l_p \sigma}{r_1} \tag{2-9}$$

Where σ is the porosity of each of the two perforated sections
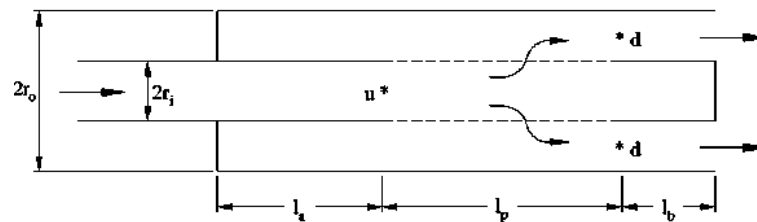
Fig 2.10: Cross flow expansion
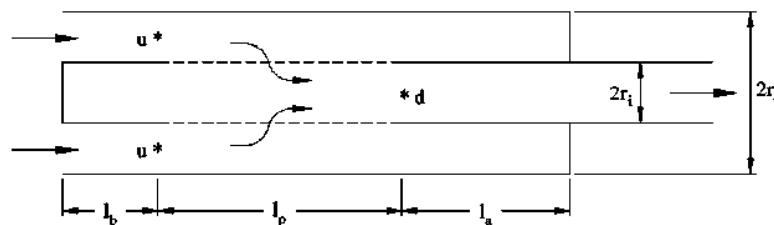
Fig 2.11: Cross flow contraction

Pressure loss coefficient of the muffler element with three interacting ducts (Fig. 2.12):
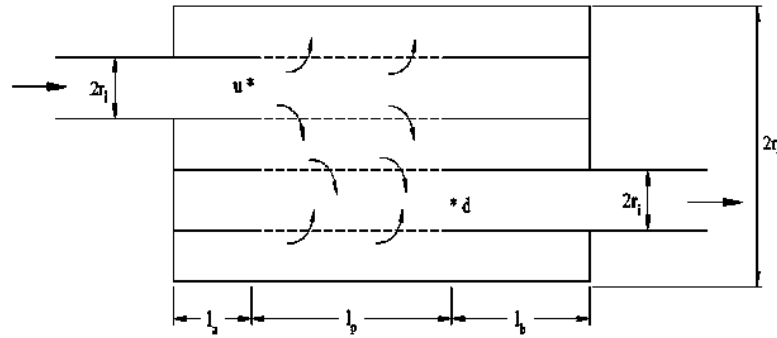
Fig 2.12: Cross flow, three duct, closed-end element

$$K = 4.2e^{-0.06x} + 16.7e^{-2.03x} \qquad (2\text{-}10)$$

By contrast, pressure loss coefficient of a concentric tube resonator (Fig. 2.3) is as small as

$$K = 0.06x \qquad (2\text{-}11)$$

Where x is the open-area ratio defined by Eq. (5.62).

2.1.2 Expansion chamber elements having influence on backpressure

A conventional muffler of internal combustion engine is mostly constructed as a mixture or combination of perforated ducts, baffle or perforated baffle, expansion chamber, etc.,

2.1.2.1 Head pipe or the Inlet Pipe

In general, a longer head pipe will bring about more bottom-end power at the cost of peak power. A small head pipe generally brings stronger peak power and subtracts bottom-end. Practically tapered head pipes are relatively more difficult to manufacture and costly too, so they are rare in conventional vehicles. Tapered head pipes have proven to boost performance and relatively ease pipe tuning in their main area of influence.

2.1.2.2 Convergent and Divergent Cones

The length, volume and taper of the divergent cone strongly influence the amount of peak power. A relatively short, steeply tapered, divergent cone creates high peak power. What happens after an engine's power peaks is nearly as important as the peak itself? Controlling power after the peak i.e. the overrun is the divergent cone's job. A relatively longer, gently tapered final cone will give more overrun. A short, steep final cone gives less.

2.1.2.3 Straight Section

The length or volume adjustments are compensated for "ideal" head pipe, divergent cone,

and convergent cone and tailpiece/silencer dimensions at the pipes mid-section. The pipe's straight section can be enlarged, shortened or lengthened to bring about the same results like "ideal" designs.
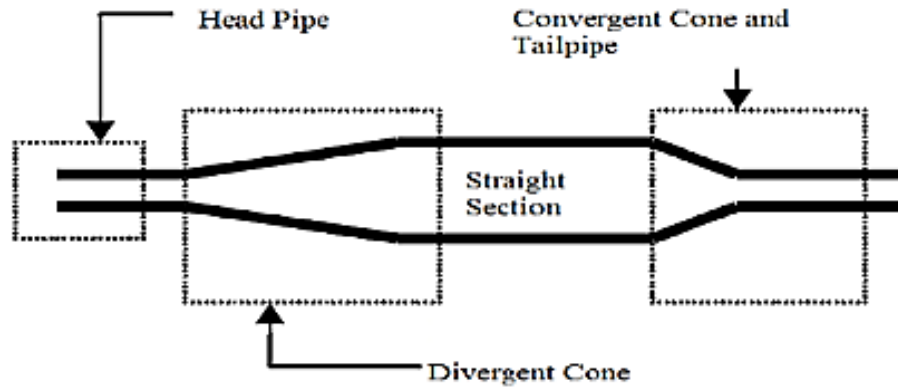
Fig 2.13: Components of an expansion chamber

2.1.2.4 The Tailpiece or Outlet Pipe

Tailpiece size and its length influences peak power and bottom-end, and can even affect an engine's resistance to pistons. In general, smaller tailpiece diameters create more peak horsepower but increase the occurrence of thermal breakdown because it accumulates the exhaust heat. Big tailpiece diameters increase bottom-end at the cost of peak power and excessively large tailpiece diameters can reduce performance at all engine speeds due to insufficient back pressure. Tailpiece length is also important, because it is the part of the total pipe length and volume. Generally, longer tailpiece is used when low and midrange power is required. The tailpipe itself acts as a resonant cavity that couples with the muffler cavity. The noise reduction capability of a muffler gets changed, if designed tail piece is not used.

2.1.2.5 Perforations on Internal connecting tubes or cross flow perforated tube

The most critical component regarding backpressure of any commercial muffler is cross flow perforated tube. The diameter and porosity of the perforations are most critical. A smaller hole diameter but higher porosity creates high peak power with acceptable backpressure value. While a larger hole diameters with higher porosity reduce performance due to insufficient back pressure. Sound energy gets dissipated considerably while moving through the perforations and it adds to the total attenuation in perforated tubes

The most critical component regarding backpressure of any commercial muffler is cross flow perforated tube in which the diameter of the perforated tube hole and porosity of the perforations are most critical.

Varying the porosity of the muffler has pronounced effect on the backpressure. The Backpressure is reduced greatly if the porosity is doubled. Also if the diameter of the hole is increased the backpressure decreases sharply. The change in diameter of holes has remarkable effect. There is sharp change in backpressure values even if hole diameter is slightly changed.

2.2 Noise & Acoustics

A popular definition of noise is, "an undesirable sound". To what extent a sound can be characterized as noise is, of course, a personal evaluation. However, if the sound level is so high as to be damaging to health, it will normally be considered by one and all as undesirable and, therefore, as noise.

Noise reduction is one of the highest prior target for IC engine development because of the stricter engine noise limits. The Ministry of Environment and Forests (MOEF) of the Government of India, on the advice of the National Committee for Noise Pollution Control (NCNPC) has been issuing Gazette Notifications prescribing noise limits as well as rules for regulation and control of noise pollution in the urban environment.

Internal combustion engine noise has been drawing significant attention from automotive manufacturers. This noise pollution level can be greater than 80 dB which is injurious for human ears. To effectively reduce the noise level of a diesel engine the first step is the identification of different engine noise sources.

An IC engine noise signal is composed of many components from different sources. The overall noise produced by an automobile is a contribution from the different sources which are classified as under.

2.2.1 Classification by noise characteristics

One typical engine noise classification technique separates the aerodynamic noise, combustion noise and mechanical noise.

1. Aerodynamic noise
2. Combustion noise
3. Mechanical noise

2.2.1.1 Aerodynamic noise

Aerodynamic noise includes exhaust gas and intake air noise as well as noise generated by cooling fans, auxiliary fans or any other air flow.

2.2.1.2 Combustion noise

Combustion noise refers to noise generated by the vibrating surfaces of the engine structure, engine components and engine accessories after excitation by combustion forces.

The combustion noise is produced by a rapid rate of pressure rise, which besides being a source of engine structural vibrations also excites resonance in the gas inside a combustion chamber cavity. The latter is also a source of vibration and noise. The contribution of the combustion to the whole noise signal is some transient components. In abnormal condition, the combustion noise is mostly in a frequency range above a few 100 hertz as the combustion energy below this range is mostly transformed into useful work by pushing pistons forward. In the case of abnormal conditions, degradation in the combustion quality may produce some low frequency content in the combustion noise. A rise in the cylinder pressure pushes the piston from the top dead center advancing to the bottom dead center. In this movement, the clearance between the piston and the cylinder or damage to piston rings can cause the piston to impact with the cylinder, the phenomenon of piston slap, which is another major source of engine noises. As

the piston slap is caused by both the combustion and the clearance, the noise level reflects the combustion quality and changes in the clearance.

2.2.1.3 Mechanical noise

Mechanical noise refers to noise generated by the vibrating surfaces of the engine components and engine accessories after excitation by reciprocating or rotating engine components.

2.2.2 Classification by engine noise sources

2.2.2.1 Exhaust system noise

Exhaust system noise includes the noise from exhaust gas pulses leaves the muffler or tail pipe and noise emitted from the vibrating surfaces of the exhaust system components. Noise emitted from the surfaces of exhaust system components results from two different types of excitation forces: those generated by the pulsating exhaust gas flow and those transmitted from the vibrating engine to exhaust system components. Additional considerations in the reduction of exhaust system noise include proper selection of piping lengths and diameters, proper mounting of exhaust system components and proper positioning of the exhaust outlet.

2.2.2.2 Intake system noise

Intake system noise includes noise generated by the flow of air through the systems air inlet and noise emitted from the vibrating surface components. As with exhaust systems surface radiated noise results from two different types of excitation process: those generated by the pulsating intake air flow and those transmitted from the vibrating engine to intake system components. In many instances, an engines air cleaner will provide significant attenuation of intake air noise. If additional attenuation is required, an intake air silencer can be added to the system. To minimize intake system surface radiated noise, proper design, selection and mounting of intake system components are essential.

Intake noise generated by interruption of airflow at inlet valves transmitted via air cleaner radiated by air duct.

2.2.2.3 Cooling system noise

Water cooled engines are typically cooled by using a radiator as a heat exchanger – with an axial flow fan is used to draw cooling air through the radiator. Air-cooled engines generally use a centrifugal fan in conjunction with shrouding to direct cooling air across the engine. Fan noise consists of both discrete frequency tones and broadband noise. The broadband components of fan noise are caused by the shedding of vortices from the rotating fan blades and by turbulence in the fans air stream.

Cooling fan noise this results from the sound of air being moved at high speed across the engine and through the radiator.

2.2.2.4 Engine surface radiated noise

Noise produced due to the vibration of the engine surface radiated through the atmosphere.

2.2.3 Basics of acoustics

Sound waves constitute alternate compression and rarefaction pulses travelling in the medium. It is the result of mechanical vibrations occurring in an elastic medium e.g. air. When the air starts to pulsate, the variations in air pressure will spread from the source through the transfer of energy from molecule to molecule. The more energy transferred, the higher the sound level.
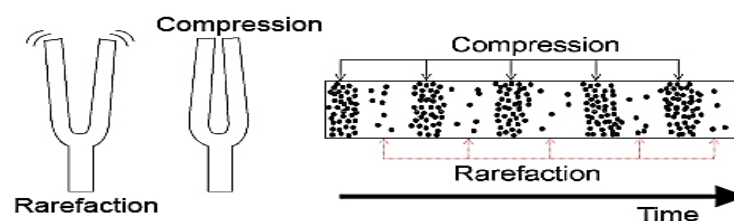
Fig 2.14: Sound propagation phenomenon

As the vibrating surface moves to the right, the fluid adjacent to the surface is compressed. This compression effect moves outward from the vibrating surface as a sound wave. Similarly, as the surface moves toward the left, the fluid next to the surface is rarefied. The vibratory motion of the solid surface causes pressure variations above and below the fluid bulk pressure (atmospheric pressure, in many cases) to be transmitted into the surrounding fluid.

However, sound is audible only if the frequency of alteration of pressure is between 20 Hz to 20,000 Hz. These limits are subjective and may vary slightly from person to person. An average human ear is not able to detect disturbance in the medium if the frequency is outside this range.

The, waves with frequency below the audible range are called infrasonic waves and the waves with frequency above the audible range are called ultrasonic waves. The compression and rarefaction in a sound wave is caused due to the back and forth motion of the particles of the medium. This motion is along the direction of propagation of sound and hence the sound waves are longitudinal.

A longitudinal wave in a fluid (liquid or gas) can be described either in terms of the longitudinal displacement suffered by the particles of the medium or in terms of the excess pressure generated due to the compression or rarefaction

All directions, perpendicular to the direction of propagation, are equivalent and hence, a sound wave cannot be polarized.

The surface through the points, having the same phase of disturbance, is called a wave front. For a homogeneous and isotropic medium, the wave fronts are normal to the direction of propagation. For a point source placed in a homogeneous anisotropic medium, the wave fronts are spherical and the wave is called a spherical wave. If sound is produced by vibrating a large plane sheet, the disturbance produced in front of the sheet will have the same phase on a plane parallel to the sheet. The wave fronts are then planes (neglecting the end effects) and the direction of propagation is perpendicular to these planes. Such waves are called plane waves.

Sound requires a medium for its propagation and its speed varies accordingly depending on the material medium. The following table gives an idea of, speed of sound, in various substances.

Table2.1: Speed of sound in various substances (CRC Handbook)

GASSES(0°C)	Substance	Speed of sound(*m/s*)
	Carbon dioxide	259
	Hydrogen	1284
	Helium	965
	Nitrogen	334
	Oxygen	316
	Air (21% Oxygen,78% Nitrogen)	331
	Air (20°C)	344
LIQUIDS(25°C)	Glycerol	1904
	Sea water (3.5% salinity)	1535
	Water	1493
	Mercury	1450
	Kerosene	1324
	Methyl Alcohol	1103
	Carbon Tetrachloride	926
SOLIDS	Diamond	12000
	Pyrex glass	5640
	Iron	5960
	Granite	6000
	Aluminium	5100
	Brass	4700
	Copper(annealed)	4760
	Gold	3240
	Lead (annealed)	2160
	Rubber (gum)	1550

The wavelength and speed of sound for a simple harmonic wave are related by:

$$\lambda = {}^{c}/_{f} \qquad (2\text{-}12)$$

Another parameter that is encountered in analysis of sound waves is the *wave number (k),* which is defined by

$$k = \frac{2\pi}{\lambda} = \frac{2\pi f}{c} \qquad (2\text{-}13)$$

2.2.3.1 Acoustic pressure and particle velocity

The ***acoustic pressure (p)*** is defined as the instantaneous difference between the local pressure (p) and the ambient pressure (p_o) for a sound wave in the material. The acoustic pressure for a plane simple harmonic sound wave moving in the positive x-direction may be represented by the following.

$$p(x,t) = p_{max} \sin(2\pi ft - kx) \qquad (2\text{-}14)$$

The quantity p_{max} is the amplitude of the acoustic pressure wave.

Acoustic instruments, such as a sound level meter, generally do not measure the amplitude of the acoustic pressure wave; instead, these instruments measure the root-mean-square (rms) pressure, which is proportional to the amplitude. The relation between the pressure wave amplitude and the rms pressure is demonstrated in the following.

Suppose we define the variable $\theta = 2\pi t/\tau$, so $d\theta = 2\pi\, dt/\tau$. The rms pressure is defined as the square root of the average of the square of the instantaneous acoustic pressure over one period of vibration τ:

$$(p_{rms})^2 = \frac{1}{\tau} \int_0^\tau p^2(x,t)\, dt = \frac{(p_{max})^2}{2\pi} \int_0^{2\pi} \sin^2(\theta - kx)\, d\theta \qquad (2\text{-}15)$$

Carrying out the integration, we find:

$$(p_{rms})^2 = \frac{(p_{max})^2}{2\pi} [\frac{1}{2}(\theta - kx) - \frac{1}{4}\sin(2\theta - 2kx)]_0^{2\pi} \qquad (2\text{-}16)$$

$$(p_{rms})^2 = \frac{1}{2}(p_{max})^2 \qquad (2\text{-}17)$$

The rms pressure is related to the pressure amplitude for a simple harmonic wave by:

$$p_{rms} = \frac{p_{max}}{\sqrt{2}} \qquad (2\text{-}18)$$

The rms pressure is defined as the square root of the average of the square of the instantaneous acoustic pressure over one period of vibration τ:

The instantaneous *acoustic particle velocity (u)* is defined as the local motion of particles of fluid as a sound wave passes through the material. The rms acoustic particle velocity is the quantity used in engineering analysis, because it is the quantity relevant to energy and intensity measurements.

The rms acoustic pressure and the rms acoustic particle velocity are related by the specific acoustic impedance (Z_s):

$$p = Z_s u \qquad (2\text{-}19)$$

The specific acoustic impedance is often expressed in complex notation to display both the magnitude of the pressure–velocity ratio and the phase angle between the pressure and velocity waves. The SI units for specific acoustic impedance are *Pa-s/m*. This combination of units has been given the special name *rayl*, in honor of Lord Rayleigh, who wrote the famous book on acoustics: i.e. $1\ rayl \equiv 1\ Pa\text{-}s/m$

For plane acoustic waves, the specific acoustic impedance is a function of the fluid properties only. The specific acoustic impedance for plane waves is called the characteristic impedance (Z_o) and is given by:

$$Z_o = \rho c / g_c \qquad\qquad (2\text{-}20)$$

(gc is a unit's conversion factor, it is often omitted from equations, and it is assumed that consistent units will be maintained when substituting values in the equations)

Table 2.2: Characteristic impedance of solids, liquids & gases [13]

MATERIAL	Characteristic impedance, Z_O (rayl)
SOLIDS:	
Aluminium(pure)	17.28×10^6
Brass	39.76×10^6
Brick(common)	7.47×10^6
Concrete	7.44×10^6
Copper	43.48×10^6
Glass (window)	15.00×10^6
Glass (Pyrex)	11.96×10^6
Ice	2.94×10^6
Lead	22.47×10^6
Lucite	2.16×10^6
Polyethylene	1.85×10^6
Steel (C1020)	44.58×10^6
Wood (oak)	3.31×10^6
Wood (pine)	3.04×10^6
Zinc	30.49×10^6
LIQUIDS:	
Ethyl alcohol (25ºC)	0.900×10^6
Ethylene glycol (25ºC)	1.808×10^6
Gasoline (25ºC)	0.820×10^6
Kerosene (25ºC)	1.086×10^6
Sea water (20ºC)	1.539×10^6

Water (15ºC)	1.461×10^6
Water (20ºC)	1.481×10^6
Water (25ºC)	1.490×10^6
Water (30ºC)	1.499×10^6
GASES AT 25ºC (77ºF) AND 1 ATM.	
Air	409.8
Ammonia	302.4
Carbon Oxide	484.7
Helium	166.2
Hydrogen	108.5
Methane	293.7
Nitrogen	403.0
Oxygen	429.6
Steam at 100ºC	282.6

2.2.3.2 Acoustic power & Acoustic intensity

The acoustic intensity (I) is defined as the average energy transmitted through a unit area per unit time, or the acoustic power (W) transmitted per unit area.

The total acoustic power radiated by a source, W, can be found by integrating the intensity over a closed hypothetical surface enclosing the source. Thus,

$$W = \oint I \, dS \qquad (2\text{-}21)$$

Wave front or phase surface is a hypothetical surface where all these particles have the same instantaneous velocity. Thus, the total power flux associated with a plane wave in a duct of cross-sectional area S, where the particle velocity u is axial and hence normal to the wave front, would be given by

$$W = S \, \overline{p \cdot u} = \overline{p \cdot v_v} \qquad (2\text{-}22)$$

Where v_v, related to the particle velocity u as

$$v_v \equiv Su \qquad (2\text{-}23)$$

is called the (acoustic) volume velocity,

Defining (acoustic) mass velocity as

$$v = S\rho_o u \qquad (2\text{-}24)$$

one can write acoustic power flux W as

$$W = \frac{1}{\rho_o} \overline{p \cdot v} \qquad (2\text{-}25)$$

$$= \frac{1}{\rho_o} p_{rms} v_{rms} \qquad (2\text{-}26)$$

Use of the mass velocity variable v is preferred in hot exhaust systems. Thus, the two variables adopted in this thesis are acoustic pressure p and acoustic mass velocity v.

For sinusoidal p and v,

$$p = P \, e^{j\omega t} \qquad (2\text{-}27)$$

$$v = V \, e^{j\omega t} \qquad (2\text{-}28)$$

$p_{rms} = P/\sqrt{2}, \qquad v_{rms} = V/\sqrt{2}$, and therefore

$$W = \frac{1}{2\rho_o} (PV) \cos\theta \qquad (2\text{-}29)$$

Where θ is the phase difference between P and V. in the case of reciprocating and rotating machinery, all sound is periodic in nature. As every periodic signal can be looked upon as a Fourier series of sinusoidal signals, the theory of mufflers is developed for sinusoidal signals.

The SI units for acoustic intensity are W/m^2. The conventional units $ft\text{-}lbf /sec\text{-}ft^2$ are not used in acoustic work at the present time. For plane sound waves, as shown in Fig. 2.15, the acoustic intensity is related to the acoustic power and the area (S) by Eq. 2-30:
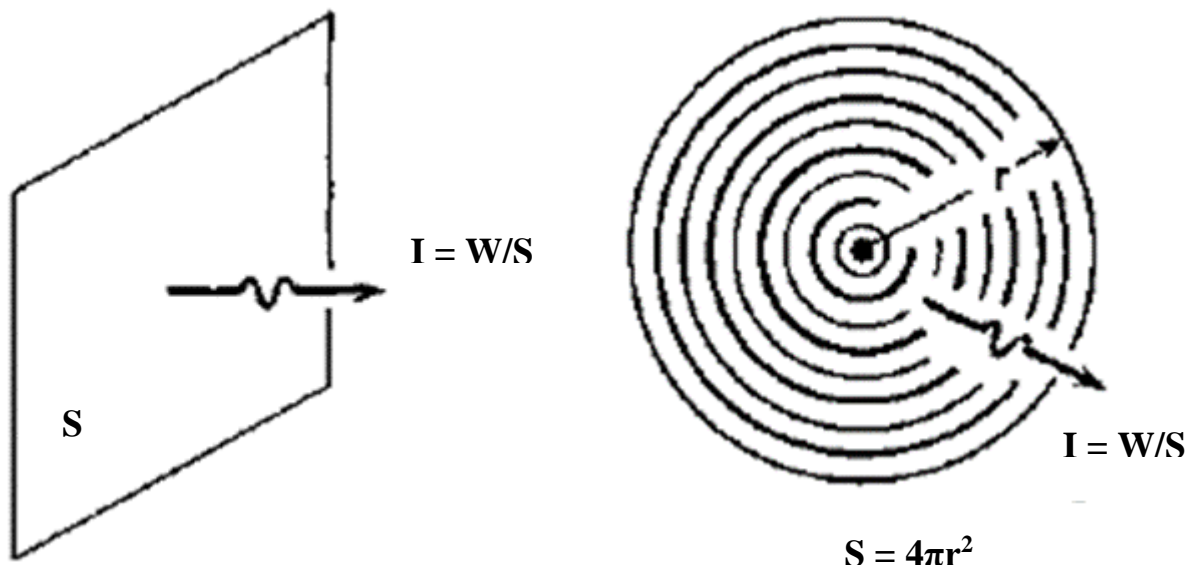
Fig 2.15: Intensity for (A) plane waves and (B) spherical waves

35

Intensity is directional in nature. It is directly proportional to the sound power and inversely proportional to the area. Therefore, if the incident area is more in a particular direction then the sound intensity is more in that direction.

$$I = \frac{W}{S} \tag{2-30}$$

The acoustic intensity may be related to the rms acoustic pressure. The average acoustic power per unit area, averaged over one period for the acoustic wave, is given by:

$$I = \frac{1}{\tau} \int_0^{\tau} p(x,t)\, u(x,t)\, \mathrm{d}t = \frac{1}{2\pi} \int_0^{2\pi} p(x,t)\, u(x,t)\, \mathrm{d}\theta \tag{2-31}$$

Where $\theta = 2\pi f t = (2\pi/\tau)t$. Let us use the following expressions for the acoustic Pressure and acoustic particle velocity for a plane wave:

$$p(x,t) = \sqrt{2}p_{rms}\sin(2\pi t - kx) \tag{2-32}$$

$$u(x,t) = (\sqrt{2}p_{rms}/\rho c)\sin(2\pi t - kx) \tag{2-33}$$

Making these substitutions into Eq. (2-31), we find:

$$I = \frac{1}{2\pi} \int_0^{2\pi} \frac{2(p_{rms})^2}{\rho c}\, sin^2(\theta - kx)\mathrm{d}\theta \tag{2-34}$$

$$I = \frac{2(p_{rms})^2}{2\pi\rho c}\left[\frac{1}{2}(\theta - kx) - \frac{1}{4}\sin(2\theta - 2kx)\right]_0^{2\pi} \tag{2-35}$$

The final expression for the acoustic intensity becomes:

$$I = \frac{p^2}{\rho c} \tag{2-36}$$

where $p = p_{rms}$. We will show that this same expression also applies for a spherical sound waves and for a non-spherical sound wave.

2.2.3.3 Levels and the decibel

The range of the quantities used in acoustics, such as acoustic pressure, intensity, power, and energy density, is quite large. For example, the undamaged human ear can detect sounds having an acoustic pressure as small as20 mPa, and the ear can withstand sounds for a few minutes having a sound

Pressure as large as 20 *Pa*. As a consequence of this wide range of magnitudes, there was an interest in developing a scale that could represent these quantities in a more convenient manner. In addition, it was found that the response of the human ear to sound was more dependent on the ratio of intensity of two different sounds, instead of the difference in intensity. For these reasons, a logarithmic scale called the level scale was defined.

The level of any quantity is defined as the common logarithms to the base 10 of the ratio of an energy-like quantity to a standard reference value of the quantity.

An energy-like quantity (for example, p^2) is used, because energy is a scalar quantity and an additive quantity. This means that all levels may be combined in the same manner, if an energy-like quantity is used.

Although the level is actually a dimensionless quantity, it is given the unit of bel, in honor of Alexander Graham Bell. It is general practice to use the decibel (*dB*), where 1 decibel is equal to 0.1 *bel*.

The level is usually designated by the symbol *L*, with a subscript to denote the quantity described by the level

For example, the acoustic power level is designated by L_w. The acoustic power level is defined by:

$$L_w = 10 \log_{10}(W/W_{ref}) \qquad (2\text{-}37)$$

The factor 10 converts from *bels* to *decibels*. The reference acoustic power W_{ref} is $10^{e\text{-}12}$ *watts* or 1 *pW*.

The sound intensity level and sound energy density level are defined in a similar manner, since both of these quantities (*I* and *D*) are proportional to energy:

$$L_I = 10 \log_{10}(I/I_{ref}) \qquad (2\text{-}38)$$
$$L_D = 10 \log_{10}(D/D_{ref}) \qquad (2\text{-}39)$$

Where the reference quantities are:

$I_{ref} = 10^{-12}$ *W/m²* $= 1pW/m^2$

$D_{ref} = 10^{-12}$ *J/m³* $= 1pJ/m^3$

The reference quantities were not completely arbitrarily selected. At a frequency of 1000 *Hz*, a person with normal hearing can barely hear a sound having an acoustic pressure of

20 *mPa*. For this reason, the reference acoustic pressure was selected as:

$p_{ref} = 20\mu Pa = 20\times10^{-6}\ Pa$

The characteristic impedance for air at ambient temperature and pressure is approximately $Z_o \approx 400\ rayl$. The acoustic intensity corresponding to a sound pressure of 20 *mPa* moving through ambient air is approximately

$I_{ref} = (20\times10^{-6})^2\ /\ (400) = 10^{-12}\ W/m^2$ or *1pW*

The acoustic power corresponding to the reference intensity and a ''unit'' area of $1m^2$ is

$W_{ref} = (10^{-12})\ (1) = 10^{-12}\ W$ or *1pW*

The reference acoustic energy $D_{ref} = 1\ pJ/m^3$ was somewhat arbitrarily selected, because the acoustic energy density for a plane sound wave in ambient air with the reference sound pressure level is approximately 0.003 pJ/m^3.

We note that the acoustic pressure is not proportional to the energy, but instead, p^2 is proportional to the energy (intensity or energy density). For this reason, the sound pressure level is defined by:

$$L_P = 10\log_{10}(p^2/p_{ref}^2) = 20\log_{10}(p/p_{ref}) \qquad (2\text{-}40)$$

Table 2.3: Reference quantities for acoustic levels [13]

Quantities	Definition, dB	Reference
Sound pressure level	$L_p = 10\log_{10}(p/p_{ref})$	$p_{ref} = 20\mu Pa$
Intensity level	$L_I = 10\log_{10}(I/I_{ref})$	$I_{ref} = 1pW/m^2$
Power	$L_W = 10\log_{10}(W/W_{ref})$	$W_{ref} = 1pW$
Energy	$L_E = 10\log_{10}(E/E_{ref})$	$E_{ref} = 1pJ$
Energy density	$L_D = 10\log_{10}(D/D_{ref})$	$D_{ref} = 1pJ/m^3$
Vibratory acceleration level	$L_a = 10\log_{10}(a/a_{ref})$	$a_{ref} = 10\mu m/s^2$
Vibratory velocity level	$L_v = 10\log_{10}(v/v_{ref})$	$v_{ref} = 10nm/s$
Vibratory displacement level	$L_d = 10\log_{10}(d/d_{ref})$	$d_{ref} = 10pm$
Vibratory force level	$L_F = 10\log_{10}(F/F_{ref})$	$F_{ref} = 1\mu m$
Frequency level	$L_{fr} = 10\log_{10}(f/f_{ref})$	$f_{ref} = 1Hz$

2.2.4 Theory of acoustic wave propagation

2.2.4.1 Plane wave theory

For plane wave propagation in a rigid straight pipe of length L, constant cross section S, and transporting a turbulent incompressible mean flow of velocity V (see Fig. 2.16), the sound pressure p and the volume velocity v anywhere in the pipe element can be represented as the sum of left and right traveling waves. The plane wave propagation model is valid when the influence of higher order modes can be neglected. Using the impedance analogy, the sound pressure p and volume velocity v at positions 1 (upstream end) and 2 (downstream end) in Fig. 1 ($x=0$ and $x=L$, respectively) can be related by

$$p_1 = Ap_2 + Bv_2 \tag{2-41}$$

and

$$v_1 = Cp_2 + Dv_2 \tag{2-42}$$
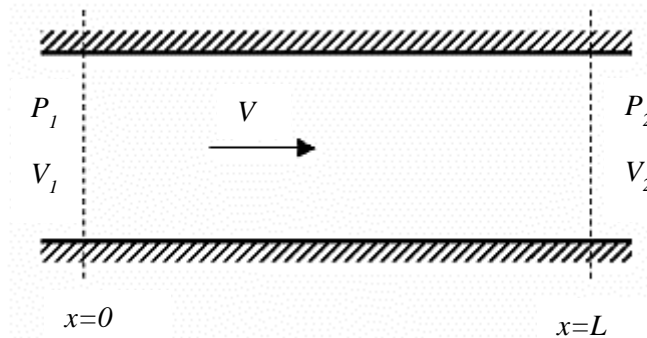
Fig 2.16: Plane wave propagation in a rigid straight pipe transporting a turbulent incompressible mean flow

where A, B, C, and D are usually called the four-pole constants. They are frequency-dependent complex quantities embodying the acoustical properties of the pipe (Pierce, 1981).

A study of propagation of waves is central to the analysis of muffler for its acoustic performance. In a rigid walled tube with sufficiently small cross dimensions (specific limits on the cross dimensions as a function of wavelength are given) filled with a stationary ideal (non-viscous) fluid small amplitude waves travel as plane waves. Therefore, the derivation and solution of the equations derived are based on the theory of plane wave propagation.

In other words, only a plane wave would propagate (all higher modes, even if present, being

cut-off, that is, attenuated exponentially) if the frequency is small enough so that

$$\lambda > 2h \quad or \quad f < \frac{a_o}{2h} \tag{2-43}$$

Where h is the larger of the two dimensions of the rectangular duct,

$k_o r_o = 3.83$. if the frequency is small enough (or wave length is large enough such that)

$$k_o r_o < 1.84, \quad or \quad k_o r_o < 1.84 \quad or \quad f < \frac{1.84}{\pi D} a_o \tag{2-44}$$

Where D is the diameter $2r_o$, then only the plane waves could propagate

Fortunately, the frequencies of interest in exhaust noise of internal combustion engines are low enough so that for typical maximum transverse dimensions of exhaust mufflers Eq. (2-44) is generally satisfied. Therefore, plane wave analysis has proved generally adequate. In the following pages, as indeed in most of the current literature on exhaust mufflers, one-dimensional wave propagation has been used throughout, with only a passing reference to the existence of higher modes or three-dimensional effects.

2.2.4.2 Plane waves in an inviscid stationary medium

In the ideal case of a rigid-walled tube with sufficiently small cross dimensions filled with a stationary ideal (non-viscous) fluid, small-amplitude waves travel as plane waves. The acoustic pressure perturbation (on the ambient static pressure) p and particle velocity u at all pints of a cross section are same. The wave front or phase surface, defined as a surface at all points of which p and u have the same amplitude and phase, is a plane normal to the direction of wave propagation, which in the case of a tube is the longitudinal axis.

The basic linearized equations for the case are:

Mass continuity

$$\rho_o \frac{\partial u}{\partial z} + \frac{\partial \rho}{\partial t} = 0 \tag{2-45}$$

Dynamical equilibrium

$$\rho_o \frac{\partial u}{\partial t} + \frac{\partial \rho}{\partial z} = 0 \tag{2-46}$$

Energy equation (isentropicity)

$$\left(\frac{\partial p}{\partial \rho}\right)_s = \frac{\gamma(p_o + p)}{\rho_o + p} \simeq \frac{\gamma \rho_o}{\rho_o} = a_o^2 \text{(say)}; \tag{2-47}$$

Where z is thee axial or longitudinal coordinate,

p_o and ρ_o are ambient pressure and density of the medium, s is entropy

$p/p_o \ll 1$, $\rho/\rho_o \ll 1$

Eq. (2-47) implies that

$$\rho = \frac{p}{a_o^2}; \qquad \frac{\partial \rho}{\partial t} = \frac{1}{a_o^2}\frac{\partial p}{\partial t}; \qquad \frac{\partial \rho}{\partial z} = \frac{1}{a_o^2}\frac{\partial p}{\partial z} \qquad (2\text{-}48)$$

The equation of dynamical equilibrium is also referred to as momentum equation. Similarly, the equation for mass continuity is commonly called continuity equation.

Substituting Eq. (2-48) in Eq. (2-45) and eliminating u from Eq. (2-45) and Eq. (2-46) by differentiating the first with respect to t, the second with respect to z, and subtracting, yields

$$\left[\frac{\partial^2}{\partial t^2} - a_o^2 \frac{\partial^2}{\partial z^2}\right] p = 0 \qquad (2\text{-}49)$$

This linear, one-dimensional (that is, involving one space coordinate), homogenous partial differential equation with constant coefficients (ao is independent of z and t) admits a general solution:

$$p(z,t) = C_1 f(z - a_o t) + C_2 g(z + a_o t) \qquad (2\text{-}50)$$

If the time dependence is assumed to be of the exponential form $e^{j\omega t}$, then the solution of Eq. (2-50) becomes

$$p(z,t) = C_1 e^{j\omega(t - z/a_o)} + C_2 e^{j\omega(t + z/a_o)} \qquad (2\text{-}51)$$

The first part of this solution equals C_1 at $z = t = 0$ and also at $z = a_o t$. therefore, it represents a progressive wave moving forward unattenuated and unaugmented with a velocity ao. similarly, it can be readily observed that the second part of the solution represents a progressive wave moving in the opposite direction with the same velocity a_o. Thus, a_o is the velocity of wave propagation, Eq. (2-49) is a wave equation, and solution (2-51) represents superposition of two progressive waves with amplitudes C_1 and C_2 moving in opposite directions.

Eq. (2-49) is called the classical one-dimensional wave equation, and the velocity of wave propagation ao is also called phase velocity or sound speed. As acoustic pressure p is linearly related to particle velocity u or, for that matter, velocity potential Φ defined by the relations

$$u = \frac{\partial \Phi}{\partial z}; \qquad p = -\rho_o \frac{\partial \Phi}{\partial t} \tag{2-52}$$

The dependent variable in Eq. (2-49) could as well be u or Φ. In view of this generality, the wave character of Eq. (2-49) lies in the differential operator

$$L \equiv \frac{\partial^2}{\partial t^2} - a_o^2 \frac{\partial^2}{\partial z^2} \tag{2-53}$$

Which is called the classical one-dimensional wave operator

Upon factorizing this wave operator as

$$\frac{\partial^2}{\partial t^2} - a_o^2 \frac{\partial^2}{\partial z^2} = \left(\frac{\partial}{\partial t} + a_o \frac{\partial}{\partial z}\right)\left(\frac{\partial}{\partial t} - a_o \frac{\partial}{\partial z}\right) \tag{2-54}$$

One may realize that the forward-moving wave [the first part of solution (2-50) or (2-51) is the solution of the equation]

$$\frac{\partial p}{\partial t} + a_o \frac{\partial p}{\partial z} = 0 \tag{2-55}$$

And the backward-moving wave [the second part of solution (2-50) or (2-51)] is the solution of the equation

$$\frac{\partial p}{\partial t} - a_o \frac{\partial p}{\partial z} = 0 \tag{2-56}$$

Eq. (2-51) can be rearranged as

$$p(z,t) = [C_1 e^{-jkz} + C_2 e^{+jkz}] e^{j\omega t} \tag{2-57}$$

Where $k = \omega/a_o = 2\pi/\lambda$

k is called the wave number or propagation constant, and λ is the wavelength

As particle velocity u also satisfies the same wave equation, one can write

$$u(z,t) = [C_3 e^{-jkz} + C_4 e^{+jkz}] e^{j\omega t} \tag{2-58}$$

Substituting Eq. (2-57) and Eq. (2-58) in the dynamical equilibrium equation Eq. (2-46) yields

$$C_3 = C_1/\rho_o a_o \qquad \qquad C_4 = -C_2/\rho_o a_o$$

and therefore

$$u(z,t) = \frac{1}{Z_o}(C_1 e^{-jkz} - C_2 e^{+jkz})e^{j\omega t} \qquad (2\text{-}59)$$

Where $Z_o = a_o \rho_o$ is the characteristic impedance of the medium, defined as the ratio of the acoustic pressure and particle velocity of a plane progressive wave.

For a plane wave moving along a tube, one coould also define a volume velocity (=Su) and mass velocity

$$v = \rho_o Su \qquad (2\text{-}60)$$

Where S is the area of cross section of the tube. The corresponding values of charterstic impedance (defined now as the ratio of the acoustic pressure and the said velocity of a plane progressive wave) would then be

$$
\begin{aligned}
&\text{Particle velocity, v:} && \rho_o a_o \\
&\text{Volume velocity, v:} && \rho_o a_o / S \\
&\text{Mass velocity, v:} && a_o / S && (2\text{-}61a)
\end{aligned}
$$

For the later two cases, the characteristic impedance involves the tube area S. As it is not a property of the medium alone, it would be more appropriate to call it characteristic impedance of the tube. For tubes conducting hot gases, it is more appropriate to deal with acoustic mass velocity v. The corresponding characteristic impedance is denoted in these pages by symbol Y for convenience

$$Y_o = a_o / S \qquad (2\text{-}61b)$$

Equations (2-59) and (2-61) yield the following expression for acoustic mass velocity:

$$v(z,t) = \frac{1}{Y_o}(C_1 e^{-jkz} - C_2 e^{+jkz})e^{j\omega t} \qquad (2\text{-}62)$$

Subscript 0 with Y and k indicates nonviscous conditions. Constants C_1 and C_2 in Eqs. (2-57) and (2-62) are to be determined by the boundary conditions imposed by the elements that precede and follow the particular tubular element under investigation.

2.2.4.3 Plane waves in an inviscid moving medium

Wave propagation is due to the combined effect of inertia (mass) and elasticity of the medium, and therefore a wave moves relative to the particles of the medium. When the medium itself is moving with a uniform velocity U, the velocity of wave propagation relative to the medium reamins a. Therefore, relative to a stationary frame of reference (that is, as seen by a stationary observer), the forward wave would move at an absolute velocity

of $U + a$ and the backward moving wave at $U - a$. The waves are said to be convected downstream by mean flow. This is borne out by the following analysis.

Let the medium be moving with a velocity U, the gradients of which in the r direction as well as z direction are negligible. The basic linearized equations for this case are the same as for stationary medium [Eqs. (2-45) -(2-47)] except that the local time derivative $\partial/\partial t$ is replaced by substantial derivative D/Dt, where

$$\frac{D}{Dt} = \frac{\partial}{\partial t} + U\frac{\partial}{\partial z} \tag{2-63}$$

Thus the mass continuity and momentum equations are

$$\rho_o \frac{\partial u}{\partial z} + \frac{D\rho}{Dt} = 0 \tag{2-64}$$

and

$$\rho_o \frac{Du}{Dt} + \frac{\partial\rho}{\partial z} = 0 \tag{2-65}$$

Respectively. The third equation is, of course, the isentropicity relation (2-47).

Eliminating ρ and μ from these three equations yields the convective one-dimensional wave equation

$$\left[\frac{D}{Dt^2} - a_o^2 \frac{\partial^2}{\partial z^2}\right] p = 0 \tag{2-67}$$

Or

$$\frac{\partial^2 p}{\partial t^2} + 2U\frac{\partial^2 p}{\partial z\partial t} + (U^2 - a_o^2)\frac{\partial^2 p}{\partial z^2} = 0 \tag{2-68}$$

Making use of the separation of variables and assuming again a time- dependence function $e^{j\omega t}$, the wave equation (2-68) may be seen to admit the following general solution:

$$p(z, t) = [C_1 e^{-j\omega/(a_o+U)z} + C_2 e^{+j\omega/(a_o-U)z}]e^{j\omega t} \tag{2-69}$$

$$= [C_1 e^{-jk_o z/(1+M)} + C_2 e^{+jk_o z/(1-M)}]e^{j\omega t} \tag{2-70}$$

Writing

$$u(z, t) = [C_3 e^{-jk_o z/(1+M)} + C_4 e^{+jk_o z/(1-M)}]e^{j\omega t} \tag{2-71}$$

Substituting Eqs. (2-70) and (2-71) in eq (2-65) and equating the coefficients of $e^{-jk_o z/(1+M)}$ and $e^{+jk_o z/(1+M)}$ separately to zero yields

$$C_3 = \frac{C_1}{\rho_o a_o} \qquad C_4 = -\frac{C_2}{\rho_o a_o}$$

Thus, acoustic mass velocity v *(z, t)* is given by

$$v(z,t) = \rho_o S u(z,t) = \frac{1}{Y_o}(C_1 e^{-jk_o z/(1+M)} - C_2 e^{+jk_o z/(1-M)})e^{j\omega t} \qquad (2\text{-}72)$$

Where the characteristic impedance Y_o is the same as for stationary medium Eq(2-61b)

Eq. (2-69) indicates(symbolically) the convective effect of mean flow on the two components of the standing waves, as mentioned in the opening paragraph of this section.

2.2.4.4 Mode cut on frequencies, and effects of multidimensional propagation

In a duct exposed to multiple frequencies waves may be travelling in one, two, and three dimensions all at the same time. The low frequency waves will be the most likely to travel in one dimension, while the high frequency waves will be the most likely to travel in three dimensions. This is because the higher the frequency of wave, the smaller the wavelength will be. As mentioned before, when the wavelength is small compared to the duct size the wave will have room to propagate in multiple directions instead of just axially. One dimensional waves and multidimensional waves are shown in the same finite cylinder at different frequencies in Fig. 2.17. Modes 1 and 2 show a one dimensional wave in the cylinder. The pressure is uniform across the cross section of these modes. Modes 10 and 11 both have multidimensional waves present them. The pressure is not uniform across their cross sections. If these cylinders were longer, the patterns seen in the figure would repeat to form a wave pattern in the pipe.

Mode: 001, Frequency: 228 Hz.   Mode: 010, Frequency: 398 Hz

Mode: 002, Frequency: 452 Hz.   Mode: 011, Frequency: 458 Hz
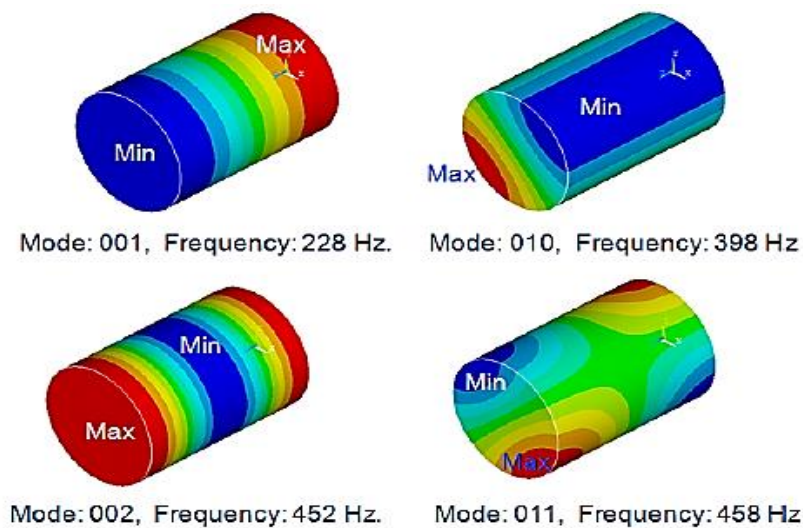
Fig. 2.17: Plane wave and higher order modes

A three dimensional wave can be described by the mode shape in which it is propagating. Each

mode shape has a particular "cut on frequency" above which it is allowed to propagate. To better illustrate this idea, a rectangular duct is considered. For a rectangular duct the cut on frequency is given by

$$f_c = \frac{c}{2\pi}\left[\left(\frac{m\pi}{a}\right)^2 + \left(\frac{n\pi}{b}\right)^2\right]^{0.5}\sqrt{1-M^2} \qquad (2\text{-}73)$$

where f_c is the cut on frequency, c is the speed of sound in the duct medium, M is the Mach number, a and b are the duct dimensions while m and n are the number of cross nodes along the duct dimensions a and b respectively (Fig. 2.18) illustrates the mode shapes for a rectangular duct. In this figure the solid lines represent the walls of the duct while the dotted lines represent the nodal or zero acoustic pressure lines of the waves. The area in between the lines represents the alternating maximum and minimum pressure regions of the wave as denoted by the "+" and the "– "signs respectively.
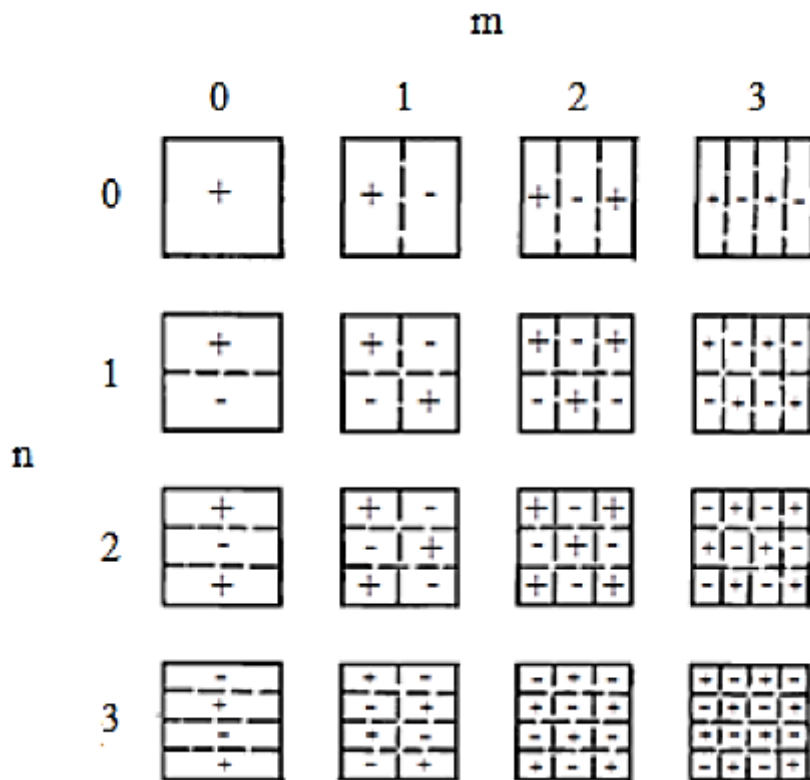
Fig. 2.18: The mode shapes of the first three cut on frequencies for either duct dimension

The cut on frequencies for a circular duct also behave in a similar fashion. The difference being that the diameter is the measurement of interest and instead of cross modes in two

46

directions there are cross modes and radial modes. The cut off frequencies for a circular duct are given by

$$f_c = J_{m,n} \times \frac{c}{\pi D} \sqrt{1 - M^2} \qquad (2\text{-}74)$$

where D is the diameter of the duct, and $J_{m,n}$ is the zero of a Bessel function for the mode of interest, m is the order of the Bessel function and the number of cross nodes and n is the number of radial nodes. The Mach number is the ratio of the flow speed in the duct to the speed of sound ($M=v/c$). This labeling scheme is shown in Fig. 2.19. The Bessel function zero associated with each mode is listed underneath the mode. Plus, and minus signs are added to the antinodes in the first few modes where there was room to do so.
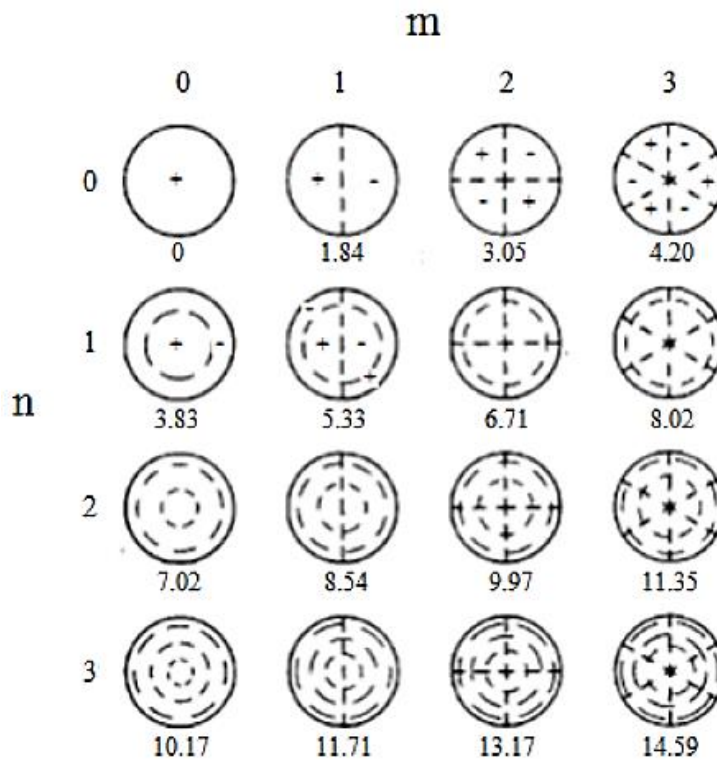
Fig. 2.19: Mode labelling scheme for circular ducts

Each higher order mode traveling in the duct of a muffler can also reach a resonance point, causing the problem of attenuating the noise within the muffler to become even more complex. If these modes are allowed to propagate through and escape the muffler, the performance of the muffler will be drastically compromised. There are two ways in which one of these higher order modes may escape the muffler. The first way is through simple propagation. In this case the muffler and tailpipe are large enough to have one of these modes become excited and propagate through the duct until it escapes. The second way is when the tailpipe and/or the muffler are too small to allow the propagation of a higher order

47

mode that has been excited. When the excited mode reaches a duct region that is too small for it to propagate in, it is attenuated over the course of a wavelength or two. This is the point that the mode becomes evanescent. If the region that does not allow the propagation of the mode, is shorter than a

couple of wavelengths for a given evanescent mode, then the evanescent mode will still escape the muffler without being fully attenuated.

2.2.4.5 Three-dimensional (3-D) wave propagation

The point where the 1-D plane wave theory breaks down is known as the cut-off frequency, f_c. At this frequency, the acoustic pressure waves begin to propagate in dimensions other than along the longitudinal axis. In this scenario, higher order modes need to be accounted for within the state variables. The new governing equation is the 3-D wave equation shown in Equation (2-75).

$$\frac{\partial^2 p}{\partial t^2} - c^2 \nabla^2 p = 0 \tag{2-75}$$

where:

$$\nabla^2 = \frac{\partial^2}{\partial x^2} + \frac{\partial^2}{\partial y^2} + \frac{\partial^2}{\partial z^2} \qquad \text{in cartesian coordinate}$$

$$= \frac{\partial^2}{\partial r^2} + \frac{1}{r}\frac{\partial}{\partial r} + \frac{1}{r^2}\frac{\partial^2}{\partial \theta^2} + \frac{\partial^2}{\partial z^2} \qquad \text{in cylindrical polar coordinate}$$

The acoustic pressure state variable for a cylindrical duct is given by the equation [2]

$$p(r,\theta,z,t) = \sum_{m=0}^{\infty}\sum_{n=0}^{\infty} J_m\left(k_{r,m,n}r\right)e^{jm\theta}$$
$$\left(C_{1,m,n}e^{-jk_{z,m,n}z} + C_{2,m,n}e^{+jk_{z,m,n}z}\right)e^{j\omega t} \tag{2-76}$$

For the acoustic pressure state variable shown in Equation (2-76), $k_{r,m,n}$ represents the radial wave number, k_r, for the (m, n) mode and is shown in Equation (2-77). After calculating $k_{r,m,n}$, the longitudinal transmission wave number, $k_{z,m,n}$, can be calculated as shown in Equation

(2-78). It should be noted that for plane wave propagation, $k_{r,m,n}$ is equal to zero, $k_{z,m,n}$ is equal to k_o and Equation (2-76) becomes Equation (2-57).

$$k_r^2 = k_o^2 - k_z^2 \tag{2-77}$$

$$k_{z,m,n} = \sqrt{k_o^2 - k_{r,m,n}^2} \tag{2-78}$$

The variable, J_m, in Equation (2-76) represents the Bessel function of the first kind of order m. Imposing a zero radial velocity boundary condition at the cylindrical walls require the first derivative of the Bessel function to be equal torero. Higher modes will begin to propagate in a cylindrical duct at a frequency governed by Equation (2-79), where D is the diameter of the cylindrical duct.

$$f = \frac{\alpha_{m,n}c}{\pi D} \qquad for\ m, n\ =\ 0, \infty \qquad (2\text{-}79)$$

The first two roots, $\alpha_{0,1}$ and $\alpha_{1,0}$ of the Bessel Function Derivative have values of 1.841 and 3.832, respectively [2].

By using Equation (2-79) and assuming ambient conditions (where the speed of sound is calculated to be 340 m/s), the cut-on frequency can be determined. The cut-on frequency for the first diametrical and axisymmetric higher order mode effects of a cylindrical tube can be seen in Fig. 2.20. If the inlet and outlet tube are symmetric about the center, then the effects of the diametrical modes will not affect TL.
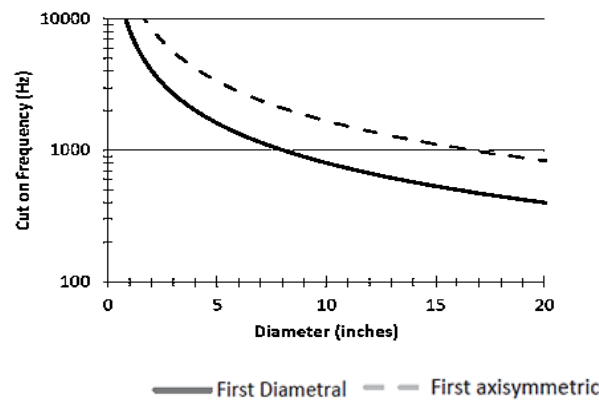
Fig 2.20: The cut on frequency of higher order mode effects in a cylindrical muffler as a function of diameter

2.2.4.6 4-Pole transfer matrix method

The development of the 4-pole method is well known and can be found in almost any textbook on acoustics or silencer design. Time will then be spent in explaining the resulting formulas and how to implement them in a FEM/Remodeling scheme. Using the 4-pole method, a silencer system is evaluated at the inlet and outlet sections by the sound pressure and normal particle velocity (see Fig 2.16) as given by Eq. (2-41) and Eq. (2-42) at positions 1 (upstream end) and 2 (downstream end) i.e. at $x=0$ and $x=L$, respectively

$$p_1 = Ap_2 + Bv_2$$

and

$$v_1 = Cp_2 + Dv_2$$

The corresponding equations (in matrix format) are:

$$\begin{bmatrix} p_1 \\ v_1 \end{bmatrix} = \begin{bmatrix} A & B \\ C & D \end{bmatrix} \begin{bmatrix} p_2 \\ v_2 \end{bmatrix}$$

(2-80)

$$T_1 = \begin{bmatrix} A & B \\ C & D \end{bmatrix}$$

(2-81)

is the *2x2* transfer matrix. This matrix relates the total sound pressure and volume velocity at two points in a muffler element, such as the straight pipe discussed in the previous section. A transfer matrix is a frequency-dependent property of the system. Reciprocity principle requires that the transfer matrix determinant be 1. In addition, for a symmetrical muffler A and D must be identical.

vector of convective state variables p_c and u_c is related to the vector of classical state variables (for stationary medium) p and u by means of the linear transformation.

Let $\{S\} = \{p, u\}^T$ and $\{S_c\} = \{p_c u_c\}^T$. Below, vectors are denoted by braces { } and matrices by brackets [ ]
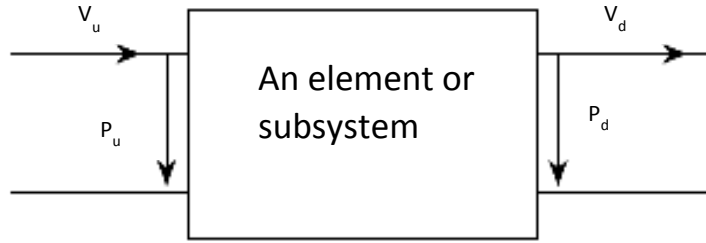
Fig 2.21: upstream and downstream flow parameters of an element

Subscripts u and d denote the upstream end and downstream end respectively of a muffler element, and

$$\{S\}_u = [T]\{S\}_d$$

(2-82)

$$\{S_c\}_u = [T_c]\{S_c\}_d$$

(2-83)

Where [T], [Tc] are transfer matrices for stationary and moving medium respectively, then

$$[T_c] = [C]_u[T][C]_d^{-1}$$

(2-84)

Conversely:

$$[T] = [C]_u^{-1}[T_c][C]_d$$

(2-85)

Where [C] is the transformation matrix:

$$[C] = \begin{bmatrix} 1 & M\underline{Z}_o \\ M/\underline{Z}_o & 1 \end{bmatrix}$$

$\underline{Z}_o = {\rho c}/{S}$ Characteristic impedance

Thus, one can work with classical state variables or convective state variables as per personal preference and skip from one system to the other at the end as necessary.

Fig. 2.22 illustrates the measurement locations for a single expansion chamber silencer
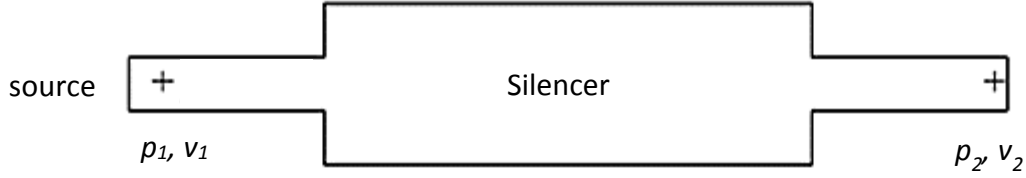
Fig. 2.22: 4-pole transfer matrix method measurement points

Where: p_1 = sound pressure at the inlet, p_2 = sound pressure at the exit, v_1 = normal particle velocity at the inlet, v_2 = normal particle velocity at the exit, and

$$A = (p_1/p_2)|_{v_2=0, \ v_1=1} \qquad\qquad B = (p_1/v_2)|_{p_2=0, \ v_1=1} \qquad \text{(2-86a, b)}$$

$$C = (v_1/p_2)|_{v_2=0, \ v_1=1} \qquad\qquad D = (v_1/v_2)|_{p_2=0, \ v_1=1} \qquad \text{(2-86c, d)}$$

Finally

$$TL = 20 \log_{10} \left(\frac{1}{2} \left| A + \frac{B}{\rho c} + C\rho c + D \right| \right) \qquad\qquad \text{(2-87)}$$

Where, ρc is the characteristic impedance of the acoustic medium.

Once the geometry and environmental conditions (speed of sound and air density) have been set, the next step is to impose the boundary condition of a unit particle velocity at the face of the inlet section ($v_1=1$, $v_2=0$). At this point, the FEM/BEM run can be performed and the values of sound pressure and particle velocity can be determined at the inlet and exit. Parameters A and C can now be calculated using Eqs. (2-86a) and (2-86c) and stored for future use. Next, the second boundary condition of zero pressure at the exit ($v_1=1$, $p_2=0$) can be imposed and the FEM/BEM run is performed again. Once again the pressures and velocities are determined, parameters B and D can be calculated using Eqs. (2-86b) and (2-86d). With all four of the parameters known, the TL can be calculated using Eq. (2-87) at each of the frequencies evaluated. One important item to note is that when the values of p_1 and p_2 are calculated, they will be in complex format. The numbers must remain complex for the duration of the calculations in order to ensure that the phase information is not lost, as would be the case if the complex values were initially converted to absolute values (like when measuring with a real time analyzer).

Another important point to note is that in order to use the 4-pole method, both the pressures

and velocities are required. This does not lend itself to easy verification in a laboratory or fully functioning installation. While acoustic pressures are relatively easy to obtain, the velocities are much more difficult to accurately measure. This is in contrast to the traditional and 3-point methods where only the pressures are required.

Transfer matrix representation is ideally suited for the analysis of cascaded one-dimensional systems like acoustic filters or mufflers. The performance of a muffler may be obtained readily in terms of the four pole parameters or transfer matrix of the entire system, which in turn may be computed by means of successive multiplication of the transfer matrices of the constituent elements.

In practice, there are different elements connected together in a real muffler, as shown in Fig. 2.23. However, the four-pole constants value of each element are not affected by connections to elements upstream or downstream as long as the system elements can be assumed to be linear and passive. So, each element is characterized by one transfer matrix, which depends on its geometry and flow conditions. Therefore, it is necessary to model each element and then to relate all of them to obtain the overall acoustic property of the muffler.
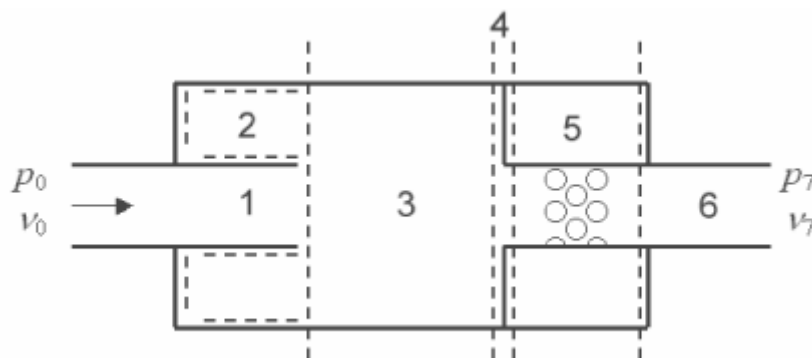
Fig. 2.23: Different elements of a real muffler

If several muffler elements, such as sudden expansions, sudden contractions, extended-tubes and/or perforated tubes are connected together in series, then the overall transfer matrix of the entire system is given by the product of the individual system matrices. For example, the muffler shown in Fig. 2.23 includes a straight extended tube, sudden expansion and extended inlet, uniform tube, sudden contraction, concentric resonator with perforated tube and a straight tail pipe. Then, for this particular muffler we can write

$$q_0 = T_o\, q_1 \tag{2-88}$$

where $q_i = [p_i v_i]^T$, i=1,2 and

Since $q_1 = T_1 q_2$, Eq. (2-88) can be written as

$$q_1 = T_o T_1 q_2 \qquad (2\text{-}89)$$

It is observed that $q_n = T_n q_{n+1}$, for $0 \leq n \leq 6$. Consequently, we obtain the final expression

$$q_0 = T_o T_1 T_2 T_3 T_4 T_5 T_6 q_7 = \prod_{i=0}^{6} T_i q_7 \qquad (2\text{-}90)$$

which relates the pressure and velocity variables at two points (inlet and exhaust) in a muffler.

It can be seen that this matrix formulation is very convenient particularly for use with a digital computer. The only information needed to model any complex muffler are the transfer matrices entries. The four-pole constants (entries for the transfer matrix) can be found easily for simple muffler elements such as straight pipes and expansion chambers.

The four pole constants for Uniform Tube with Flow and Viscous Losses are (Munjal,1975)

$$A = exp(-jMk_cL)cos(k_cL) \qquad (2\text{-}91)$$
$$B = j(\rho c/S)exp(-jMk_cL)sin(k_cL) \qquad (2\text{-}92)$$
$$C = j(S/\rho c)exp(-jMk_cL)sin(k_cL) \qquad (2\text{-}93)$$

and

$$D = exp(-jMk_cL)cos(k_cL) \qquad (2\text{-}94)$$

Where $M=V/c$ is the mean flow Mach number ($M<0.2$), c is the speed of sound (m/s),

$$k_c = k/(1 - M^2)$$

Is the convective wave number (*rad/m*), $k=\omega/c$ is the acoustic wavenumber (*rad/m*), ω is the angular frequency (*rad/s*), ρ is the fluid density (*kg/m³*), and j is the square root of -1. Substitution of *M=0* in Eqs. (2-91) to (2-94) yields the corresponding relationships for stationary medium.

But for a complex element its four-pole constants can take very complicated forms which are not easily determined mathematically. An alternative is to use the finite element method

to obtain numerically each constant (Craggs, 1989).

Fortunately, a large number of transfer matrices have been theoretically developed and reported in the literature. Some of them include the convective effects of a mean flow. Several formulas of transfer matrices of different elements constituting commercial mufflers have been compiled in the book by Munjal (1987) and, more recently, in the book by Mechel (2002). They also included an extensive list of relevant references.

It has to be noticed that, in addition to the geometric characteristics and flow conditions, some transfer matrices depend on additional parameters such as the drop in stagnation pressure and heat conductivity. When using perforate tube elements, the transfer matrices depend on the porosity (number of perforations per unit length of pipe axis) and particularly on the normalized partition impedance of the perforate. This impedance can be evaluated by means of empirical expressions given for different flow conditions, such as stationary medium (Sullivan and Crocker, 1978), perforates with cross-flow (Sullivan, 1979), and perforates with grazing flow (Rao and Munjal, 1986).

2.2.4.7 Muffler performance parameters

The performance of the exhaust system can be characterized in a variety of ways. However, the proper selection of the performance parameter is essential to properly draw conclusions on the overall effectiveness of the exhaust system.

The performance of a muffler is measured in terms of one of the following parameters:

a) Insertion loss, *IL* (easy to measure, difficult to calculate)
b) Transmission loss, *TL* (easy to calculate, difficult to measure)
c) Level difference, *LD* or noise reduction, *NR*
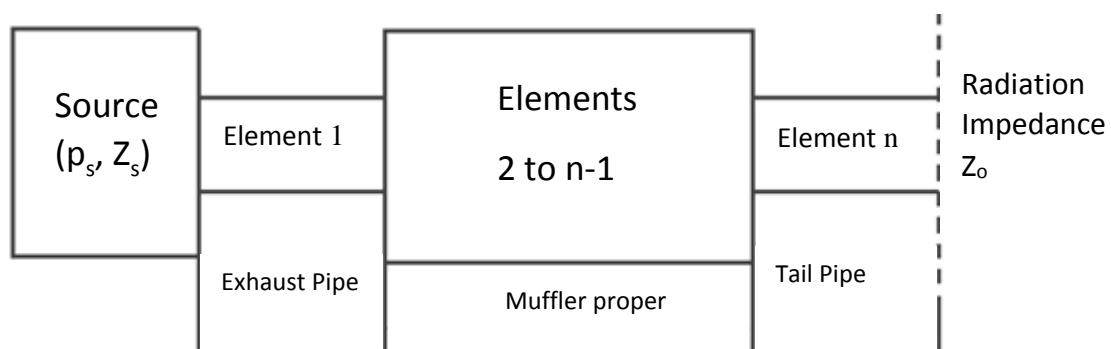
Fig. 2.24: Typical exhaust system

a) Insertion Loss (IL)

As stated previously, Insertion Loss, IL, is the difference in acoustical power of the exhaust system with the muffler attached and then replaced by a straight pipe. The equation of IL can be seen in Equation (2-97). In the equation, L_w is the sound power level in decibels (dB) whereas W is the sound power level in Pascal's (Pa). The subscript 1 represents the straight pipe configuration and subscript 2 represents the muffler configuration.

$$IL = L_{w1} - L_{w2} = 10 \log_{10} \left(\frac{w1}{w2}\right) \qquad \text{(2-97)}$$

The derivation of IL was done by Munjal and can be seen in Equation (2-98) [2]. From the equation, the subscript o represents the location just outside of the tailpipe in the atmosphere and the subscript s represents the source. In the formula, R represents the real or "resistive" part of the characteristic impedance, Z. Assuming that the density of the atmosphere just outside of the tailpipe with and without the muffler installed is relatively constant, the first term in the logarithm is equal to one. Also, it has been shown in the works of Munjal that the real part of the radiation impedance is primarily a function of the tailpipe radius [2]. This allows the second part of the logarithm to equal one. With these assumptions, IL can be reduced to Equation (2-99). The last term, VR, represents the velocity ratio between the source and radiation. As shown in Equation (2-99), with the given assumptions IL becomes a function of the source impedance, the radiation impedance of the straight pipe configuration, and the velocity ratio between the source and the radiation exiting the tailpipe. The velocity ratio is a function of the four-pole parameters of the muffler and the radiation impedance of the muffler configuration to the environment. Due to the required knowledge of source and termination properties, this type of calculation can be very difficult to predict numerically. As a result, IL is much more commonly determined experimentally.

$$IL = 20 \log_{10} \left(\left(\frac{\rho_{rad2}}{\rho_{rad,1}}\right)^{\frac{1}{2}} \left(\frac{R_{rad,1}}{R_{rad,2}}\right)^{\frac{1}{2}} \left|\frac{Z_s}{Z_s + Z_{rad,1}}\right| \left|\frac{v_s}{v_{rad}}\right| \right) \qquad \text{(2-98)}$$

$$IL = 20 \log_{10} \left(\left|\frac{Z_s}{Z_s + Z_{rad,1}}\right| |VR_{s,rad}| \right) \qquad \text{(2-99)}$$

b) Transmission Loss (TL)

Transmission Loss, TL, is the difference in the acoustical power of the forward traveling "incident" pressure wave at the inlet of the muffler to the forward traveling "transmitted" pressure wave at the outlet. Transmission Loss requires an anechoic termination at the

outlet which results in having no reflective waves in the outlet tube. This is not the case in the inlet tube. It will be shown in a later chapter that for experimental analysis having an anechoic termination is unfeasible, thus testing needs to be done in two configurations. The equation for

TL is shown in Equation (2-95) where the subscripts 1 and 2 represent the total measured sound

pressure (including reflective waves) at the inlet and outlet, respectively.

$$TL = 20 \log_{10} \left(\left| \frac{p_{in}}{p_{tr}} \right| \right) + 10 \log_{10} \left(\frac{S_i}{S_o} \right) \tag{2-95}$$

S_i, S_o represent the cross sectional areas of the inlet and outlet, respectively. Usually the cross-sectional area of the inlet and outlet are identical. As a result, the second term in the TL can be removed. Using FEM techniques, this formulation of TL can be very useful. The particle velocity at the inlet can be defined as a known boundary condition (usually a unit vector) and an anechoic termination can be easily modeled. Using the FEM, only a total of two measurement points are required for the calculation of TL. This is not true experimentally as the mass velocity in the inlet tube cannot be determined using a single measurement point. It is also not feasible to recreate an anechoic termination. Thus, experimentally it is ideal to incorporate the 4-pole parameters into the TL calculation. The derivation of TL using the 4-pole parameters was done by Munjal [2]. Making the necessary assumptions that the TL was measured with no temperature gradients, the TL with the 4-pole parameters can be simplified to the equation shown in Equation (2-96) [2].

$$TL = 20 \log_{10} \left(\left| \frac{1}{2} \left[A + \frac{B}{\rho c} + C \rho c + D \right] \right| \right) + 10 \log_{10} \left(\frac{S_i}{S_o} \right) \tag{2-96}$$

c) Level Difference (LD) Noise reduction (NR)

Level Difference is the overall noise reduction of an exhaust system at any arbitrary point in the inlet of the muffler to an arbitrary point in the outlet of the muffler and can be seen in Equation (2-100). Because of its simplicity and as it does not distinguish between transmitted and reflective waves, its usefulness is fairly limited except for comparison purposes.

Unlike the transmission loss, the definition of level difference makes use of standing wave pressures and does not require an anechoic termination.

$$LD/NR = 20 \log_{10}\left(\frac{p_i}{p_o}\right) \qquad (2\text{-}100)$$

2.2.4.8 Comparison of the three performance parameters

Of the three performance parameters just discussed, insertion loss is clearly the only one that represents the performance of the muffler truly, as it represents the loss in the radiated power level consequent to insertion of the filter between the source and the receiver (the load). But it requires prior knowledge or measurement of the internal impedance of the source.

Transmission loss does not involve the source impedance and the radiation impedance as it represents the difference between incident acoustic energy and that transmitted into an anechoic environment. Being made independent of the terminations, TL finds favor with researches who are sometimes interested in finding the acoustic transmission behavior of an element or a set of elements in isolation of the terminations. But measurement of the incident wave in a standing wave acoustic field requires use of impedance tube technology, which may be quite laborious, unless one makes use of the two-microphone method with modern instrumentation.

Level difference, or noise reduction, is the difference of SPLs at two points: one upstream and one downstream. Like TL it does not require knowledge of source impedance and, like IL, it does not need anechoic termination. It is therefore, the easiest to measure and calculate and has come to be used widely for experimental confirmation of the calculated transmission behavior of a given set of elements (called the muffler proper in Fig. 2.24)

Thus, the various performance parameters have relative advantages and disadvantages. However, in the final analysis, for the user, insertion loss is the only criterion for the performance of a given muffler.

2.2.4.9 Theory of acoustic applied to different mufflers elements

When examining many different muffler configurations in a variety of industries, it becomes apparent that they all use the same types of elements. The elements which are commonly used are uniform tubes, extended tubes, Helmholtz resonators, perforated tubing, and absorption materials. This section will describe the function of each of these elements.

a) Uniform tube

A uniform tube can be described as a distribution element as long as plane wave propagation exists. For a circular tube of diameter, D, plane wave propagation exists,

provided that the criteria in Eq. (2-101) is satisfied. It should be noted that for the TL equations to be valid, plane waves must be present in the exhaust and tail pipe.

.

$$f < \frac{1.84}{\pi D} a_o \qquad\qquad (2\text{-}101)$$

b) Extended tube resonators

Extended tube resonators are very common in muffler design because of their ability to cause acoustical resonances in the muffler at specific frequencies, which is a function of the length of the extended tube. When the impedance tends to zero no acoustical energy is transmitted and there is a large peak in TL [2]. In which case, this is the frequency where the acoustical resonance occurs. The resonances improve the TL in a fairly wide frequency span centered around the resonance. This can be very beneficial to see the effects of the resonance at many operating conditions. In order to describe where in the frequency spectrum the resonance is located, it is necessary to describe what type of extended tube resonator is being used. There are two different types of extended tube resonators as can be seen in Fig. 2.25. The parameter of interest is *L,* which causes a structural resonance at frequencies described in Eq. (2-102) and is where a quarter wavelength of the sound wave is equal to *L*. This type of element is commonly referred to as a quarter wave resonator.

$$f = \frac{c}{4L}(2n + 1) \qquad\qquad for\ n\ =\ 0,1,2 \qquad\qquad (2\text{-}102)$$

(a)   **(b)**
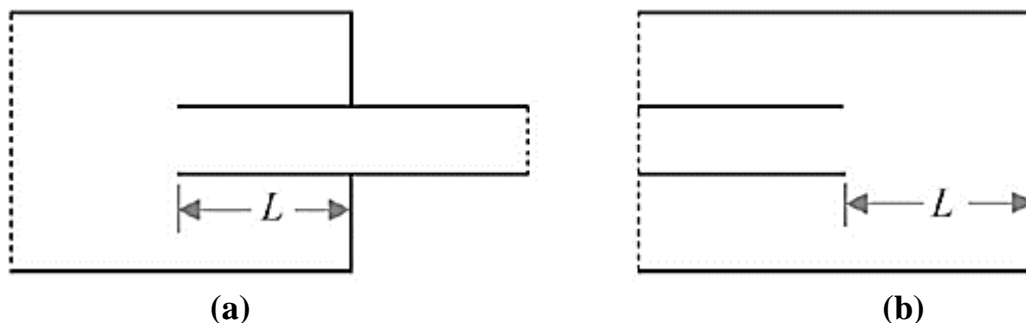
Fig. 2.25: Quarter wave resonator diagrams for (a) extended inlet/outlet (b) flow reversal

(expansion/contraction)

c) Helmholtz and Concentric hole-cavity resonator

Much like the quarter wave resonators shown in the last section, these elements are tuned to a certain frequency which causes an acoustical resonance. The equivalent impedance of the resonator can be calculated using Eq. (2-103). In this equation, tw is the tube thickness, L_{eq} is the equivalent length of the neck, and S_n is the neck cross sectional area.

$$Z = \left(\frac{\omega^2}{\pi \cdot c} \right) + j \left(\omega \frac{l_{eq}}{S_n} - \frac{c^2}{\omega \cdot V_o} \right) \qquad (2\text{-}103)$$
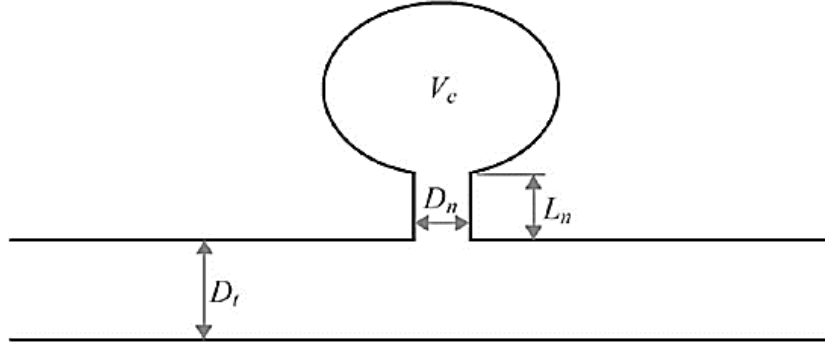
Fig. 2.26: Diagram of Helmholtz resonator

Where:

$$l_{eq} = L_n + t_w + 0.85 D_n$$

$$S_n = \frac{\pi}{4} D_n^2$$

From Eq. (2-103), the 4-pole parameters of the element can be determined which can be used to determine the Transmission Loss of the element. The calculation for TL can be seen in Eq. (2-104) where Z_{rl} is the real portion of the impedance and Z_{img} is the imaginary portion. An example of the TL of a Helmholtz resonator is shown in Fig. 2.27, where the parameters are given in Table 2.4

$$TL(dB) = 20 \log_{10} \left(\sqrt{\left(2 + \left(\frac{c}{S_o} \right) \frac{Z_{rl}}{Z_{rl}^2 + Z_{img}^2} \right)^2 + \left(2 + \left(\frac{c}{S_o} \right) \frac{Z_{rl}}{Z_{rl}^2 + Z_{img}^2} \right)^2} \Big/ 2 \right) \qquad (2\text{-}104)$$

Table2.4: Sample Helmholtz resonator properties used for calculation of transmission loss

Helmholtz Resonator properties		
Volume of cavity, V_c	10	in^2
Neck length, L_n	1	in
Neck diameter, D_n	1	in
Tube Diameter, D_t	1	in
Tube thickness, t_w	0.1	in
Speed of sound, c	348	m/s
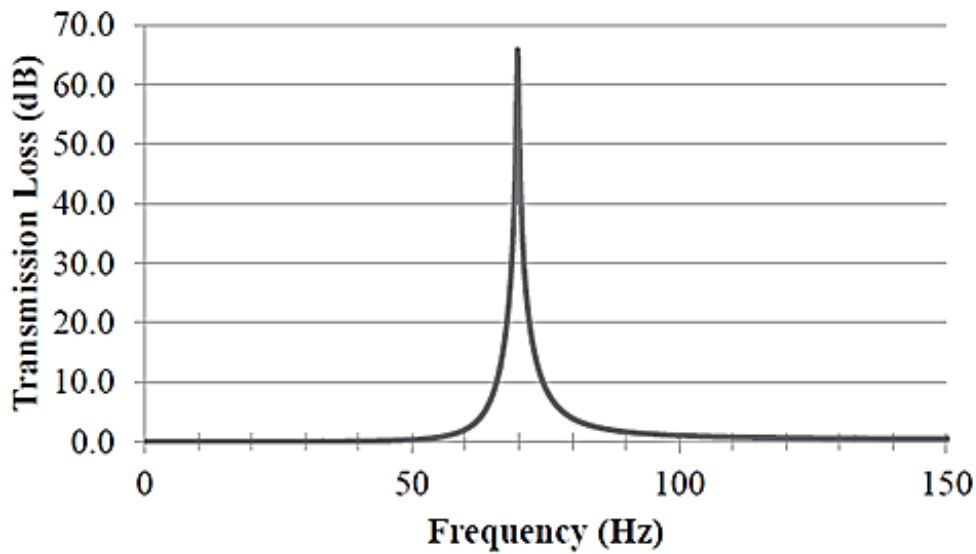
Fig. 2.27: Transmission loss of a simple Helmholtz resonator

A more popular form of a Helmholtz resonator in muffler design is a concentric tube resonator. The concentric tube resonator is a tube that contains a series of perforations in a specific location that opens into an expansion tube. A diagram showing the concentric tube resonator is shown in Fig. 2.28. This type of resonator is more ideal for muffler design for several reasons. The performance of the resonator is significantly more efficient when there is flow in the exhaust system. The space requirements are also less due to its concentric shape and the transmission loss has a slightly higher broadband performance due to the resistivity of the perforated tubing. The equation used to calculate the equivalent impedance is shown in Eq. (2-105). In the equation, n_h represents the number of holes in a circumferential row, d_h is the diameter of the perforated holes, t_w is the wall thickness, l_{eq} is the equivalent length, S_h is the surface area of each hole, S_c is the cross sectional area of the expansion tube, and Y_c is the characteristic impedance of the expansion tube. The same calculation shown in Eq. (2-104) can be used to calculate TL.
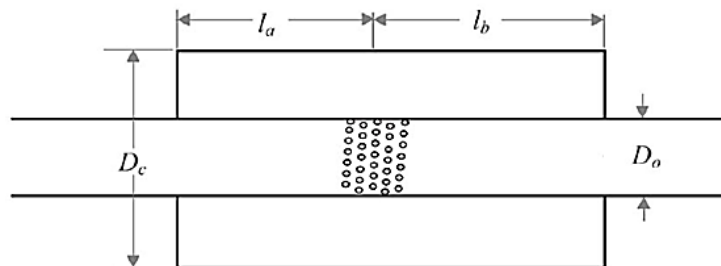
Fig. 2.28: Diagram of a concentric tube resonator

$$Z = \left(\frac{\omega^2}{n_h \cdot \pi \cdot c}\right) + j\left(\left(\frac{\omega \cdot l_{eq}}{n_h \cdot S_h}\right) - \frac{Y_c}{\tan(k_o \cdot l_a) + \tan(k_o \cdot l_b)}\right) \qquad (2\text{-}105)$$

Where:

$$l_{eq} = t_w + 0.85 \cdot d_h$$

$$S_h = \frac{\pi}{4} d_h^2$$

$$S_c = \frac{\pi}{4}(D_c^2 - D_o^2)$$

$$Y_c = \frac{c}{S_c}$$

d) Perforated tubing

Perforated tubing is in nearly all commercial mufflers and is quite beneficial when large flow velocities are seen inside of the muffler. When an exhaust stream exits out of a tube within the muffler there is typically a flow jet that forms. In order to combat this phenomenon, perforated tubing is used to steady the flow and force the flow to expand into the entire chamber. Perforated tubing can also be considered a dissipative element. When the acoustical pressure

wave moves past the perforations it feels a resistance which converts the acoustical energy into heat. The driving parameter in the performance of the perforated section is the equivalent impedance, Z_{perf}. The perforated impedance consists of areal part, R_{perf} (resistance) and an imaginary part, X_{perf}, (reactance). This is shown in Eq. (2-106)

$$Z_{perf} = R_{perf} + j \cdot X_{perf} \qquad (2\text{-}106)$$

The calculation for the resistance and reactance of the perforated impedance is seen in Eq. (2-107) and Eq. (2-108), respectively. These can be used for both sheets and tube. These equations hold true in the linear range and when the sheet is not too thick. In the equations ε represents the porosity of the surface, η is the dynamic viscosity of air which is primarily a function of

temperature, ρ_o is the density of the medium, t is the surface thickness, R_h is the radius of the holes, and CF is a correction factor which is dependent on the hole pattern, spacing, and diameter.

$$R_{perf} = \frac{1}{\varepsilon}\sqrt{8\omega\eta\rho_o}\left(1 + \frac{t}{2 \cdot R_h}\right) \qquad (2\text{-}107)$$

$$X_{perf} = \frac{1}{\varepsilon} \omega \rho_o (t + 2 \cdot CF) \tag{2-108}$$

Modeling small holes can be very exhaustive and requires a significant number of elements. This leads to an exponential increase in simulation time. Also, because the spacing of the perforated holes is very close together, the results achieved tend to be fairly inaccurate. It is often more convenient to model the perforated tubing as a continuous sheet and apply a transfer admittance property that relates the state variables p and v for the inner and outer face. This admittance relationship is shown in Eq. (2-109); where k is a correction factor that takes into account the thickness of the pipe (24). In the case of a perforated baffle or sheet, k would equal to zero.

$$\begin{bmatrix} v_{in} \\ v_{out} \end{bmatrix} = \begin{bmatrix} 1/Z_{perf} & -1/Z_{perf} \\ -k/Z_{perf} & k/Z_{perf} \end{bmatrix} \begin{bmatrix} p_{in} \\ p_{out} \end{bmatrix} \tag{2-109}$$

Many parametric studies have been performed on the effects of perforation Properties. All the results have revealed that by decreasing the porosity the TL is increased at all frequencies slightly.

e) Absorptive material

The use of sound absorption material in an exhaust system serves to dissipate the energy of the acoustic waves into heat and also to store heat energy from the exhaust stream. Using absorptive material can greatly increase the transmission loss of an exhaust system in the mid to high frequency ranges. In the muffler system, however, the absorption material is typically not thick enough to perform attenuation of the low frequencies. For the material to provide attenuation, the material thickness needs to be at least *1/10th* of the wavelength for the frequency of interest. Most of the low frequency attenuation is a result of the expansion into the chamber. By placing the acoustic material in the cavity, the overall effective expansion area is reduced. As a result, there is a potential for a drop in TL at the low frequencies. These affects should be minimized because most of the acoustical energy exists in these frequencies. The properties for the complex acoustical impedance, $\bar{Z}$, and wave number, $\bar{k}$, of an element can be seen in Eq. (2-110) and Eq. (2-111). These properties are primarily a function of density, ρ_o, and flow resistivity, σ.

$$\frac{\bar{Z}}{Z_o} = 1.0 + 0.0954 \left(\frac{\rho_o f}{\sigma}\right)^{-0.754} - j\, 0.085 \left(\frac{\rho_o f}{\sigma}\right)^{-0.732} \tag{2-110}$$

$$\frac{\bar{k}}{k_o} = 1.0 + 0.16 \left(\frac{\rho_o f}{\sigma}\right)^{-0.577} - j\, 0.189 \left(\frac{\rho_o f}{\sigma}\right)^{-0.595} \tag{2-111}$$

For the FEM software packages, when modeling absorptive materials, the input variables are the flow resistivity, porosity, and tortuosity, as well as the properties of the medium c and ρo. If the sound absorption properties were measured experimentally, it is typically done with the two-cavity method. The flow resistivity can be back calculated from Eq. (2-110). Flow resistivity is primarily a function of the material density and inversely proportional to the thickness. Also, all glass fiber materials have roughly the same flow resistivity values relative to their density. Therefore, the flow resistivity can be estimated for glass-fiber materials and produce accurate results regardless if the true values are nearly double or half that of which was estimated.

CHAPTER 3
MEASUREMENT & CALCULATION

As mentioned in the previous chapter, there are three standard ways to study the acoustic performance of a muffler. They are insertion loss, transmission loss, and noise reduction. Each offers its own advantages and disadvantages. In this section, the focus will mainly be on transmission and insertion loss. These are the two measurement methods that are the most prominent in both industry and research.

3.1 Insertion loss (IL)

Insertion loss is defined as the difference between sound pressure levels of a silenced system and some reference system. The reference system is usually just a straight pipe of the diameter that is typical to the system in place of the muffler. This pipe should also be the same length of the muffler being tested [5]. Insertion loss is calculated by Equation (3.1)

$$IL = L_{w1} - L_{w2} = 10 \log_{10}\left(\frac{w1}{w2}\right) \tag{3-1}$$

There are two main advantages to using IL as the standard of performance. The first advantage is that, conceptually, IL is the true performance of a muffler for a given system. It is the comparison of the duct system before and after the muffler is introduced. This is why expected insertion loss is the measure of muffler performance used by many companies. The second advantage is that IL measurement is relatively easy, and only requires one microphone either inside the muffler in a pipe or outside the muffler in free space [6].

There are also a few disadvantages. IL is difficult to predict analytically, because it is very system dependent. Both the source impedance and the load impedance must be taken into account when trying to predict IL [7]. This system dependence leads to another disadvantage which is that even if the same muffler is used, the insertion loss can vary for different systems, different sources, and different loads. This is why companies generally only offer expected IL as a performance measurement.

The experimental setup for IL is relatively simple. The muffler should be situated horizontally relative to the ground, and noise source in the same way that it will be in

application, and the environment should simulate a free-field above a reflecting plane. In order to create this type of environment the muffler should be placed in an area where the noise outlet and microphone are at least thirty meters from any large reflecting surfaces including, but not limited to buildings, walls, vehicles, hills, and people. Ideally there would be no reflecting surfaces near the noise source or microphone, but if that is not possible, the following guidelines will help to minimize their effect. If possible, the measurements should be made in an anechoic chamber to eliminate any effects from wind, background noise, or reflecting surfaces near the microphone. When an anechoic chamber is not available, then measurements should be taken at a time when wind and background noise are at a minimum. The effects from these two sources should be at least 10 dB less than the noise source being measured [8]. If this is not possible, then time must be given to let the noise die down, or a new measurement environment must be selected. The reflecting plane in this case is the ground and should be either concrete or asphalt. The muffler should be replaced with a simple pipe of equal length for the reference system [2]. The microphone should be placed approximately one meter from the outlet of the exhaust system. This distance should help to reduce contamination from background noise in the measurement field. The measurements should also be taken at a number of positions around the outlet of the exhaust system in a circular pattern, in particular 0, 45,90, and 100 degrees. Once everything is set in place nothing in the setup should change when switching between the reference system and the silenced system. Figure 3.1 illustrates some of these guidelines.
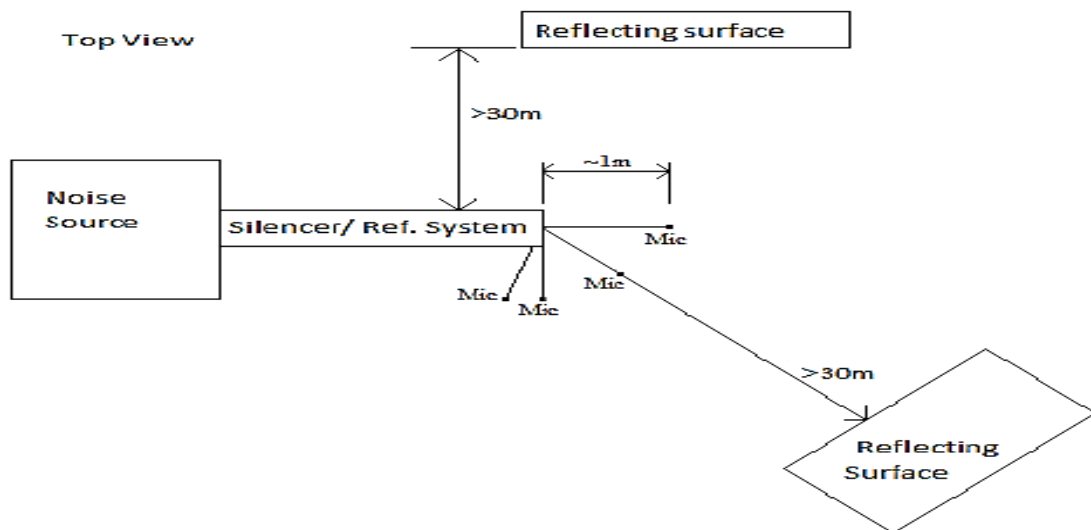
Fig. 3.1: Top view of typical IL setup

3.2 Transmission loss (TL)

Transmission loss is defined as the ratio of incident sound power and transmitted sound power across the muffler being examined

$$TL = 10 \log_{10} \left(\frac{W_i}{W_o} \right) + 10 \log_{10} \left(\frac{S_i}{S_o} \right) \tag{3-2}$$

$$TL = 20 \log_{10} \left(\left| \frac{p_{in}}{p_{tr}} \right| \right) + 10 \log_{10} \left(\frac{S_i}{S_o} \right) \tag{3-3}$$

where W_i is the incident sound power, W_t is the transmitted sound power, and TL is the transmission loss. Before we get started, it is worth mentioning that all methods of measuring TL are based on plane wave theory.

The Transmission Loss of a muffler can be calculated in a variety of ways, including the use of the decomposition method, two load method, and the two source-location method. The methods other than the decomposition method are the most practiced
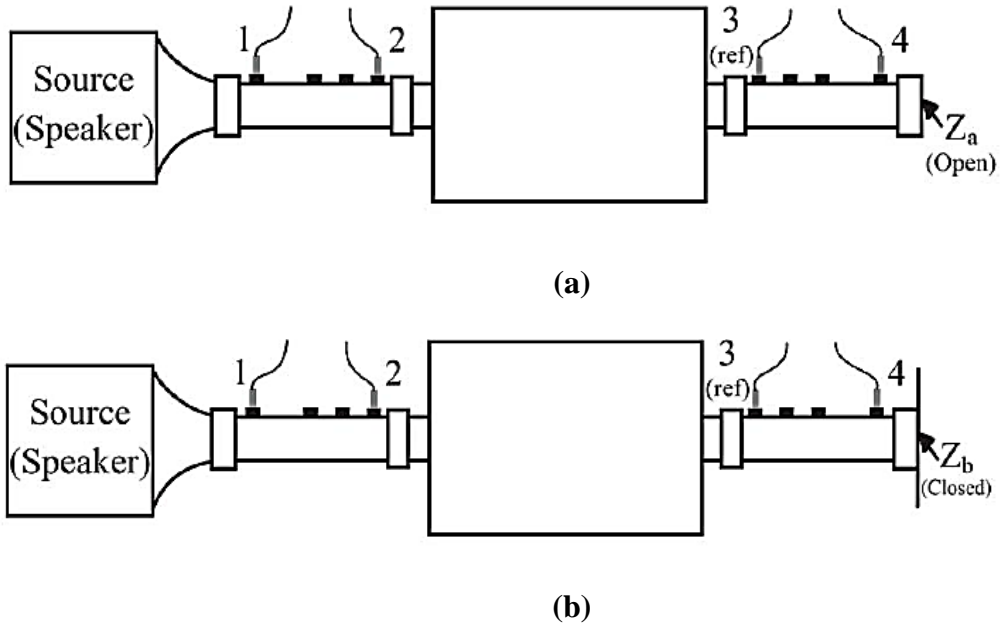
3.2.1 Two load method

Because an anechoic termination cannot accurately be applied to the outlet of the muffler, different testing techniques such as two load method need to be practiced. The two-load method consists of four microphones. Two microphones are place both in the inlet piping and outlet piping to determine both the progressive and reflective waves. This technique is used to derive the 4-pole parameters of the muffler and then, using these, Transmission Loss can be calculated. As there are four unknowns (4-pole parameters) and only two equations relating the state variables, there must be two loading conditions. Typically, this is done by leaving the termination open to the atmosphere and proceeded by closing the outlet tubing using a rigid termination, such as a steel plate. The diagrams of the two test configurations are depicted in Figure 3.2a, b.

In Figure 3.2 the numbers represent the channel number of the microphone at that specific location. Given the two test configurations, six total Frequency Response Functions (FRF) are calculated; where channel 3 is always referred to as the reference channel. The derivation of the 4-pole parameters was described in the works of Tao et al.; only the equations will be presented in this thesis [9]. The calculation of the 4-pole parameters is

shown in Equation (3-4) through Equation (3-7). The variable, H, represents an FRF with the first number designated as

(a)

(b)

Fig. 3.2: Two Load method in determining TL of muffler for (a) Load 1: when outlet is open to atmosphere and (b) Load 2: when outlet is rigidly closed.

the output channel, the second number represents the reference channel (Ch. 3), and the letter represents the test configuration. The Δ symbol is the determinant of the transfer matrix, in which case, for a uniform tube would be equal to one.

$$A_{23} = \frac{\Delta_{34}(H_{32a}H_{34b} - H_{32b}H_{34a}) + D_{34}(H_{32b} - H_{32a})}{\Delta_{34}(H_{34b} - H_{34a})} \tag{3-4}$$

$$B_{23} = \frac{B_{34}(H_{32a} - H_{32b})}{\Delta_{34}(H_{34b} - H_{34a})} \tag{3-5}$$

$$C_{23} = \frac{(H_{31a} - A_{12}H_{32a})(\Delta_{34}H_{34b} - D_{34}) + (H_{31b} - A_{12}H_{32b})(\Delta_{34}H_{34a} - D_{34})}{B_{12}\Delta_{34}(H_{34b} - H_{34a})} \tag{3-6}$$

$$D_{23} = \frac{B_{34}(H_{31a} - H_{31b}) + A_{12}(H_{32b} - H_{32a})}{B_{12}\Delta_{34}(H_{34b} - H_{34a})} \tag{3-7}$$

As presented in the equations above, the 4-pole parameters of the uniform tubes between microphones 1-2 and 3-4 must be known. The four pole parameters between 1-2 are

67

calculated using Equation (3-8). To calculate the 4-pole parameters between microphones 3-4 the same equation is used. Replacing the necessary variables for the pipe between microphones 1-2, the 4-pole parameters of 3-4 are calculated and can be seen in Equation (3-9). Typically, the diameters and lengths are identical, resulting in identical 4-pole parameters.

$$\begin{bmatrix} A_{12} & B_{12} \\ C_{12} & D_{12} \end{bmatrix} = \begin{bmatrix} Coskl_{12} & j\rho c\,Sinkl_{12} \\ jsinkl_{12}/\rho c & Coskl_{12} \end{bmatrix}, \quad \Delta_{12} = 1 \tag{3-8}$$

$$\begin{bmatrix} A_{34} & B_{34} \\ C_{34} & D_{34} \end{bmatrix} = \begin{bmatrix} Coskl_{34} & j\rho c\,Sinkl_{34} \\ jsinkl_{34}/\rho c & Coskl_{34} \end{bmatrix}, \quad \Delta_{34} = 1 \tag{3-9}$$

Where k is the wave number and l_{ij} is the length of the pipe between position i, j.

The limitation of using the two-location method is, if there are not substantial differences between the two loads attached at the termination, then the equation for TL breaks down. It might be assumed that by closing the outlet, the load is sufficiently changed. As the load is a function of frequency, this would not always be the case, particularly at the lower frequencies. A much more feasible and accurate method is the two source-location method which is not limited to these shortcomings.

3.2.2 Two source – location method

The two source-location method is an improved method based on the two location method stated previously. In this method, the source is moved from the inlet to the outlet location for the second configuration. Because of the two different testing configurations, the terminations do not need to be identical nor anechoic. Typically, however, one needs to minimize the background noise. Due to this, it would be advantageous to place some absorptive material at the end of the outlet/inlet. A diagram of the two test configurations is shown in Figure 3.3. All of the previous equations presented for two load method are used in the calculation of TL and the nomenclature remains the same.

(a)

(b)
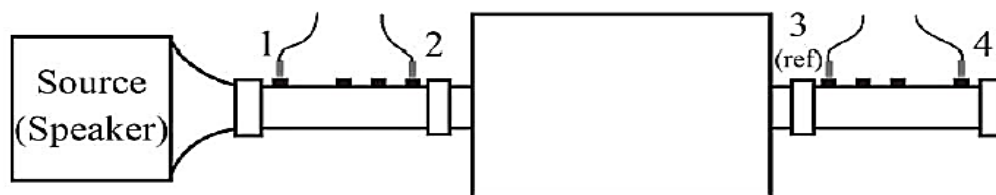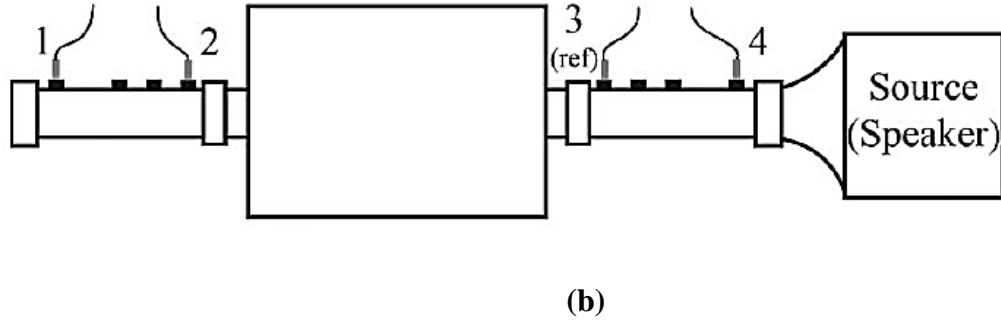
Fig. 3.3: Two Source-Location method in determining TL of muffler for (a) Config.1: when source is at inlet and (b) Config.2: when source is at outlet.

3.2.3 Decomposition method

For the proper calculation of TL incident and transmitted waves must be isolated. This can be difficult because in the portions of piping immediately upstream and downstream of the muffler, there exists forward moving and reflected waves. These reflected waves are a result of the impedance mismatch

The incident wave is isolated through the method of wave decomposition. In the wave decomposition method, two microphones are placed upstream of the muffler. In a case where flow is present, a way to measure flow through the pipe will also need to be installed, because the wavenumber is affected by the flow rate, as seen in Equation (3-11). The information from these two microphones is then manipulated to separate the incident and reflected auto spectral densities. A spectral density represents how the square of a signal is distributed across the frequency range of that signal. In this case, the signal will be the voltage from the microphone. That voltage will then be related to the pressure through the sensitivity provided by the manufacturer. Since auto and cross spectral densities can be calculated from measured pressures very readily by many mathematical programs and FFT analyzers, the calculation boils down to a simple formula for the auto spectral density of the incident wave:

$$S_{ii} = \frac{S_{11} + S_{22} - 2C_{12}cos(k_r\Delta x) + 2Q_{12}sin(k_r\Delta x)}{4sin^2\big((k_i + k_r)\Delta x/2\big)} \qquad (3\text{-}10)$$

$$k_i = \frac{k}{(1+M)}, \qquad k_r = \frac{k}{(1-M)} \qquad (3\text{-}11)$$

69

$$k = \frac{2\pi f}{c} \tag{3-12}$$

Where S_{ii} is the auto spectral density of the incident wave, S_{11} and S_{22} are the auto spectral densities of the acoustic pressures measured by microphones one and two respectively. C_{12} and Q_{12} are the real and imaginary parts of the cross spectral density, S_{12}, between the total acoustic pressures measured at microphones 1 and 2 respectively. k is the wavenumber, k_i and k_r are the incident and reflected wave numbers respectively. $\varDelta x$ is the distance between the microphones. M is the Mach number, f is the frequency of the acoustic wave, and c is the speed of propagation of the acoustic wave. The subscript i stands for the incident wave, 1 and 2 are for measurements made at microphones 1 and 2 respectively, and r stands for the reflected wave.

On the downstream side of the muffler the auto spectral density of the transmitted wave must be obtained. Unfortunately, for this side of the muffler, the decomposition method is not applicable. Not only does the transmitted wave reflect from the end of the duct, but that reflected wave again reflects when it reaches the muffler. This double reflection causes the decomposition method to produce inaccurate results. One way to deal with this problem is to create an anechoic termination. This anechoic termination is designed to reduce the reflections from the termination to a significant level, and the spectral density of the transmitted wave may be calculated directly from the downstream measurement. From both the incident and transmitted wave, the incident and transmitted acoustic power, W_i and W_t respectively, can be calculated using Equations 3-13 and 3-14.

$$p_i = \sqrt{S_{ii}}, \qquad p_t = \sqrt{S_{tt}} \tag{3-13}$$

$$W_i = \frac{p_i^2}{\rho_i c_i} A_i, \qquad W_t = \frac{p_t^2}{\rho_t c_t} A_t \tag{3-14}$$

decomposition method to produce inaccurate results. One way to deal with this problem is to create an anechoic termination. This anechoic termination is designed to reduce the reflections from the termination to a significant level, and the spectral density of the transmitted wave may be calculated directly

where the subscripts i and t represent the incident and transmitted variables respectively, p is the pressure. ρ is the density of the medium, c is the speed of sound propagation in the medium, A is the cross sectional area of the duct, and S is the auto spectral density. The setup and placement of certain elements in the measurement of TL can greatly affect the accuracy of the results. A typical setup for TL measurement is shown in Figure 3.4.
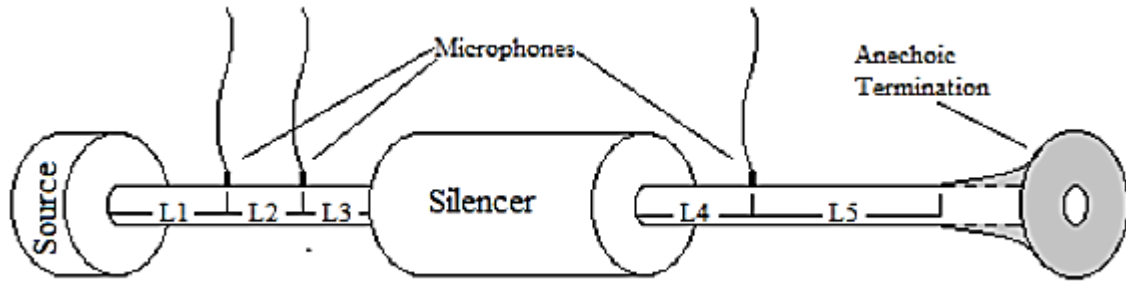
Fig. 3.4: Typical setup for TL measurement

To minimize the error from the measurement, the distances L1,2,3,4,5 should be chosen according to the guidelines laid out by Seybert and Ross [10]. Lengths 3 and 4 should be made as small as possible.

Placing the microphones close to the muffler will reduce attenuation effects in the duct so that the measured transmitted and incident waves are as close as possible to the true transmitted and incident waves. Both length 5 and Length 1 should be as long as the space permits. This will minimize any measurement contamination due to reflections from the source or the anechoic termination. Since a perfectly anechoic termination is impossible to construct, this is a necessary guideline. Length 2 is the length that the most attention must be paid to. There are a number of constraints on it. Ideally, length 2should be as small as possible. Length 2 needs to be small for two reasons. The first reason is to reduce the amount of wave attenuation between the two measurements, and the second being that when the microphone spacing is equal to a multiple of the half wavelength of the pressure wave, the decomposition theory equations produce sharp discontinuities in the data. To avoid this discontinuity, the spacing of the microphones should be chosen according to Equation (3-15), which states that the spacing should be less than half the wavelength of the highest frequency being measured.

$$\Delta x \leq \frac{c}{2f_m} \tag{3-15}$$

where f_m is the maximum frequency, c is the speed of sound, and Δx is the microphone spacing. The limiting factor of the spacing between the microphones is that it should still be large enough that the position of the microphones may be approximated as the centerline of each microphone. This is why the spacing must be much larger than the microphone diameter. This may cause the discontinuity to be present in some of the measured

frequencies. If one of these discontinuities is encountered the data point may be simply ignored, and a curve fit may be used to estimate the data at the frequency.

However, Equation (3-15) is an ideal spacing for the microphones. Many other factors in the measurement and calculation must be taken into account when deciding upon the spacing. An error analysis by Abom and Boden [11] resulted in a general formula that reduces error in the entire decomposition process by defining an acceptable frequency range for a given microphone spacing. Equation (3-16) should be used in accordance with the above mentioned constraint that the spacing of the microphones should be much larger than the diameter of the microphones.

$$\frac{0.05 c_o (1 - M^2)}{\Delta x} < f < \frac{0.4 c_o (1 - M^2)}{\Delta x} \tag{3-16}$$

where c_o is the speed of sound, M is the Mach number (for cases with flow), Δx is the microphone spacing, and f is the frequency.

3.3 Level difference/Noise reduction (NR)

Noise reduction is defined as the sound pressure level difference between two points in a system. For a muffler, one point should be upstream and one point should be downstream of the muffler. Noise reduction is much like insertion loss in that it is very easy to measure, but is also source and load dependent making it hard to predict and calculate.

$$LD/NR = 20 \log_{10} \left(\frac{p_i}{p_o} \right) \tag{3-17}$$

Not much work has been done with NR, and thusly standards and research papers on it are hard to find. The reason for this is that NR itself does not tell us anything absolute about the performance of the muffler in the system or acoustic properties of the muffler, and the purpose of it is somewhat undecided. However, in many cases, NR is by far the simplest and easiest measurement to make in terms of the performance. Also, NR can be used as an approximation of the TL in many systems. For these two reasons NR is widely used in muffler performance studies.

3.4 Experimental Setup

The transmission loss of a sample muffler is measured on the test rig. Sample muffler is shown in the Fig. 3.5. Transmission loss is measured using two load method with a random noise signal as an excitation by a speaker source.

The diaphragm of the microphone is placed flush with the inside of the test tube. Through personal experience, if the diaphragm of the microphone was not placed exactly flush with the tube, there would be distortion of the TL curve. This was a result of the microphone causing interferences with the plane waves in the tube which, in turn, caused unwanted reflections.

Fig. 3.5: Sample muffler

Larger microphone spacings will more accurately calculate lower frequency TL due to the large wavelengths. The shorter microphone spacings will more accurately calculate the higher frequency TL.

At near locations of the microphone spacing where the calculation of the progressive wave breaks down, the TL takes on the appearance of an acoustical resonance. The calculation for the progressive wave is shown in Equation (3-18), where 1 and 2 represents microphones 1 and 2. The equation breaks down when the $\sin(kl_{12})$ goes to zero. The frequencies when this occurs can be calculated using Equation (3-19) and is shown for the four microphone spacings in Table 3.1. The frequency-microphone spacing combination should be avoided for accurate results.

$$p_i = \frac{1}{2jsin(kl_{12})}\left[p_1(j\omega)e^{jkz_2} - p_2(j\omega)e^{jkz_1}\right] \qquad (3\text{-}18)$$

$$f_{res} = \frac{nc}{2L_{12}} \qquad for \; n = 1,2,3 \ldots\ldots \qquad (3\text{-}19)$$

It should be noted, however, that although the microphone spacing can change between measurements, the location of microphones 2 and 3 should not change as this would change the acoustical properties of the muffler.

Table. 3.1: Breakdown frequency(Hz) table for TL (c=348 *m/s*)

n	Length between Microphones (mm)			
	35	70	105	140
1	4946	2473	1649	1237
2	9893	4946	3298	2473
3	14839	7420	4946	3710
4	19786	9893	6595	4946
5	24732	12366	8244	6183

Transfer functions are measured for two acoustic load conditions first with anechoic termination (acoustic material at end of exit pipe) and second with reflective condition (Hard plate at end of exit pipe).
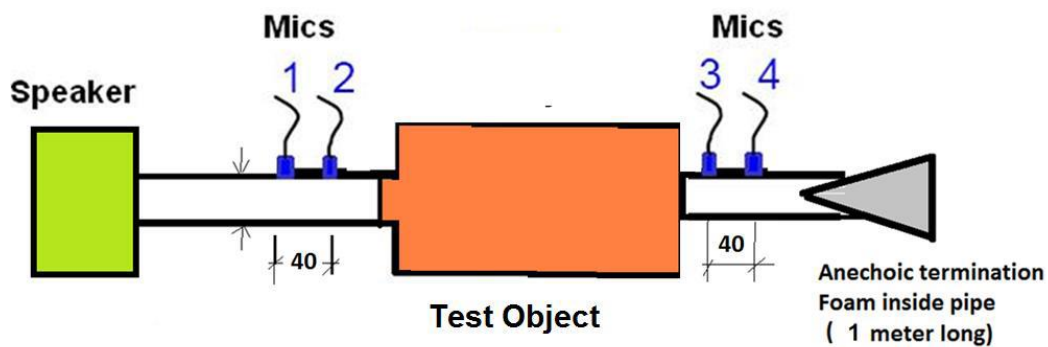
Fig. 3.6: Load 1: Anechoic termination
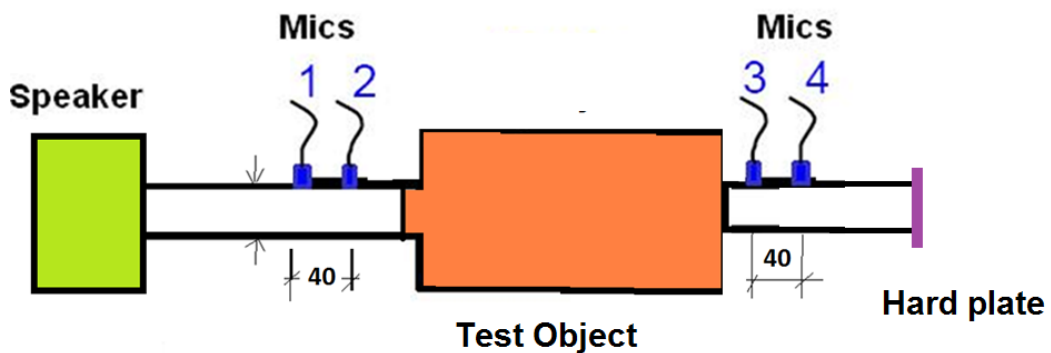
Fig. 3.7: Load 2: Reflective termination

74

3.4.1 Test equipments & test conditions

The details of the equipments used are given in the following table

Table. 3.2: Equipment details

Sr. No.	Equipment details
1	Multi-channel data acquisition system PULSE, Type 3560D, B & K Denmark Make
2	Power Amplifier, Type 2716, B&K Denmark make
3	Quarter inch condenser microphones, PCB make
4	Muffler Test Rig with Sound Source, ARAI make
5	Lower cut off Frequency = 50 Hz
6	Upper Cut off Frequency = 4200 Hz (Based on mic spacing of 40 mm)
7	Mic- spacing (S12, S34) = 40 mm
8	Temperature = Room temperature at 25ºC, No flow

In the past, measurement of the incident wave in a standing wave field required use of the impedance tube technology, leading to quite laborious experiments. However, use of the two-load method with modern instrumentation allows faster and accurate results.

1-Speaker   **2**- DAQ & Amplifier   **3**- Microphones   **4**- Muffler under test

Fig. 3.8: Actual test setup for measuring muffler transmission loss(TL)

To measure transfer functions vs. frequency across the intake system, two upstream and two downstream microphones are used. The sound source produces white noise. White noise has the characteristic that it has the same sound power at all the frequencies. The motive for using such kind of sound source is to keep the load constant with the frequencies. Loudspeaker, creates an acoustic pressure field in the tube. A preamplifier amplifies the signal picked up by the microphone before it is fed to the computer-controlled Fourier analyzer. The assessed data is the sound pressure, measured at different microphone locations.
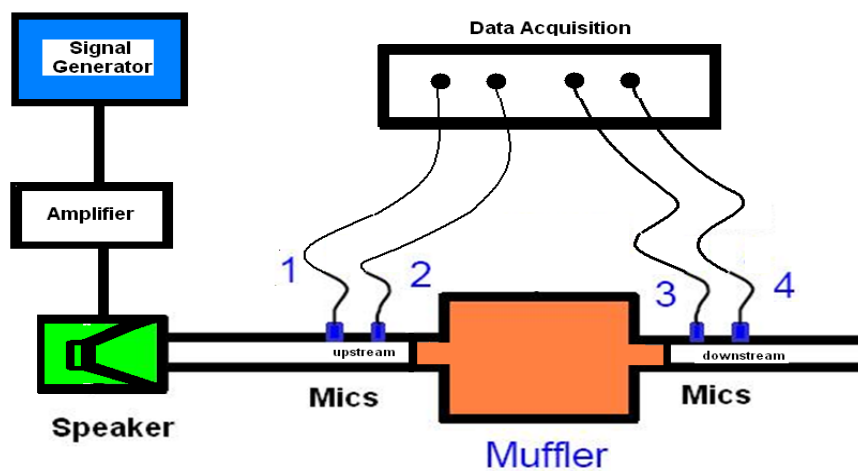

Fig. 3.9: Sample muffler under test

Fig. 3.10: Connectivity diagram of test setup

Making use of these measured data, the four pole parameters of a muffler are calculated using the equation given in the section 3.2a. Data is taken upto a frequency of 2000 Hz.

With the help of these four pole parameters the transmission loss can be easily calculated.
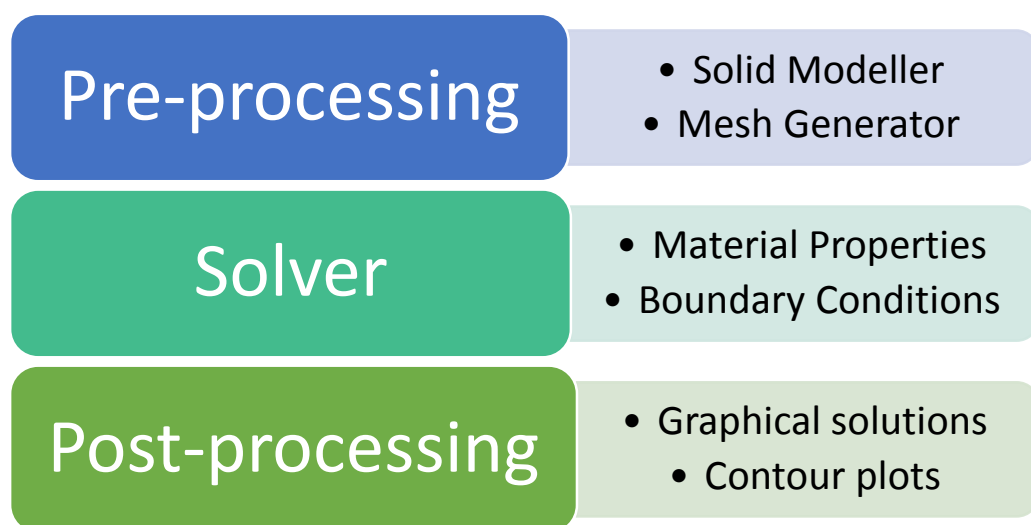
CHAPTER 4
MODELLING & SIMULATION

Manufacturing companies are bound to supply products in a restricted time frame because of the strong demand from the OEM's. Simulation comes into play to cover up these design and development (D&D) time and consecutively to reduce prototype cost.

The main objective of the present study is to build a three dimensional finite element approach (3D-FEM) for a sample muffler, to study its flow and acoustic attenuation performance.

One of the major advantages of the FEM is the possibility to analyze problems with arbitrary geometry and general boundary conditions, but at the cost of long computation times if sufficient accuracy is desired at high frequencies, due to the large number of elements required

FEM requires high computational and memory resources particularly at higher frequency, but the availability of high speed computers, also using domain decomposition and parallel processing techniques have led to overcome this defect. Also dividing the solution scheme into models with different element size; coarser mesh model for lower frequencies and finer model mesh for higher frequencies reduce the analyses time.

There are three basic steps involved in any finite element (FE) analysis, see Fig.4.1

Pre-processing	• Solid Modeller • Mesh Generator
Solver	• Material Properties • Boundary Conditions
Post-processing	• Graphical solutions • Contour plots

Fig. 4.1: Flow diagram of Finite Element (FE) analysis

4.1 Computational fluid Dynamics (CFD) analysis

Predicting and controlling fluid flow is critical in optimizing the efficiency of so many products and processes. Computational fluid dynamics (CFD) uses applied mathematics, physics and computational software to visualize how a gas or liquid flows, as well as how the gas or liquid affects objects as it flows past. Computational fluid dynamics is based on the Navier-Stokes equations. These equations describe how the velocity, pressure, temperature, and density of a moving fluid are related.

4.1.1 Introduction to Solver: AcuSolve

AcuSolve is a leading general-purpose finite element-based Computational Fluid Dynamics (CFD) flow solver with superior robustness, speed, and accuracy. It is a coupled solver based on galerkin's least square finite element method which works at nodal level and solves equations simultaneously.

AcuSolve uses a single solver for all flow regimes with very few parameters to adjust. It has the capability to solve fully coupled pressure-velocity problem for all supported flow regimes, fully coupled temperature-flow problem for highly buoyant flows, incompressible and sub-sonic compressible Stokes and Navier-Stokes equation and many more. It produces results rapidly by solving the fully-coupled pressure-velocity equation system using industry leading, scientifically proven numerical techniques. This yields rapid linear and nonlinear convergence rates for both steady state and transient simulations

One of the keys to its numerical methods accuracy is the use of equal order interpolation for all variables. This results in second order spatial accuracy for all governing equations. This focus on accuracy further enhances the speed of the solver by enabling you to achieve high levels of accuracy with AcuSolve using far less mesh than what is required to achieve comparable results using other CFD solvers. In addition to requiring less mesh to produce a comparable result, it is able to retain its second order accuracy on all element topologies. You can confidently simplify your pre-processing by using tetrahedral elements to mesh your domain without sacrificing robustness or accuracy.

In addition to exceptional spatial accuracy, AcuSolve provides second-order accuracy in time as well. This provides you with unmatched transient simulation capabilities. Running a transient in AcuSolve is easy as specifying that the simulation is transient, selecting a suitable time step to resolve the physics, and then launching the solver. No complex solver

settings to adjust, and no concerns about the simulation diverging due to improper solver selection!

There are different turbulence models available in AcuSolve such as Large Eddy Simulation (LES) Model, Dynamic LES model, Constant coefficient Smagorinsky LES model, Detached Eddy Simulation (DES) Model, Spalart-Allmaras based Detached Eddy Simulation (DES-1997, DDES, IDDES), SST based Detached Eddy Simulation (SST-DES), Reynolds Averaged Navier-Stokes(RANS) models, Spalart-Allmaras, SST, k-omega.

In this problem Spalart-Allmaras model is used because it is best suited for internal flows and heat transfer problems.

4.1.2 Model description

The first step, as with any FEM simulation, is to start with the design of the model. In this thesis, a solid modelling package NX (a Siemens product) was used to create the muffler model. When designing the mesh, only the skins of the muffler are needed. Accordingly, the muffler can either be modeled using sheets or the skins need to be extracted from the solid geometry. Each component should be created using a separate body in the part to allow for easy distinction between the components when generating the mesh. A picture showing the muffler model used in the research is shown in Figure 4.2
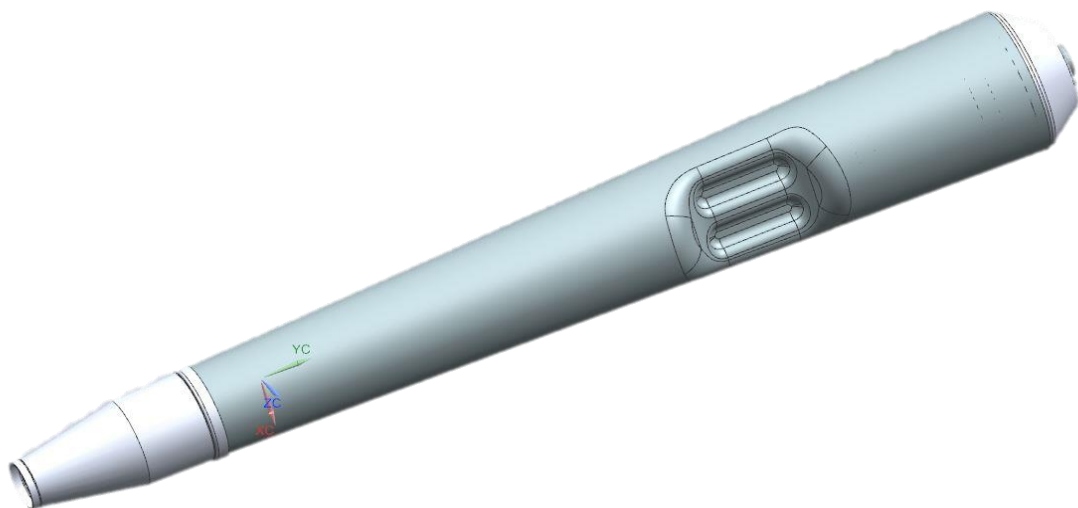
Fig. 4.2: Solid model of sample muffler
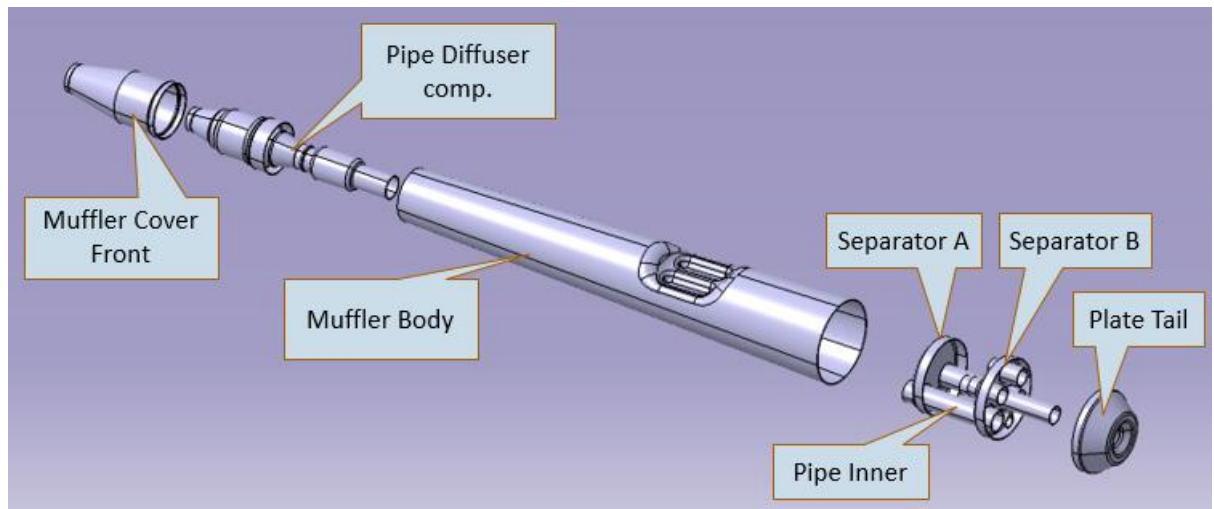
Fig. 4.3: Exploded view of sample muffler

After the model is created it needs to be output to a readable format for the mesh generating software. The model can be saved as either a step file (.stp) or Initial Graphics Exchange Specification file (.iges), or Parasolid (.x_t), however, a Parasolid or step file is recommended because there is less worries of losing the surface geometry while exporting the model.

4.1.3 Mesh generation

If the muffler is fairly sophisticated, the meshing of the muffler is the most time consuming process which can take over a day for the most complicated mufflers. The meshing software used in this thesis was Altair's HyperMesh 13.0 because of the sophisticated control over the mesh generated. Each of the muffler components created inside of the muffler should have their own mesh component. This helps to decrease the model setup time in AcuSolve significantly. Then each surface of every component needs to be meshed using 2-D elements. For the models used in this thesis, the maximum element size was set to 1mm.

While creating the 2-D mesh of different components it should be kept in mind that the connectivity must be maintained between the dissimilar meshes. For this the keep connectivity option must be turned on while meshing. All of the internal components inside of the muffler should be completely closed at the end of this process.

After creating the 2-D mesh, a 3-D tetra mesh can be created for the muffler model. To see the effect of boundary layer, 3-D meshing requires the no. of boundary layers, the thickness of boundary layer and the boundary layer growth rate (see fig 4.5). The 2-D surface

elements are the triangular elements and the 3-D fluid elements are the tetrahedral elements
The 2-D elements should be placed in a different component after this step.
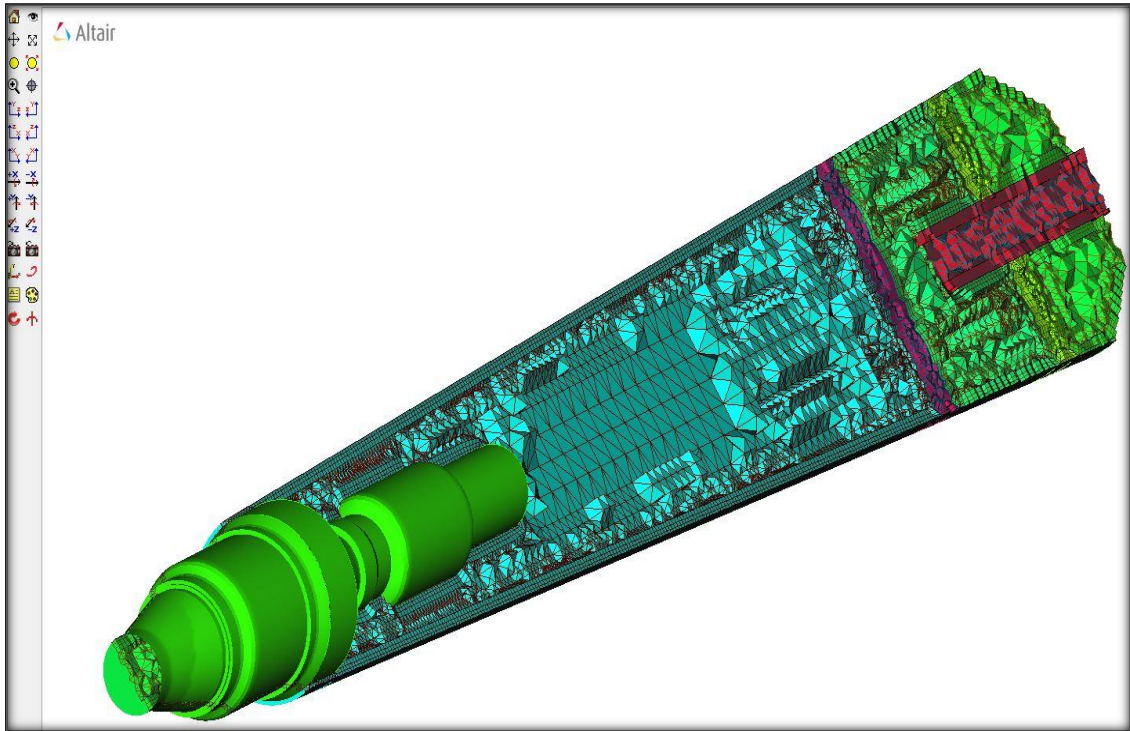
Fig. 4.4: Volume mesh of sample muffler (GUI: AcuConsole)
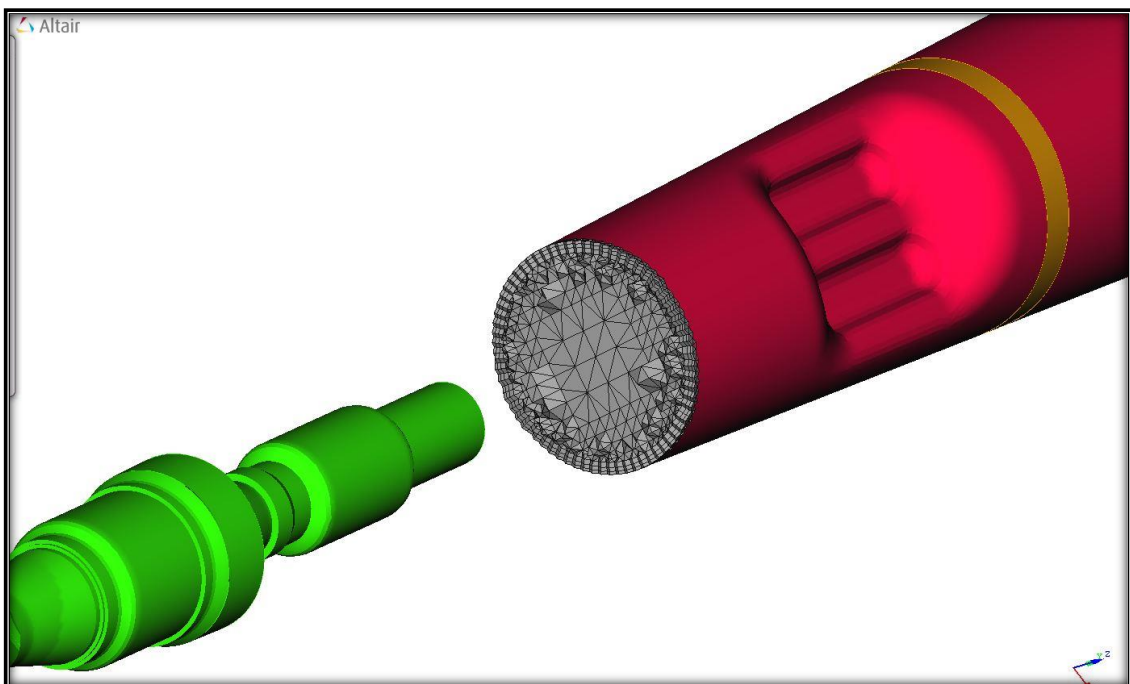
Fig. 4.5: 3-D mesh with boundary layers (GUI: AcuConsole)

4.1.4 Material properties and boundary conditions

The fluid elements (3-D) are given the material property of air and the wall elements (2-D) are given the property of solid. Gravitational forces are also assigned in transverse direction to the flow of air. The boundary conditions are defined at inlet and outlet to the muffler and the flow calculation at the inlet and outlet to the perforations are performed by the solver itself. One just needs to define them as inlet and outlet according to the flow direction. The simulation is performed for both states, steady state and transient state. The boundary conditions and solver settings are different for both the cases.

4.1.4.1 Steady state analysis of Exhaust Muffler

The steady state analysis gives a spatial description of the flow inside the muffler. It is very easy to perform and takes relatively less time in comparison to the transient one. The boundary conditions for the steady state are given in the table 4.1

Table 4.1: Steady state boundary conditions

Inlet boundary conditions	
Inlet gas velocity	10.24 m/s
Gas temperature	633 k
Outlet boundary conditions	
Outlet pressure	Atmospheric pressure (101325 N/m^2)

4.1.4.2 Transient state analysis of Exhaust Muffler

The transient analysis tells us how the system evolves with time. Therefore, an extra variable comes into picture in the transient analysis, which is time. For this case the solver settings need to be controlled for the convergence of the solution. Thus, we have to provide the convergence criteria and time step for each iteration carefully. The residual behavior for a transient simulation is useful to see that the solvers are behaving correctly, which is indicated by a relatively smooth variation with increasing iterations. The actual residual values and profiles are not significant.

Table 4.2: Transient state boundary conditions

Inlet boundary conditions	
Mass flux	0.008 Kg/sec

Gas temperature	923 k
Outlet boundary conditions	
Outlet pressure	Atmospheric pressure (101325 N/m^2)

The boundary conditions applied in the AcuConsole (a GUI for the CFD problem setup) is shown in the Fig. 4.6, 4.7

Fig. 4.6: Inflow boundary conditions (GUI: AcuConsole)

Fig. 4.7: Outflow boundary conditions (GUI: AcuConsole)

4.2 Acoustic analysis

The major factor in engine and vehicle emitted noise is the exhaust system. The untreated exhaust noise is often ten times greater than all the structural noise of the system combined which is controlled through the use of silencers or mufflers. By the acoustic analysis of mufflers, we can find out its acoustical performance and the effect of various muffler components on its performance. The acoustic analysis is based on inviscid flow with linear pressure-density relation and the continuity equation. The equations describe the sound pressure distribution and particle velocity inside the muffler.

4.2.1 Introduction to Solver: OptiStruct

OptiStruct is a modern structural analysis solver for linear and nonlinear problems under static and dynamic loadings. It is the leading solution for structural design and optimization. It is widely used to analyze and optimize structures for their strength, durability and NVH (noise, vibration and harshness) characteristics.

OptiStruct has the capability to solve various types of analysis problems:

- Heat Transfer Analysis
- Kinematics and Dynamics
- Linear and nonlinear static analysis with contact and plasticity
- Normal modes analysis for real and complex eigenvalue analysis
- Direct and modal frequency response analysis
- Random response analysis
- Response spectrum analysis
- Direct and modal transient response analysis
- Coupled fluid-structure (NVH) analysis

Acoustic analysis in OptiStruct can be solved by performing harmonic analysis. The analysis calculates the pressure distribution in the fluid due to a harmonic load. A harmonic analysis, by definition, assumes that any applied load varies harmonically(sinusoidally) with time. To completely specify a harmonic load in an acoustic analysis, two pieces of information are usually required the amplitude and the forcing frequency. Amplitude describes the intensity of the load and the forcing frequency describes the interval of the repeating motion, more the frequency more frequent is the repetition.

4.2.2 Model description

The 3-D modelling should be done in a way similar to the modelling in case of computational fluid dynamic analysis. The reason being that we require only the extracted fluid volume for this purpose. Therefore, the geometry must be trimmed or modelled in such a way that only the surface which are in contact with the fluid were left at the end.

It is not necessary to model intricate details such as protrusions or small cavities, if the acoustic wavelength is so long that the acoustic wave will not be altered by the presence of the feature.

The acoustic simulation is performed for the two cases one is the simple expansion chamber and the other is the sample muffler the description of both the models are given in the following section

4.2.2.1 Single chamber muffler

Initially the analysis is performed on a simple expansion chamber for the sake of simplicity the geometrical dimension of which is shown in the Fig. 4.8


Φ 50

Φ 150

L= 50 mm

L= 550 mm
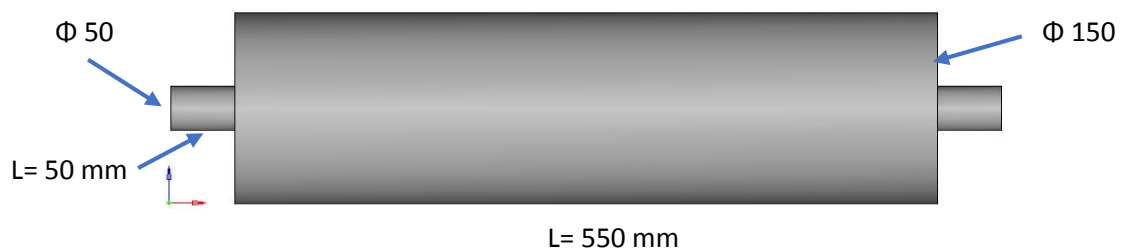
**Fig. 4.8: Single chamber muffler**

4.2.2.2 Sample muffler

The geometry of the sample muffler is same as described in the section 4.1.2. The geometry is further simplified for acoustic analysis i.e. only the part in contact with the fluid is retained and rest is removed. The various views of the sample muffler are shown in the Fig. 4.9. Although perforations can be seen on the tube connected to the diffuser but absorptive material is not modelled for the sample muffler.
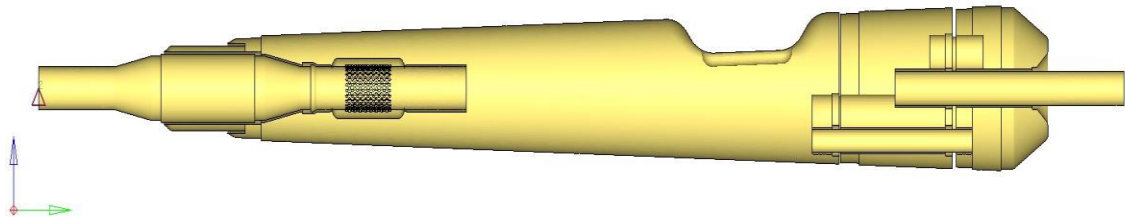
Fig. 4.9a: Front view of sample muffler
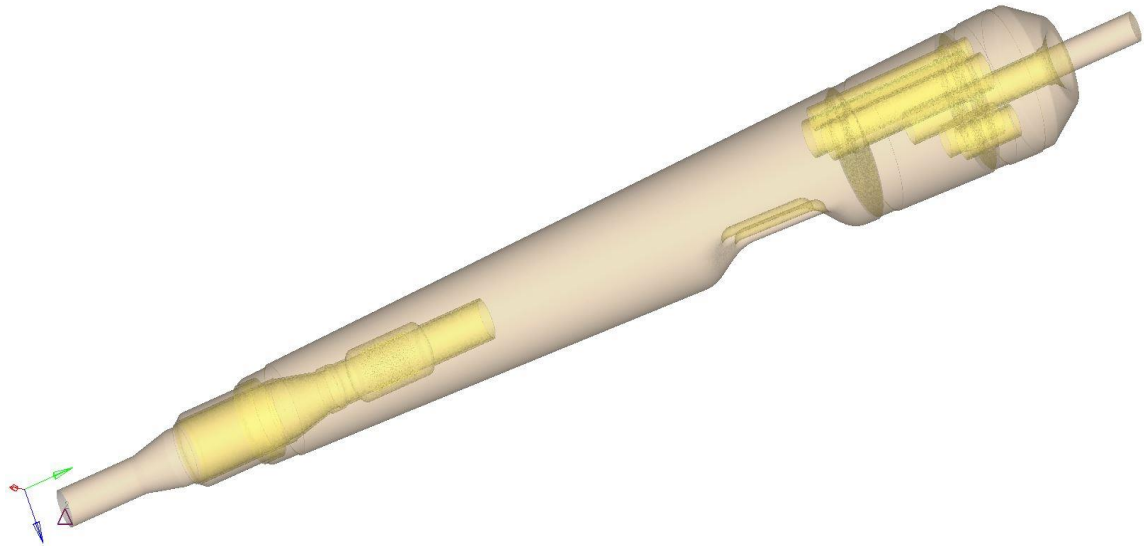
**Fig. 4.9b: Isometric view of sample muffler**
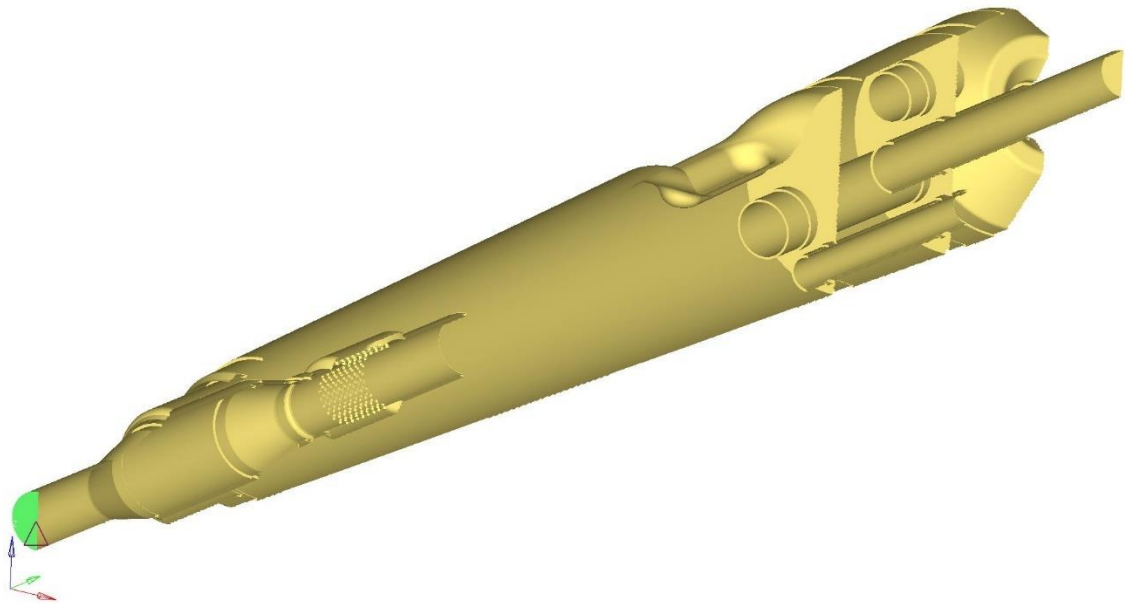
Fig. 4.9c: Section view of sample muffler

4.2.3 Mesh generation

It is very important to consider the acoustic wavelength when meshing the acoustic and structural models, as this will affect the accuracy of the results.

Finite element methods can be useful for low-frequency problems. However, as the excitation frequency increases the number of nodes and elements required in a model increases exponentially, requiring greater computational resources and taking longer time to solve. A general rule of thumb is that acoustic models should contain at least 6 elements per wavelength as starting point. For better accuracy, it is recommended to use 12 elements per wavelength.

4.2.3.1 Single chamber muffler
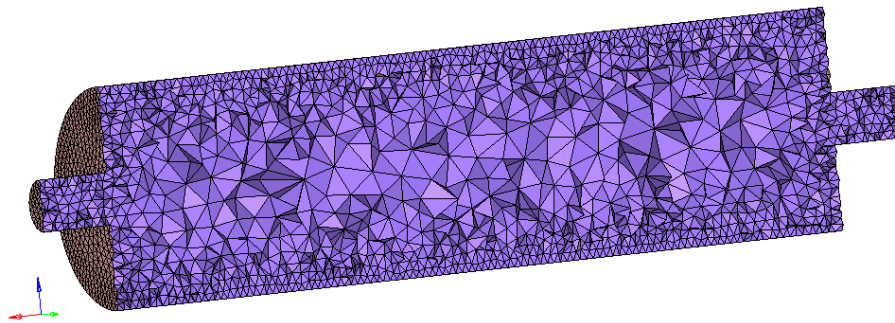
**Fig. 4.10: volume mesh Single chamber muffler**

The surface mesh is used to generate the three dimensional solid mesh for fluid The 2-D elements are triangular elements and 3-D elements are tetrahedral elements

4.2.3.2 Sample muffler

For the models used in this thesis, the maximum element size was set to 1mm. This would result in the max achievable frequency well over the max frequency of interest (2000Hz). The meshed model is shown in the Fig. 4.11

Because of less control over the solid mesh the element size is not uniform throughout. The algorithm is such that the element size keeps on growing from the surface to the inside of muffler. Thus it can be seen that there is fine mesh near the surface boundary and coarse mesh in the middle of the muffler. The perforations are meshed separately because of the small dimension, so that elements follow the surface of the perforations correctly.
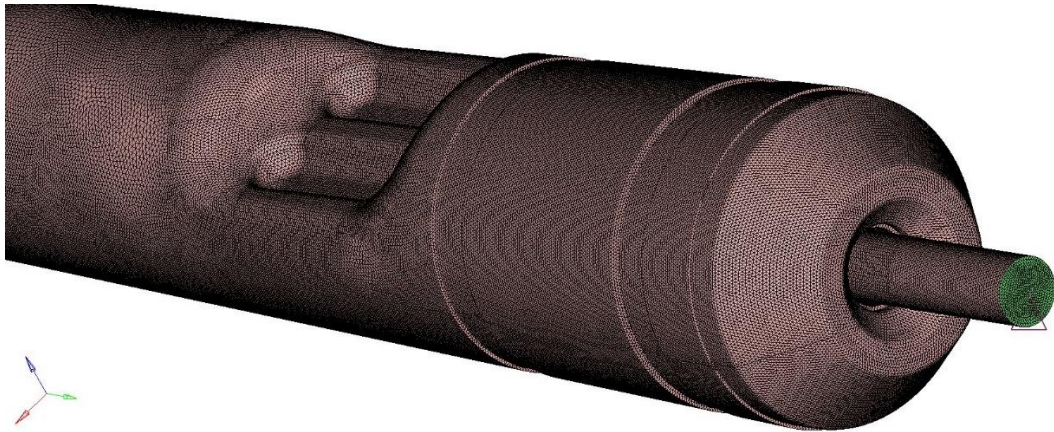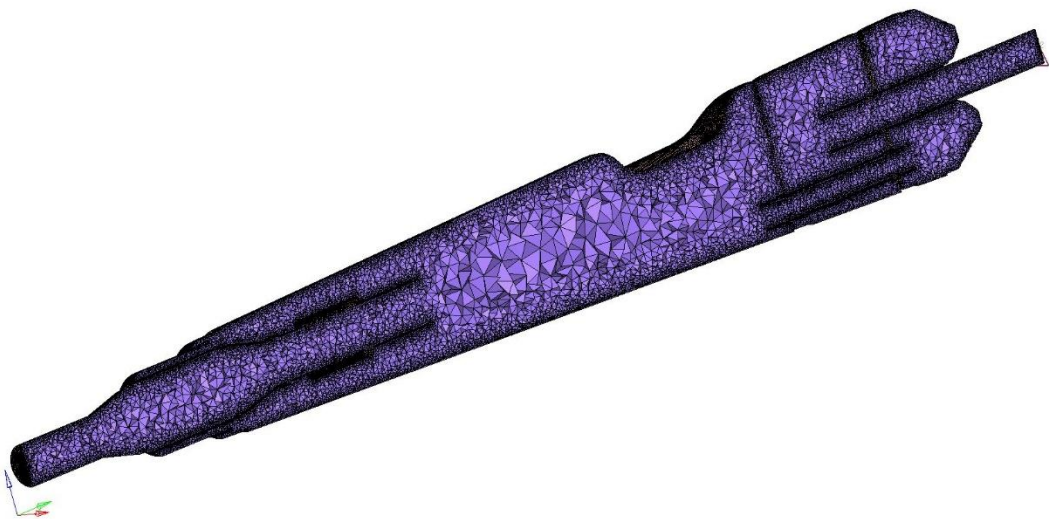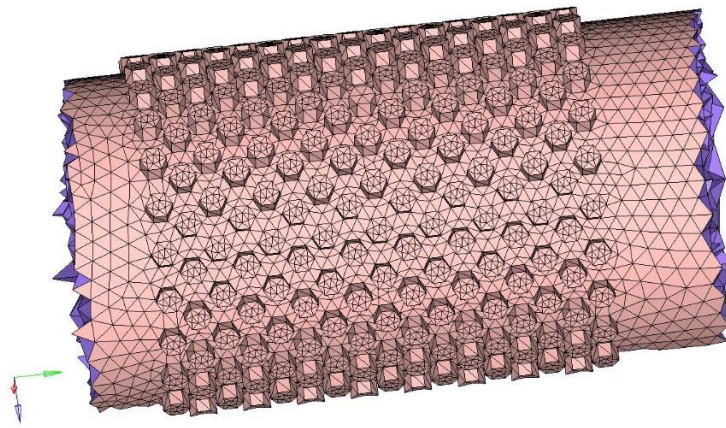
Fig. 4.11a: Surface mesh of sample muffler

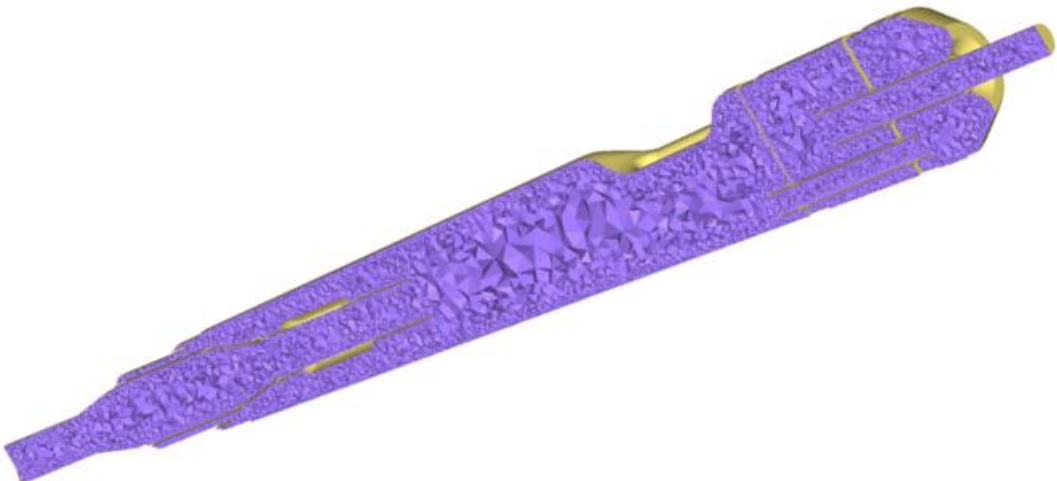**Fig. 4.11b: Section view of surface mesh of sample muffler**

Fig. 4.11c: Section view of volume mesh of sample muffler

89

Fig. 4.11d: Transparent view of volume mesh of sample muffler

Fig. 4.11e: volume mesh of perforated section

Fig. 4.11f: Section view of volume mesh with surface boundary

The 2-D surface elements are the triangular elements and the 3-D fluid elements are the tetrahedral elements. The information of the meshed model is shown in the Fig. 4.12

- **Finite element model information**

  Number of nodes: 1277134
  Number of elements: 5324574
  Number of degrees of freedom: 1967940
  Number of non-zero stiffness terms: 42306246

  - **Elements**
  Number of TRIA3 elements: 655844
  Number of PYRAF elements: 4668730

Fig. 4.12: Finite element model information of sample muffler

At regions in a model where there is a change in the acoustic impedance for example diameter change, a complex acoustic field can exist with steep pressure gradients. It is important to ensure that there is sufficient mesh density in these regions to accurately model a complicated acoustic field.

4.2.4 Material properties and boundary conditions

A coupled acoustic analysis takes the fluid-structure interaction into account. In the finite element method, the entire three-dimensional domain has to be discretized and modeled with volume elements. In deriving the discretized acoustic wave equation, there are some necessary assumptions:

- The fluid is compressible, but only relatively small pressure changes with respect to the mean pressure are allowed.
- The fluid is inviscid (no viscous dissipation).
- There is no mean flow of the fluid.
- The mean density and mean equilibrium pressure are uniform throughout the fluid.

All the meshed elements are moved into three components fluid, surface and the diaphragm. The three different are then assigned different properties which is described in the table 4.3

Table 4.3: Material properties of different elements

Surface	
Young's modulus of elasticity (E)	210000 N/mm^2
Poisson's ratio	0.33
Density	$8\times10^{-6} \text{ Kg/mm}^3$

Diaphragm	
Young's modulus of elasticity (E)	3400 N/mm^2
Poisson's ratio	0.3
Density	4.5×10^{-10} Kg/mm^3
Fluid (air)	
Density	1.2×10^{-9} Kg/mm^3
Speed of sound	343000 mm/sec

The surface and diaphragm both are assigned a property of shell elements with the thickness of 1mm and 0.05 mm respectively.

The purpose of this analysis is to develop an approach but in this case two source method is employed for the problem setup unlike the two load method in the experimental investigation because of modelling different loads in the software. And if there are not substantial differences between the two loads attached at the termination, then the equation for TL breaks down. Therefore, a much more feasible and accurate method is the two source-location method which is not limited to these shortcomings.

The output frequency range for the analysis is 2000 Hz and the Eigen modes considered for this problem are 200. The Eigen modes covers the frequency range of interest and are well above it. This is required because in the frequency response modal analysis the solver first calculates the modes of the fluid and the structure independently and after that it uses the calculated modes for the simultaneous solution of the wave equation.

The diaphragm is assigned a frequency dependent dynamic load of the form given in Eq. 4.1

$$f(\Omega) = A[C(\Omega) + iD(\Omega)]e^{i(\theta - 2\pi\Omega\tau)} \qquad (4\text{-}1)$$

Where

θ is the phase and τ is the time delay. Ω is a variable that defines the frequency range. No delay and phase are given in this problem, also unit amplitude is given.

The load is applied in such a way so that it mimics the white noise, as produced by the specially designed speaker. Therefore, it is assigned a constant value at all the frequencies by defining a dynamic load tabular function.

Fluid-structure interaction (FSI) is specified by applying a card which defines fluid-structure interface. Damping is specified for both structure and fluid as 0.06 and 0.12 using control card. This uniform structural damping coefficient is obtained by multiplying the critical damping [C/C0] ratio by 2.0. For the output of the frequency response analysis the pressure (complex) is specified as the output request in the control card.
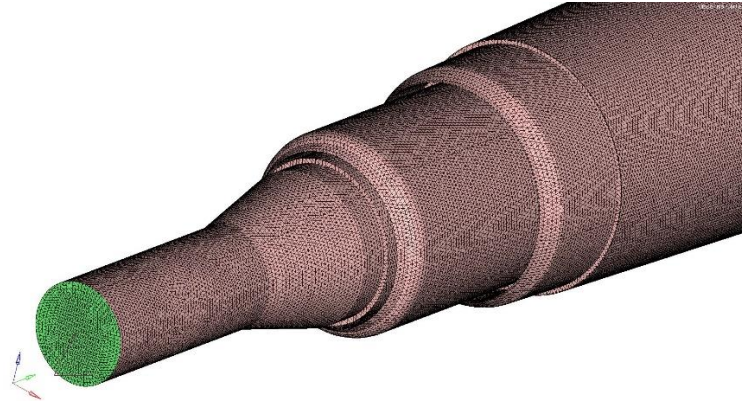
Fig. 4.13: Front source: engine exhaust side

Two runs are required for this analysis one with the diaphragm to the engine exhaust side and other with the diaphragm to the tail pipe side, which is necessary for the prediction of four pole parameters. The green color in Fig.4.12, 4.13 shows the positions of source for the two cases.
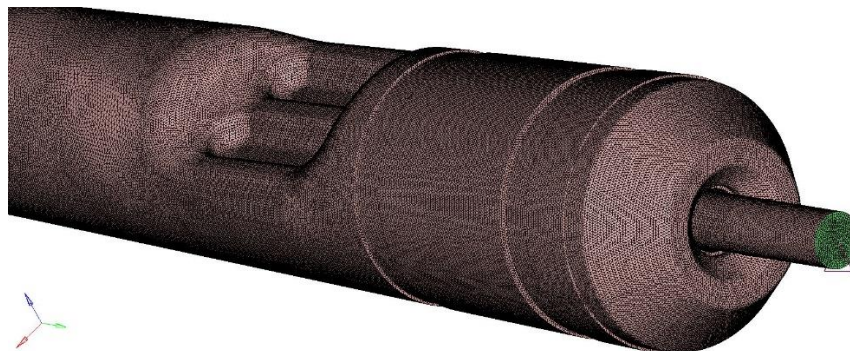
Fig. 4.14: Rear source: tail pipe side

The complex pressure values obtained from the simulation are used further to calculate the transmission loss of the muffler (as given in the section 3.2.1).

CHAPTER 5

RESULTS & DISCUSSION

The discussion from the previous chapters led to analyze the behavior of the muffler based on the findings from the experimental and simulated results. Comparing experimental results to predictions gives insight into the accuracy of the predictions, the validity of simulated results, and the performance of the muffler systems themselves.

5.1 Computational fluid dynamic analysis

The CFD results of the sample muffler are shown in the following sections. Post-processing of results was done in AcuField View 13.0, a post-processing and visualization environment for finite element and CFD analysis. The results obtained from the simulation run for both, steady state and transient state are:

5.1.1 Steady state contour plots

The steady state contour plots for the velocity, pressure and temperature are shown in the Fig. 5.1 to 5.3

Parallel streamlines to the length of the muffler can be seen between inlet of the muffler and the first baffle. After the first baffle the turbulent behavior persists.
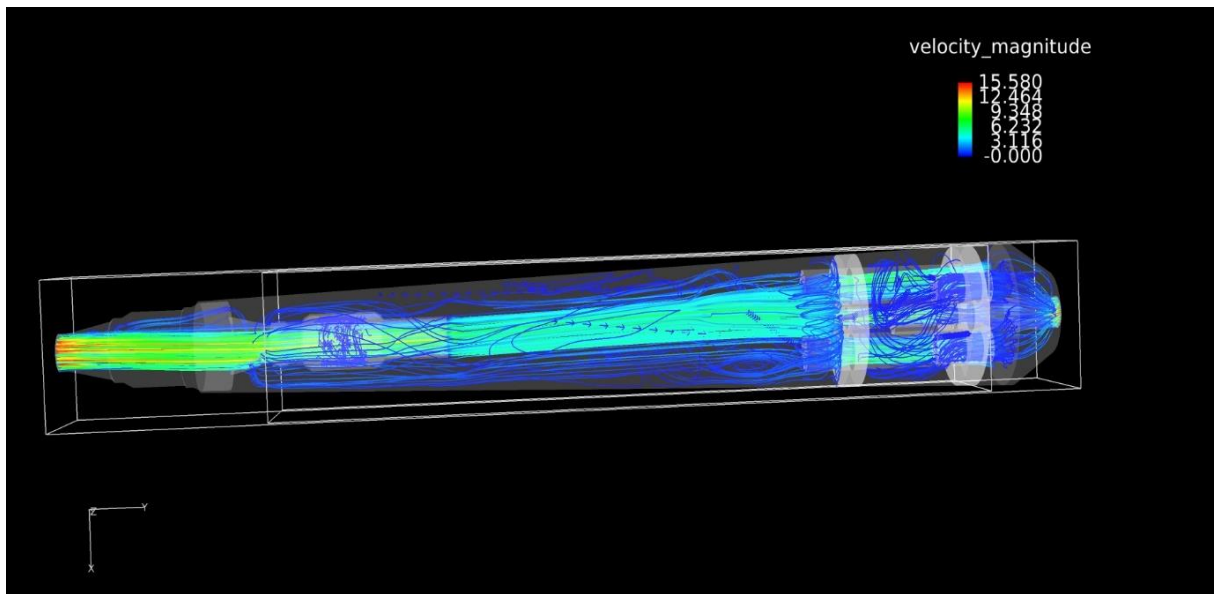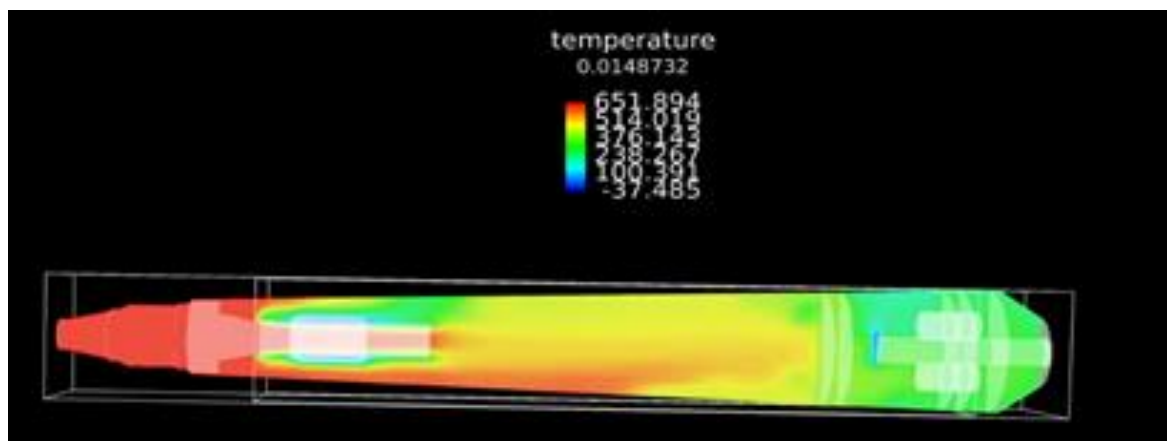

Fig. 5.1: Steady state contour plot for velocity

The maximum velocity obtained has the magnitude of 15.580m/s at the very inlet and the velocity at the boundary surface is zero or nearly zero which should be the case as the fluid has to satisfy the no slip condition.

In muffler there should be no backpressure because it will cause reduction in the volumetric efficiency which is responsible for the reduction in power (as discussed in section 2.1). It can be seen from the Fig. 5.2 that the pressure has the same magnitude over the entire length and maximum pressure has magnitude of 101.5 kpa. The pressure drop comes out to be 1.85 kpa considering the inlet of the muffler and the tail pipe
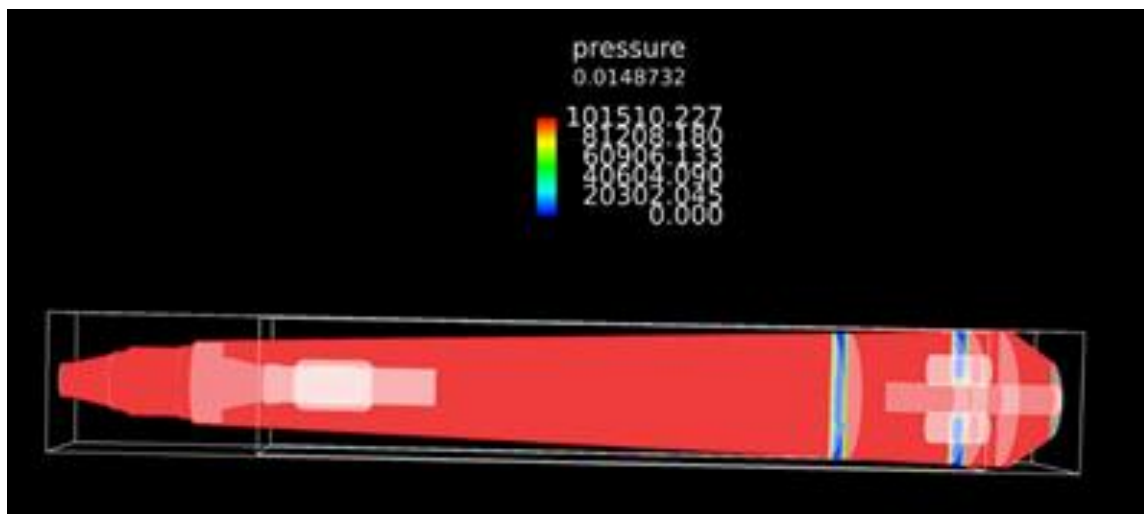
**Fig. 5.2: Steady state contour plot for pressure**

Fig. 5.3: Steady state contour plot for temperature

Maximum temperature comes out to be 651 kelvin at the inlet and as the fluid flows through the length of the muffler it loses the energy and get cools down. Therefore, the temperature at the end of muffler got reduced to 318 kelvin. The temperature drop comes out to be 333 kelvin.
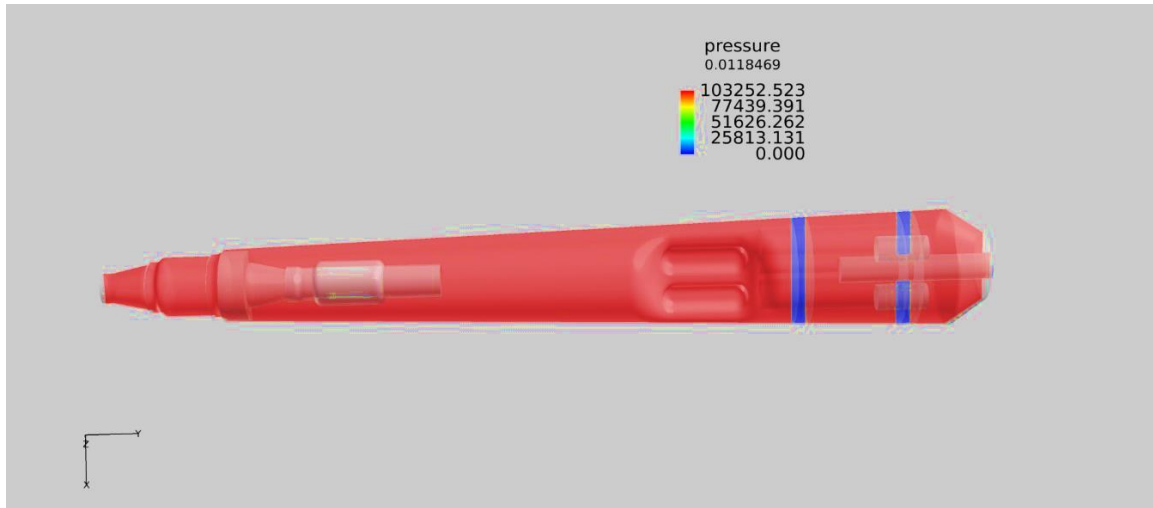
5.1.2 Transient state contour plots

The flow of gases through the exhaust port is highly unsteady therefore transient state analysis is the true representation of the flow behavior inside the muffler. Results are calculated over a time span of 120 sec. Solver controls are defined in terms of maximum time steps, final time, initial time increment and the convergence tolerance. The residual control can be taken care of with the convergence tolerance. But it should be kept in mind that the accuracy of the results also gets affected. So it must be defined in such a way that the results accuracy is not compromised. The transient state contour plots for the velocity, pressure and temperature are shown in the Fig. 5.4 to 5.6
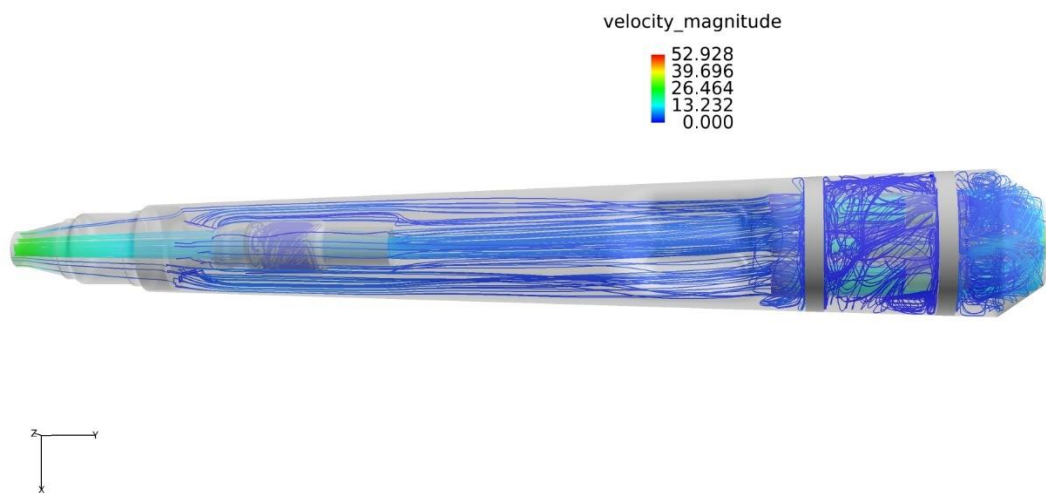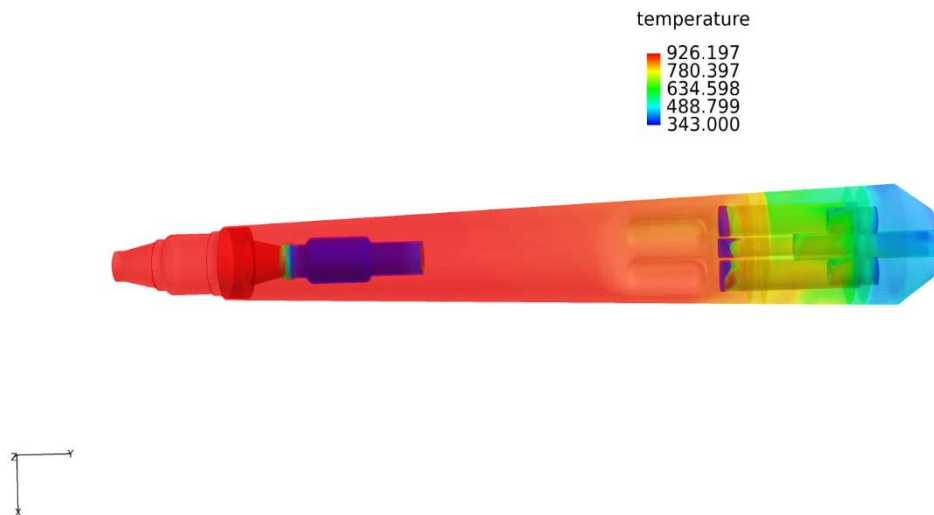

Fig. 5.4: Transient state contour plot for velocity

The velocity distribution plot shown in the Fig. 5.4 is obtained after the completion of the time step given in the solution sequence. At that time the flow is completely developed and therefore the velocity magnitude shown here is for the fully developed flow. The maximum velocity comes out to be 53 m/s (approx.). Apart from this value all other values seems to be practically feasible and the results looks satisfactory. The boundary surface velocity is zero which is the case for the no slip condition, as already discussed in the section 5.1.1 which proves that number of boundary layers taken during the meshing is sufficient to see the velocity distribution near the walls. The turbulent streamlines can be seen between the two baffles and at the exit.

Fig. 5.5: Transient state contour plot for pressure

The complete pressure distribution for the overall time span and along the length of the muffler is shown in the Fig. 5.5. It can be seen that the pressure distribution is uniform throughout the length of the muffler. Some variation in the values seen in the pressure profile is near the perforations on the tube connected to the diffuser and the shared boundary of the two baffles and the muffler main body. The maximum magnitude of the pressure is 103.25 kpa and the pressure drop between the inlet of the muffler and the tail pipe comes out to be 91 kpa.


Fig. 5.6: Transient state contour plot for temperature

Fig. 5.6 shows the variation of the variation of the temperature inside the muffler. The maximum temperature comes out to be 926 kelvin at the diffuser inlet and as the fluid

flows to the end of muffler it cools down to a temperature of around 400 kelvin. The maximum temperature drop is of the magnitude of 526 kelvin.

5.2 Experimental Testing

The calculated transmission loss with the help of experimental data using equations in the section 3.2a, for the sample muffler is shown in the Fig. 5.7
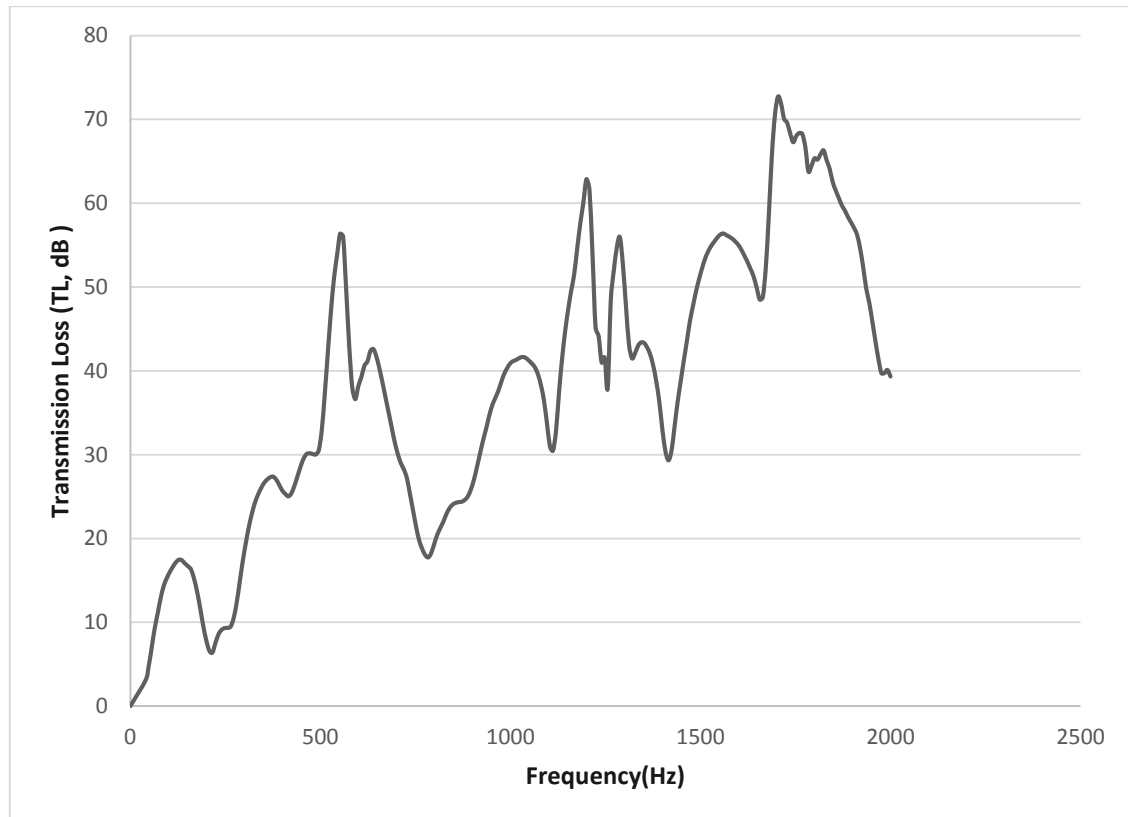
Fig. 5.7: Experimental results of sample muffler

5.2.1 Observations

▪ The average TL of the sample muffler upto frequency 2000 Hz comes out to be 38 dB

▪ Three peaks are encountered in the frequency span of 2000 Hz

▪ First peak was obtained at a frequency of 552 Hz with a TL of 56.4 dB

▪ Second peak was obtained at a frequency of 1200 Hz with a TL of 62.9

▪ Third peak was obtained at a frequency of 1704 Hz with a TL of 72.7 dB

▪ The minimum transmission loss (TL) between 1000 Hz to 2000 Hz is 30 dB

98

- Because of the presence of the absorption elements inside the muffler which mainly works in the mid to high frequency range we can also see significant transmission loss at higher frequencies

5.3 Acoustic analysis

The transmission loss results of the single chamber muffler and the sample muffler are shown in the following sections. Post-processing of results was done in HyperView 13.0 which allows to see the results in the graphical format.

5.3.1 Single chamber muffler

5.3.1.1 Front source

The complex pressure output values obtained from the graph are seen in the Fig. 5.8 and 5.9. The grid points where the output is taken in order of location 1,2,3,4 are 3, 23, 10103,10123

The distance between the first two output locations is 33.375 mm and one can see in the graphs, that while travelling this distance the sound waves magnitude is greatly reduced. Grid point 3

Grid point 3   **Grid point 23**
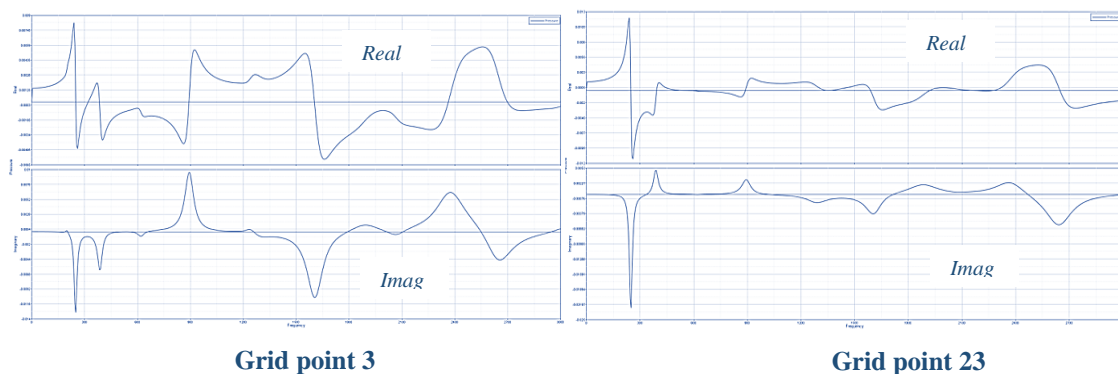
Fig. 5.8: Pressure at grid points 3 and 23 in single chamber muffler (front source)

has pressure variation throughout the frequency range but grid point 23 has significant pressure variation only in the frequency range of 0-600 Hz.

Distance between the last two output locations is 33.345 mm which is almost similar to the first case and similar pattern of pressure output can be seen in the graphs of grid point 10103 and 10123. But there is significant difference in the magnitude of obtained pressure.

Grid point 10103   Grid point 10123
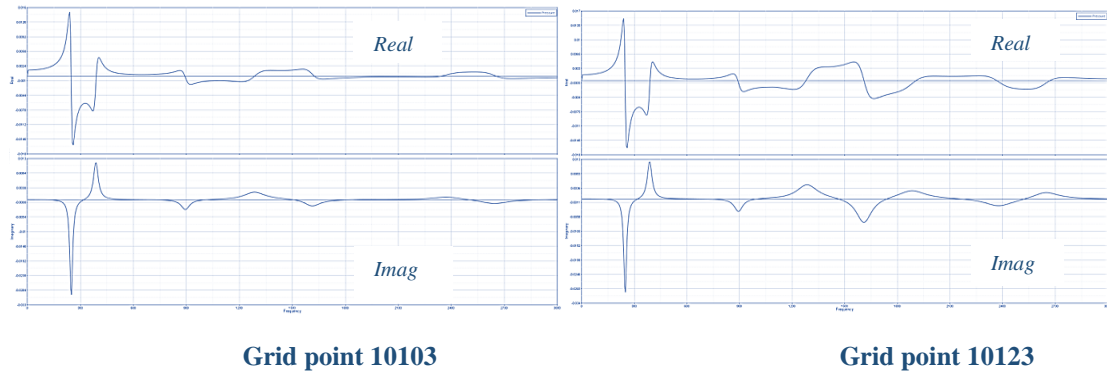
Fig. 5.9: Pressure at grid points 10103 and 10123 in single chamber muffler (front source)
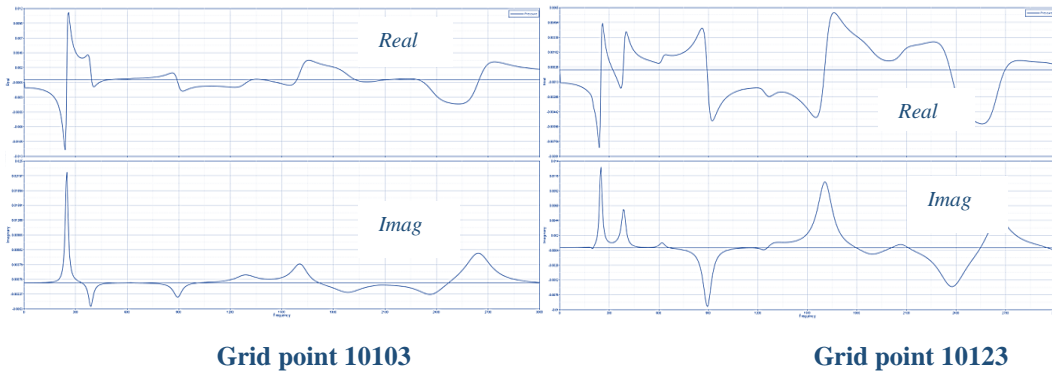
5.3.1.2 Rear source

In this case the source location is reversed and the sound pressure output are shown in the Fig. 5.10 and 5.11

If we compare the sound pressure at the grid point 3 for the two cases i.e. for the front source and the rear source we will found that there is significant difference in the pressure amplitude

Grid point 3   Grid point 23
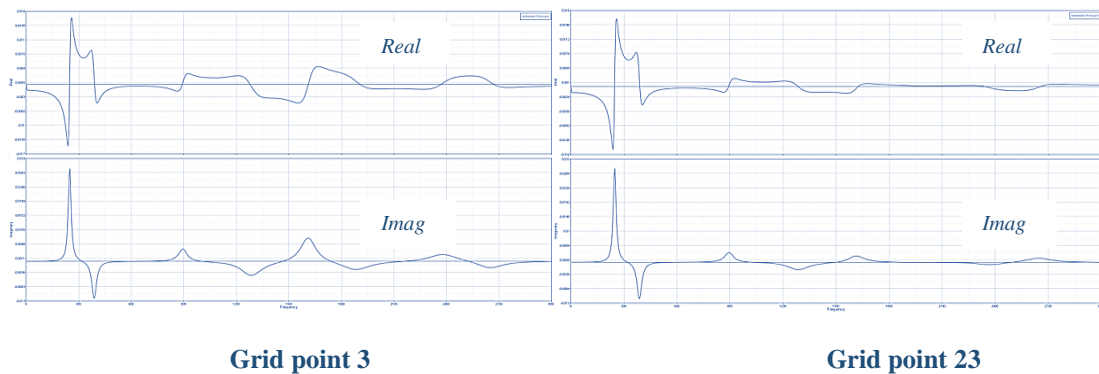
Fig. 5.10: Pressure at grid points 3 and 23 in single chamber muffler (rear source)

This is because of the change in the position of the vibrating source. The sound pressure could not be able to reach upto grid point 3 there is significant loss of sound pressure between the two far most point.

Grid point 10103   Grid point 10123

Fig. 5.11: Pressure at grid points 10103 and 10123 in single chamber muffler (rear source)

The transmission loss obtained after calculation using the above mentioned sound pressure values is shown in the Fig. 5.11

The maximum transmission loss obtained is of magnitude 24.3 dB at a frequency of 1745 Hz.
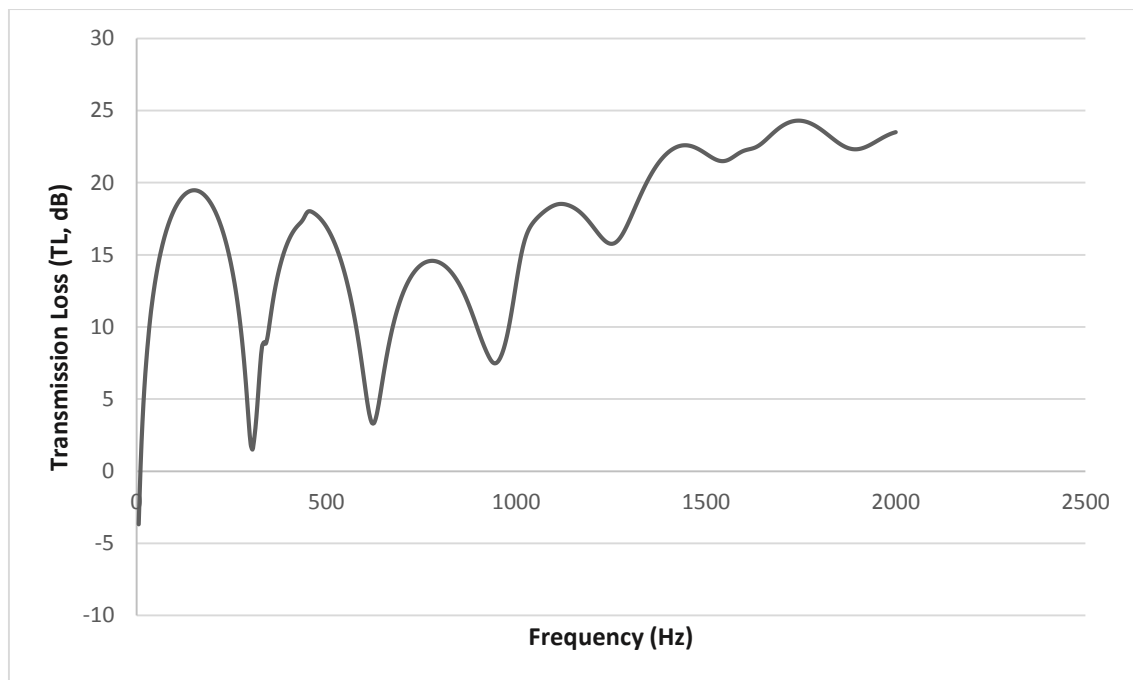
Fig. 5.12: Acoustic analysis result of single chamber muffler

5.3.1.3 Validation of results

The analytical results are obtained from the calculation based on the formula given in the appendix. A repeatable pattern can be seen in the analytical results. The TL becomes equal

to zero when the frequency is a multiple of $\frac{c}{2l}$ and its peak occurs when the frequency is a multiple of $\frac{c}{4l} + n * \frac{c}{2l}$, where c is the speed of sound and l is the length of the chamber and n is whole number. This occurs because the reflected sound wave has to travel a distance of $2l$ to reach the source of origin and it is 180° out of phase with the original sound wave. Therefore, when the two waves meet then cancellation of amplitude occurs and the resultant magnitude comes out to be zero. If the reflected wave is in phase with the original wave, then the resultant magnitude is an addition of the magnitude of two waves thus a peak occurs.

The simulation results match perfectly well with the experimental results upto a frequency of 270 Hz. There is only one absurd value of transmission loss -3 dB, which occurs at a frequency of 5 Hz except that the simulation results overlaps with the analytical, approximately.

Even upto 935 Hz frequency, the results are in good agreement with the analytical results with an offset 2 dB and 5 dB in the first and second peaks respectively.

Beyond this frequency range the results shows great deviation from the analytical results because the sound pressure at the grid locations is not significant, the possible reason for which could be the mesh density.
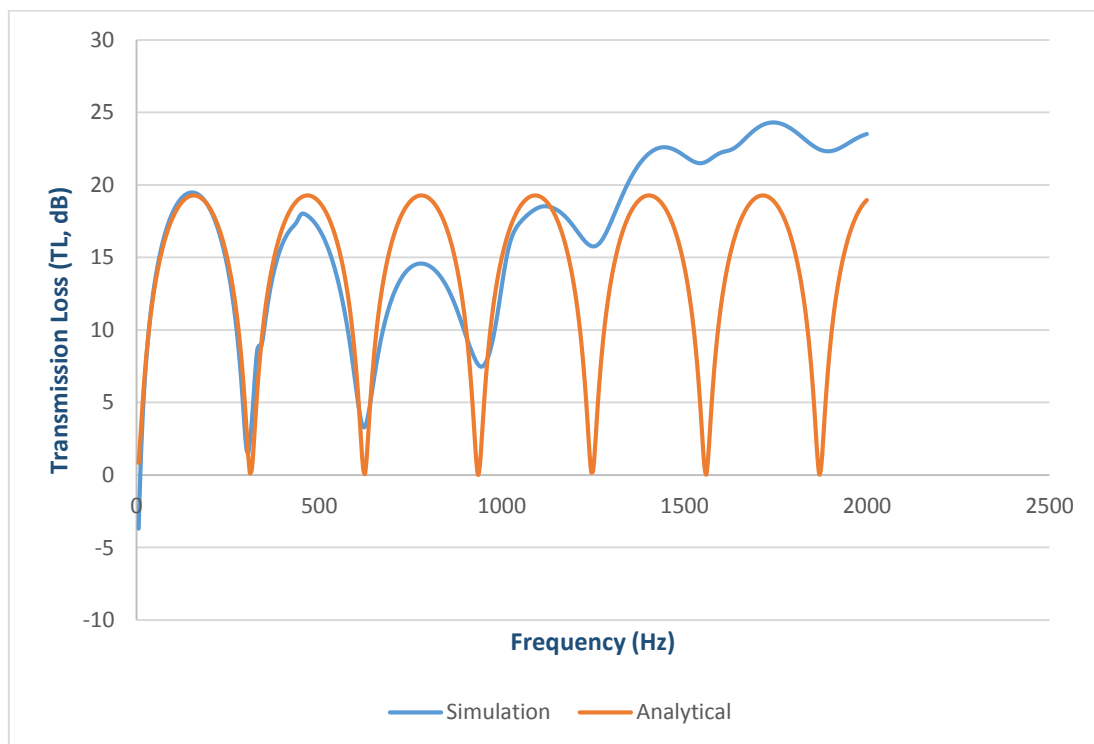

Fig. 5.13: Comparison of analytical and simulation results of single chamber muffler

5.3.2 Sample muffler
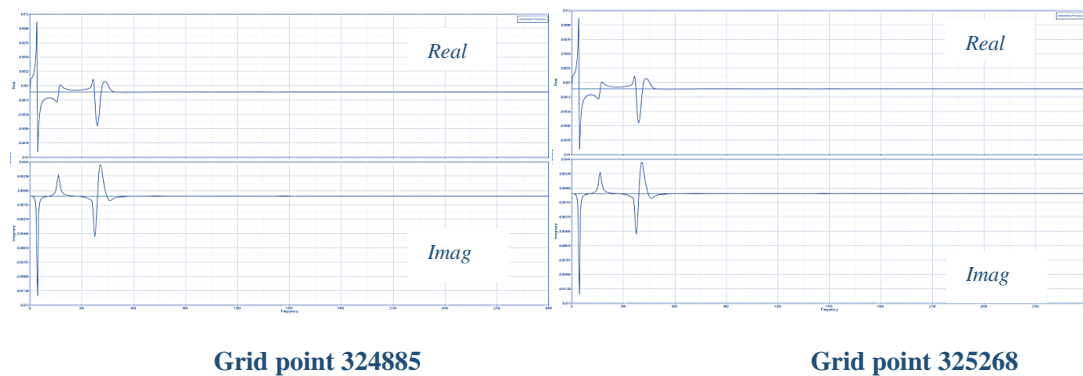
5.3.2.1 Front source

The complex pressure output values obtained from the graph are seen in the Fig. 5.14 to 5.15. The grid points where the output is taken in order of location 1,2,3,4 are 321223, 323040, 325268, 324885

The distance between the first two output locations is 8.591 mm. As the distance between the first two locations of output is small therefore not much variation can be seen in the sound pressure of these two by looking at the graphs but there is difference in the values obtained.

Grid point 321223   **Grid point 323040**
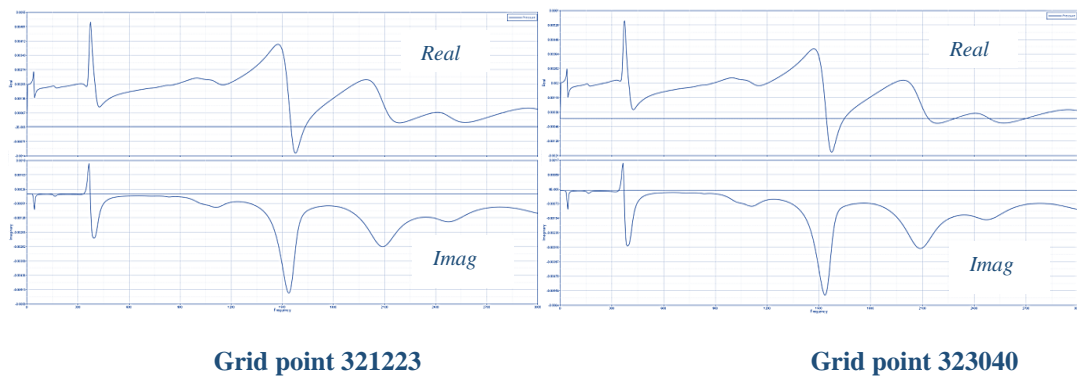
Fig. 5.14: Pressure at grid points 321223 and 323040 in sample muffler (front source)

The length of the sample muffler is very large as compared to the single chamber muffler therefore, the variations in the sound pressure could not be transferred to the end of the

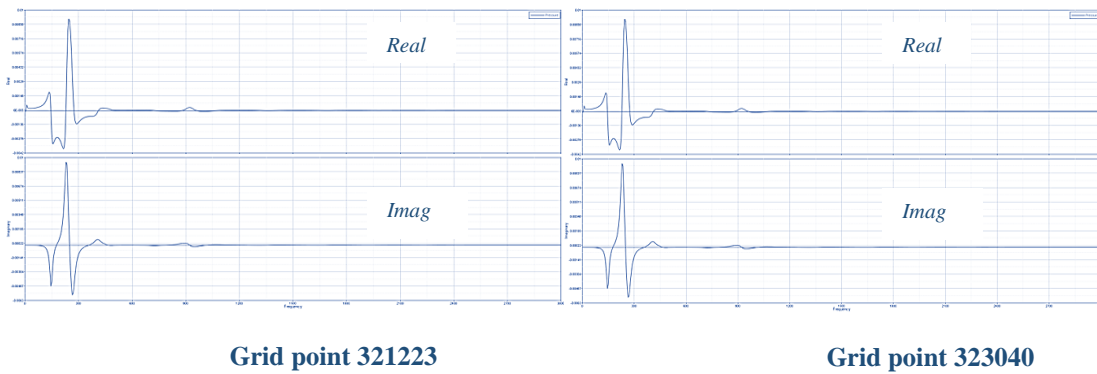**Grid point 324885**   **Grid point 325268**

Fig. 5.15: Pressure at grid points 324885 and 325268 in sample muffler (front source)

muffler resulting in a variation in the pressure only upto a certain frequency rage and beyond that it vanishes. Same behavior can be seen in the graph of the ast two locations because of a small distance of 10.005 mm.

5.3.2.2 Rear source

In this case the source location is reversed and the sound pressure output are shown in the Fig. 5.16 and 5.17

It seems that the results are reversed (although there is difference in magnitudes) which should be the case because the source are reversed.

Grid point 321223   Grid point 323040

Fig. 5.16: Pressure at grid points 321223 and 323040 in sample muffler (rear source)

Grid point 324885   Grid point 325268
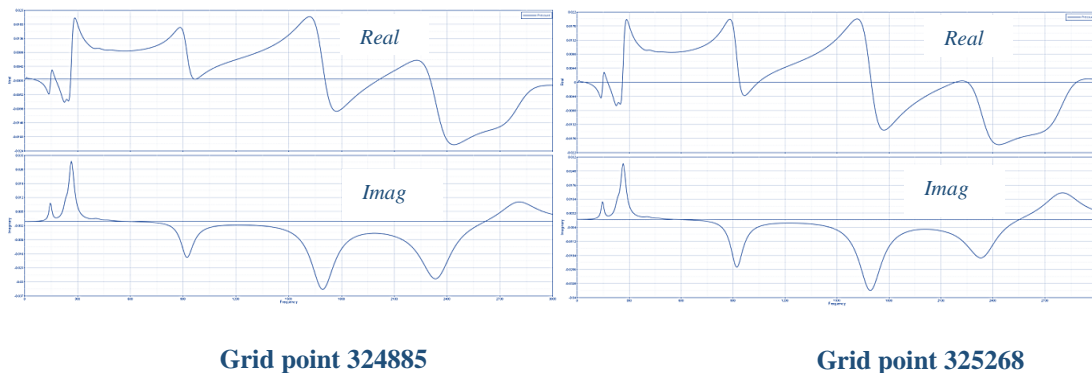
Fig. 5.17: Pressure at grid points 324885 and 325268 in sample muffler (rear source)

The transmission loss obtained after calculation using the above mentioned sound pressure values is shown in the Fig. 5.18

There is not any repeatable pattern in the graph. The maximum transmission loss obtained is of magnitude 74.4 dB at a frequency of 1815 Hz.
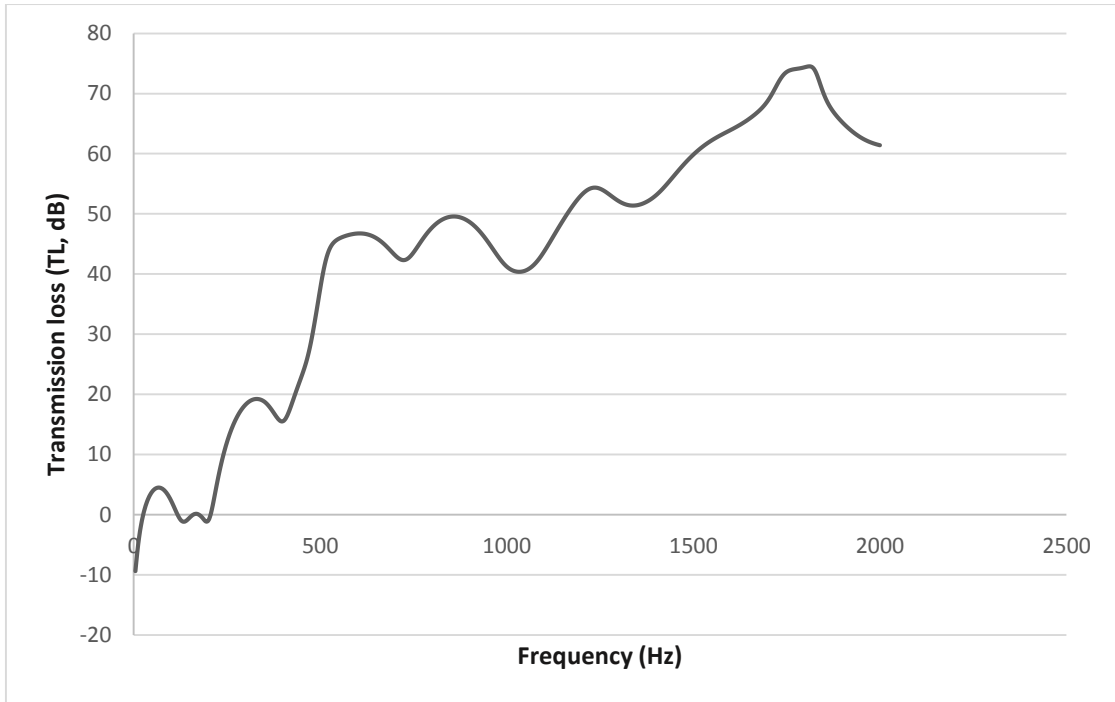
Fig. 5.18: Acoustic analysis results of sample muffler

5.3.2.3 Comparison of results
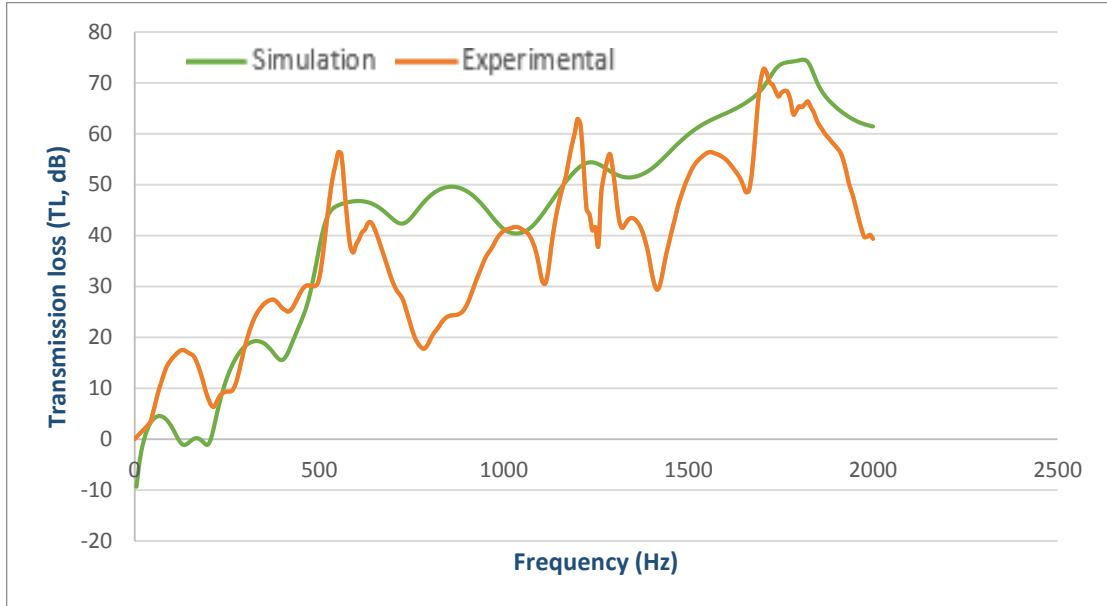
Fig. 5.19: Comparison of experimental and simulation results of sample muffler

The simulation curve follows the experimental curve upto a frequency of 560 Hz with a little offset which shows that analysis results are in good correlation with the experimental. The little offset in the results is because of the mesh density.

105

Beyond 560 Hz simulation results does not match very well with the experimental results although the maximum values at the peaks obtained in the analysis are close to the experimental values.

The reasons behind the deviation of the simulation results are that the absorptive material condition is not modelled in the simulation model which is the reason for the high frequency attenuation, plane wave condition is not cross-checked which could also be the possible reason and anechoic termination is not provided in the modelling.

CHAPTER 6
CONCLUSION & FUTURE SCOPE

The thesis is aimed to find out the performance characteristics of a two wheeler muffler for which various finite element tools was used. AcuSolve is used for the computational fluid dynamics analysis (CFD) and OptiStruct for the acoustic analysis. The CFD results are derived for sample muffler and for acoustic analysis firstly, the Transmission Loss assessment was done for a simple expansion chamber the results of which was used for comparison. Then, the same implementation procedure was applied on a sample muffler and the computational results was compared with experimental TL data.

On the basis of results and understanding of concepts the following conclusions can be made.

6.1 Conclusions

- AcuSolve is one of the best solver for the for CFD analysis. The modelling and problem setting is very easy. If problem is modelled correctly one cannot get unrealistic results

- Because of the calculations at the nodal level mesh control is not a primary importance while solving a CFD problem in AcuSolve

- Due to the gradual development transient state analysis is a true representation of the muffler's flow performance.

- The sample muffler has better attenuation of sound at mid to high level frequency as compared to low frequency with maximum transmission loss reaching upto 72 dB approx.

- There is need of optimization of design of the sample muffler for the low frequency attenuation as most of the sound in the internal combustion engines lies in the low frequency range. Improvement is also required to increase the average transmission loss of muffler which is 38 dB according to the present experimental data.

- Although the transmission loss result of the single expansion chamber shows a deviation at the higher frequencies but it is sufficient to show the capability of OptiStruct which could prove to be better and economical solver as compared to the other commercially available finite element acoustic codes.

- The distance between the locations of output also affects the accuracy of the transmission results.
- The predicted curve of transmission loss for the sample muffler well agree upto a frequency, with the experimental trend. Some amplitude and frequency shift exist which shows further improvement is required in meshing and problem setting.

6.2 Future Scope

- For the sample muffler only the reactive elements are modelled which can be extended to include the absorptive elements also.
- No sound absorption elements are present in the sample muffler model which is required for an anechoic termination
- Mean flow and temperature effects can be taken into account for a realistic simulation

References

[1] Shah, S., Kuppili, S., Hatti, K., & Thombare, D. (2010). *A Practical Approach towards Muffler Design, Development and Prototype Validation* (No. 2010-32-0021). SAE Technical Paper.

[2] Munjal, M. L. (1987). *Acoustics of ducts and mufflers with application to exhaust and ventilation system design.* John Wiley & Sons.

[3] Ferguson C, Kilpatrick A. *Internal combustion engines.* John Wiley & Sons.

[4] Munjal, M. L. (2013). *Noise and Vibration Control.* World Scientific.

[5] Bodén, H., & Glav, R. (2008). *Exhaust and intake noise and acoustical design of mufflers and silencers.* Handbook of Noise and Vibration Control, 1034-1053.

[6] Prasad, M. G., & Crocker, M. J. (1981). *Insertion loss studies on models of automotive exhaust systems.* Journal of the Acoustical Society of America, 70(5), 1339-1344.

[7] Gupta, V. H., & Munjal, M. L. (1992). *On numerical prediction of the acoustic source characteristics of an engine exhaust system.* Journal of the Acoustical Society of America, 92(5), 2716-2725.

[8] Fang, J. H., Zhou, Y. Q., Hu, X. D., & Wang, L. (2009). *Measurement and analysis of exhaust noise from muffler on an excavator.* International Journal of Precision Engineering and Manufacturing, 10(5), 59-66.

[9] Tao, Z., & Seybert, A. F. (2003). *A review of current techniques for measuring muffler transmission loss.* (No. 2003-01-1653). SAE Technical Paper.

[10] Seybert, A. F., & Ross, D. F. (1977). *Experimental determination of acoustic properties using a two-microphone random-excitation technique.* Journal of the Acoustical Society of America, 61(5), 1362-1370.

[11] Åbom, M., & Bodén, H. (1988). *Error analysis of two-microphone measurements in ducts with flow.* The journal of the acoustical society of America, 83(6), 2429-2438.

[12] Heywood J. *Internal Combustion Engine Fundamentals.* Tata McGraw-Hill

[13] Barron R F. *Industrial Noise Control and Acoustics.* CRC Press

[14] Mechel, F. P. (2013). *Formulas of acoustics.* Springer Science & Business Media.

[15] Han, H. S., Chae, S. S., & Kim, Y. C. (2000, June). *Analytical design of muffler based on transmission loss calculation.* Fisita world automotive congress. Seoul 2000

[16] Rahman, M., Sharmin, T., Hassan, A. F. M. E., & Al Nur, M. (2005, December). *Design and Construction of a Muffler for Engine Exhaust Noise Reduction.* Proceedings of the International Conference on Mechanical Engineering (ICME2005) (pp. 28-30).

[17] Potente, D. (2005, November). *General design principles for an automotive muffler.* Proceedings of ACOUSTICS (pp. 153-158).

[18] El-Sharkawy, A. I., El-Chazly, N. M. (1987). *A critical survey of basic theories used in muffler design and analysis.* Applied Acoustics, 20(3), 195-218.

[19] Mehdizadeh, O. Z., Paraschivoiu, M. (2005). *A three-dimensional finite element approach for predicting the transmission loss in mufflers and silencers with no mean flow*. Applied Acoustics, 66(8), 902-918.

[20] Dhaiban, A. A., Soliman, M. E. S., El-Sebaie, M. G. (2011). *Finite Element Simulation of Acoustic Attenuation Performance of Elliptical Muffler Chambers*. Journal of Engineering Sciences, Assiut University, 39(6), 1361-1373.

[21] Fan, W., Guo, L. X. (2016). *An Investigation of Acoustic Attenuation Performance of Silencers with Mean Flow Based on Three-Dimensional Numerical Simulation*. Shock and Vibration, 2016.

[22] Parlar, Z., Ari, S., Yilmaz, R., Özdemir, E., Kahraman, A. (2013, March). *Acoustic and Flow Field Analysis of a Perforated Muffler Design*. Proceedings of World Academy of Science, Engineering and Technology (No. 75, p. 715). World Academy of Science, Engineering and Technology (WASET).

[23] Jones, P., Kessissoglou, N. (2009). *An evaluation of current commercial acoustic FEA software for modelling small complex muffler geometries: Prediction vs Experiment*. Proc. ACOUSTICS 2009.

[24] Panicker, V. B., Munjal, M. L. (2013). *Aeroacoustic analysis of straight-through mufflers with simple and extended tube expansion chambers*. Journal of the Indian Institute of Science, 63(1), 1.

[25] El-Sharkawy, A. I., Nayfeh, A. H. (1978). *Effect of an expansion chamber on the propagation of sound in circular ducts*. The Journal of the Acoustical Society of America, 63(3), 667-674.

[26] Özdemir, E., Yılmaz, R., Parlar, Z., Arı, Ş. (September 2013). *An analysis of geometric parameters 'effects on flow characteristic of a reactive muffler*. International Research/Expert Conference" Trends in the Development of Machinery and Associated Technology", Istanbul, Turkey.

[27] Thawani, P. T., Doige, A. G. (1983*). Effect of mean flow and damping on the performance of reactive mufflers*. Canadian Acoustics, 11(1), 29-47.

[28] Byrne, K., Skeen, M., Kessissoglou, N. (2006, November). *Measurement of the sound transmission loss of a small expansion chamber muffler to consider the effects of mean flow and wall compliance*. Proceedings of ACOUSTICS (pp. 257-264).

[29] Gupta A K (April, 2016). *Transmission loss of cylindrical muffler with different length to diameter ratio by using two load method and simulation tool*. IJESMR, ISSN 2349-6193

[30] Gupta, A. K., Tiwari, A. (2015). *Enhancement on Sound Transmission Loss for Various Positioning of Inlet and Outlet Duct of the Muffler*. International Journal of Engineering and Manufacturing (Hong Kong), IJEM-V5 N, 4.

[31] Pratap, A., Kalita, U., & Kumar, S. *Effect of perforated tube on transmission loss of muffler-a review*. International Journal of Engineering Research and General Science Volume 3, Issue 3, May-June, 2015

[32] Panigrahi, S. N., & Munjal, M. L. (2007). *Backpressure considerations in designing of cross flow perforated-element reactive silencers*. Noise Control Engineering Journal, 55(6), 504-515.

[33] Liu, L. Y., Hao, Z. Y., & Liu, C. (2012*). CFD analysis of a transfer matrix of exhaust muffler with mean flow and prediction of exhaust noise*. Journal of Zhejiang University SCIENCE A, 13(9), 709-716.

[34] Rajadurai S, Sukumaran S, Madhusudhanan P. *CFD Analysis for Flow through Glass Wool as Porous Domain in Exhaust Muffler*. International Journal of Innovative Science, Engineering & Technology, Vol. 1 Issue 7, September 2014.

[35] Saripalli, P., Sankaranarayana, K. *CFD Analysis on Flow Through a Resistance Muffler of LCV Diesel Engine.* International Journal of Science, Technology and Society,2015; 3(4): 132-145

[36] Bilawchuk, S., & Fyfe, K. R. (2003). *Comparison and implementation of the various numerical methods used for calculating transmission loss in silencer systems*. Applied Acoustics, 64(9), 903-916.

[37] Gerges, S. N. Y., Jordan, R., Thieme, F. A., Bento Coelho, J. L., & Arenas, J. P. (2005). *Muffler modeling by transfer matrix method and experimental verification*. Journal of the Brazilian Society of Mechanical Sciences and Engineering, 27(2), 132-140.

[38] Andersen, K. S. (2008). *Analyzing muffler performance using the transfer matrix method*. COMSOL Conference.

[39] Nuñez, I. J. C., Marqui, D., Libardi, A. L., Cavaglieri, M., Arruda, J. R. D. F. (2008). *Investigating the transmission loss of compressor suction mufflers applying experimental and numerical methods*. International Compressor Engineering Conference

APPENDIX

A. Transmission loss of single expansion chamber muffler [13]

At the junction of the inlet tube and the expansion chamber, the instantaneous acoustic pressure in the inlet tube and in the expansion chamber are equal; and, similarly, the instantaneous acoustic pressures are equal at the junction of the expansion chamber and the outlet tube for the expansion chamber muffler. The instantaneous volumetric flow rates, $U(t) = S\,u(t)$, are equal on each side of the inlet and outlet junction.
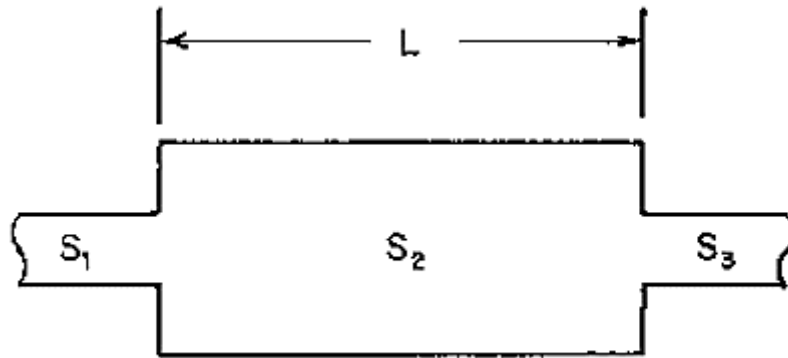
The sound power transmission coefficient for the single chamber muffler shown above is

$$\frac{1}{a_t} = 1 + \frac{1}{4}(m - 1/m)^2 \sin^2(kL) \tag{a-1}$$

Transmission loss can be calculated as:

$$TL = 10\log_{10}(1/a_t) \tag{a-2}$$

B. Transfer matrix of various muffler elements [14]

B.1 Uniform Tube with Flow and Viscous Losses

$$\begin{bmatrix} p \\ u \end{bmatrix}_u = e^{-jMk_cl} \begin{bmatrix} \cos(k_cl) & j\underline{Z}\sin(k_cl) \\ (j/\underline{Z})\sin(k_cl) & \cos(k_cl) \end{bmatrix} \begin{bmatrix} p \\ u \end{bmatrix}_d \qquad \text{(b-1)}$$

Subscripts u and d indicate points just upstream and just downstream of the sudden area discontinuity.

Incidentally, the same transfer matrix would hold for the convective state variables p_c and u_c at both ends. For inviscid stationary medium, the transfer matrix for a uniform tube reduces to

$$\begin{bmatrix} \cos(k_ol) & j\underline{Z_o}\sin(k_cl) \\ (j/\underline{Z_o})\sin(k_ol) & \cos(k_ol) \end{bmatrix} \begin{bmatrix} p \\ u \end{bmatrix}_d \qquad \text{(b-2)}$$

B.2 Sudden Area Changes

Typically, the mean flow Mach number M in the smaller diameter tube is M < 0.2.

$$\begin{bmatrix} p_{c,u} \\ u_{c,u} \end{bmatrix} = \begin{bmatrix} 1 - \dfrac{K_dM_d^2}{1-M_d^2} & K_dM_d\underline{Z_d} \\ \dfrac{(k-1)K_dM_d^3}{(1-M_d^2)\underline{Z_d}} & 1 - \dfrac{(k-1)K_dM_d^2}{1-M_d^2} \end{bmatrix} \begin{bmatrix} p_{c,d} \\ u_{c,d} \end{bmatrix} \qquad \text{(b-3)}$$

(a) Sudden contraction   (b) Sudden expansion
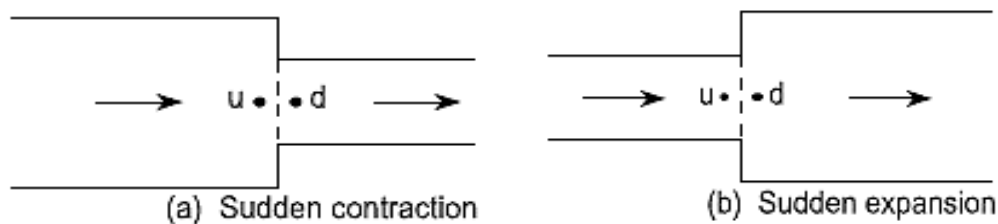
Where K_d is the K-factor indicating the drop in stagnation pressure of the incompressible mean flow in terms of the dynamic head $\rho_o V_d^2/2$

$K_d = (1 - S_d / S_u)/2$ for sudden contraction,

$K_d = (1 - S_d / S_u)/2$ for sudden expansion.

If M < 0.2 in the smaller diameter tube, the foregoing transfer matrix may be approximated as

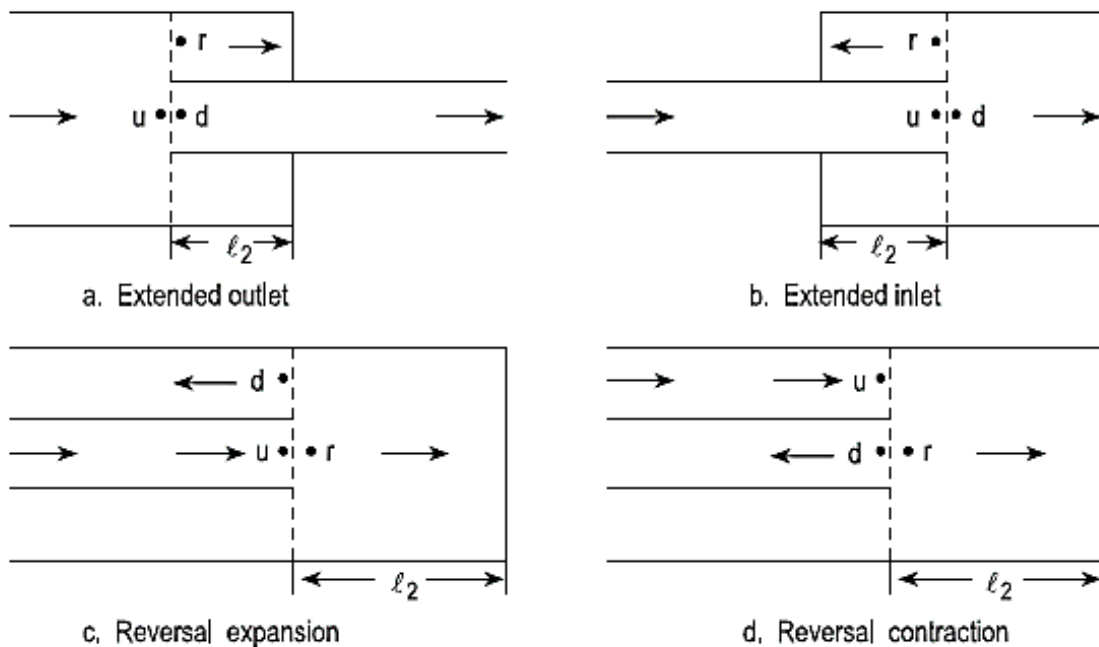$$\begin{bmatrix} p_{c,u} \\ u_{c,u} \end{bmatrix} = \begin{bmatrix} 1 & K_d M_d \underline{Z_d} \\ 0 & 1 \end{bmatrix} \begin{bmatrix} p_{c,d} \\ u_{c,d} \end{bmatrix} \tag{b-4}$$

This relation, on transformation to the classical state variables and on incorporating the low Mach number simplification, becomes:

$$\begin{bmatrix} p_u \\ u_u \end{bmatrix} = \begin{bmatrix} 1 & (1 + K_d) M_d \underline{Z_d} - M_u \underline{Z_u} \\ 0 & 1 \end{bmatrix} \begin{bmatrix} p_d \\ u_d \end{bmatrix} \tag{b-4}$$

B.3 Extended Inlet/Outlet

$$\begin{bmatrix} p_{c,u} \\ u_{c,u} \end{bmatrix} = \begin{bmatrix} 1 & K_d M_d \underline{Z_d} \\ \dfrac{C_r S_r}{C_r S_r Z_r + S_u M_u \underline{Z_u}} & \dfrac{C_r S_r Z_r - M_d \underline{Z_d}(C_d S_d + K_d S_u)}{C_r S_r Z_r + S_u M_u \underline{Z_u}} \end{bmatrix} \begin{bmatrix} p_{c,d} \\ u_{c,d} \end{bmatrix} \tag{b-5}$$

a. Extended outlet

b. Extended inlet

c. Reversal expansion

d. Reversal contraction

- S_x are cross-section areas at $x = u, d, r$;

- M_x are Mach numbers at these positions;

- $\underline{Z_d}$, $\underline{Z_u}$, $\underline{Z_2}$ are characteristic flow impedances;

- $\underline{Z_r} = -j\underline{Z_2}\cot(k_o l_2)$ is the input flow impedance of the annular cavity resonator.

Thus, $K_d = (1 - S_d / S_u)/2$ for extended outlet,

$\qquad\quad = (S_d / S_u - 1)^2$ for extended inlet,

$\qquad\quad = (S_d / S_u)^2$ for reversal expansion,

$\qquad\quad = 0.5$ for reversal contraction.

The constants Cr and Cd are given by the area compatibility equation:

$S_u + C_d\, S_d + C_r\, S_r = 0$
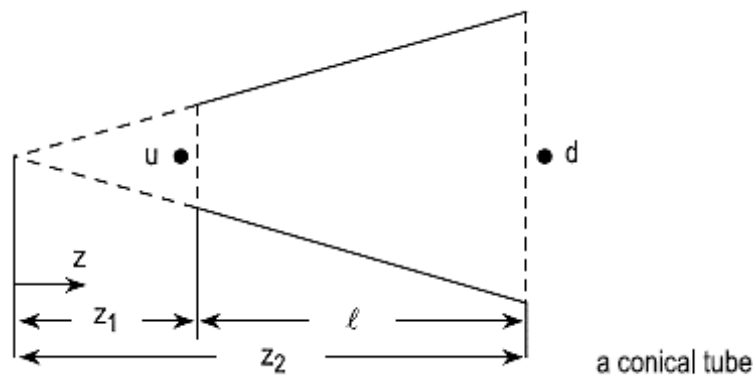
Thus, $C_d = -1$;	$C_r = -1$	for extended outlet,
$C_d = -1$;	$C_r = +1$	for extended inlet,
$C_d = +1$;	$C_r = -1$	for reversal expansion,
$C_d = +1$;	$C_r = -1$	for reversal contraction.

B.4 Conical Tube

With tube length l and tube radii r_u, r_d, the following relations are used:

$$z_1 = \frac{r_u}{r_d - r_u}\,l, \qquad z_2 = z_1 + l \tag{b-6}$$

$$\underline{Z_d} = \frac{\rho_o c_o}{\pi r_d^2} \tag{b-7}$$

a conical tube

For a stationary medium, the transfer matrix relationship for a conical tube is given by

$$\begin{bmatrix} p_u \\ u_u \end{bmatrix} = \begin{bmatrix} \dfrac{z_2}{z_1}\cos(k_o l) - \dfrac{\sin(k_o l)}{k_o z_1} & jZ_d\dfrac{z_2}{z_1}\sin(k_o l) \\ \dfrac{j}{Z_d}\left\{ \dfrac{z_1}{z_2}\left(1+\dfrac{1}{k_o^2 z_1 z_2}\right)\sin(k_o l)\dfrac{\sin(k_o l)}{k_o z_2} \\ + \dfrac{z_1}{z_2}\cos(k_o l) - \left(1-\dfrac{z_1}{z_2}\right)\dfrac{\cos(k_o l)}{k_o z_2} \right\} \end{bmatrix} \begin{bmatrix} p_d \\ u_d \end{bmatrix} \qquad (\text{b-5})$$

The expression holds for a convergent tube as well as a divergent tube.